

TRANSPORTATION RESEARCH RECORD 983

Issues in Transportation
Noise Mitigation:
Highway and Railway Studies

TRB

TRANSPORTATION RESEARCH BOARD
NATIONAL RESEARCH COUNCIL

WASHINGTON, D.C. 1984

Transportation Research Record 983

Price \$9.20

Editor: Scott C. Herman

Compositor: Lucinda Reeder

Layout: Harlow Bickford

modes

1 highway transportation

3 rail transportation

subject areas

12 planning

17 energy and environment

Transportation Research Board publications are available by ordering directly from TRB. They may also be obtained on a regular basis through organizational or individual affiliation with TRB; affiliates or library subscribers are eligible for substantial discounts. For further information, write to the Transportation Research Board, National Research Council, 2101 Constitution Avenue, N.W., Washington, D.C. 20418.

Printed in the United States of America

Library of Congress Cataloging in Publication Data

National Research Council. Transportation Research Board.

Issues in transportation noise mitigation.

(Transportation research record; 983)

1. Traffic noise—Addresses, essays, lectures. 2. Railroads—Noise—Addresses, essays, lectures. 3. Noise control—Addresses, essays, lectures. I. National Research Council (U.S.). Transportation Research Board. II. Title.

TE7.H5 no. 983 380.5 s 85-4882

[TD893.6.T7] [625.7'95] ISSN 0361-1981

Sponsorship of Transportation Research Record 983

GROUP 1—TRANSPORTATION SYSTEMS PLANNING AND ADMINISTRATION

Kenneth W. Heathington, University of Tennessee, chairman

Environmental Quality and the Conservation of Resources Section
Carmen DiFiglio, U.S. Department of Energy, chairman

Committee on Transportation-Related Noise and Vibration
Mas Hatano, California Department of Transportation, chairman
Fred L. Hall, McMaster University, secretary
Charles B. Adams, Grant S. Anderson, Timothy M. Barry, Donna Berman, Jesse Owen Borthwick, William Bowlby, Ronald M. Canner, Jr., Peter C. L. Conlon, Donna McCord Dickman, Charles C. Erhard, John S. Higgins, Harvey S. Knauer, Win M. Lindeman, Robert L. Mason, James P. Muldoon, Anthony W. Paolillo, Joseph B. Pulaski, Fred M. Romano, Harter M. Rupert, Gary D. Vest, Donald R. Whitney

Liaison Representative
Louis F. Cohn

GROUP 2—DESIGN AND CONSTRUCTION OF TRANSPORTATION FACILITIES

Robert C. Deen, University of Kentucky, chairman

Evaluations, Systems and Procedures Section
Charles S. Hughes, Virginia Highway and Transportation Research Council, chairman

Committee on Instrumentation Principles and Applications
Earl C. Shirley, California Department of Transportation, chairman
Kenneth R. Agent, Larry D. Barfield, Roy E. Benner, Richard L. Berry, William Bowlby, Bernard C. Brown, Theodore R. Cantor, Gerardo G. Clemen, John C. Cook, George H. Cramer II, Wilbur J. Dunphy, Jr., C. Page Fisher, Speros J. Fleggas, Thomas A. Fuca, James L. Melancon, Terry M. Mitchell, David H. Pederson, Ronald J. Piracci, David C. Wyant

Stephen E. Blake and Neil F. Hawks, Transportation Research Board staff

Sponsorship is indicated by a footnote at the end of each paper. The organizational units, officers, and members are as of December 31, 1983.

NOTICE: The Transportation Research Board does not endorse products or manufacturers. Trade and manufacturers' names appear in this Record because they are considered essential to its object.

Contents

NOISE STUDIES FOR THE SAN ANTONIO "Y" PROJECT Grant S. Anderson	1
EVALUATION OF T-PROFILE HIGHWAY NOISE BARRIERS J. J. Hajek and C. T. Blaney	8
NOISE-COMPATIBLE DEVELOPMENT: A PILOT DEMONSTRATION PROJECT Mark T. Stahr	18
DETERMINATION OF REFERENCE ENERGY MEAN EMISSION LEVEL IN GEORGIA Roswell A. Harris	22
RUMBLE STRIP NOISE John S. Higgins and William Barbel	27
EXAMINATION OF THE DEPENDENCE OF DIESEL-ELECTRIC LOCOMOTIVE NOISE EMISSION ON SPEED, RATED POWER, AND AGE Eric Stusnick	36
NOISE IMPACT OF RAIL PASSENGER SERVICE Mas Hatano	40
SYNTHESIS OF DISC BRAKE SQUEAL QUIETING EXPERIENCE Michael A. Staiano	43
RESEARCH ON A DEVICE FOR REDUCING NOISE Kazuyoshi Iida, Yoshikazu Kondoh, and Yasuhiro Okado	51
REVIEW OF FEDERAL NOISE EMISSION STANDARDS FOR INTERSTATE RAIL CARRIERS Eric Stusnick	54
USE OF MICROCOMPUTERS IN HIGHWAY NOISE DATA ACQUISITION AND ANALYSIS Philip J. Grealy, Simon Slutsky, and William R. McShane	57

Addresses of Authors

- Anderson, Grant S., Bolt Beranek and Newman, Inc., 10 Moulton Street, Cambridge, Mass. 02238
- Barbel, William, Division of Highways, Illinois Department of Transportation, Region 1, 1000 Plaza Drive, Schaumburg, Ill. 60196
- Blaney, C. T., Research and Development Branch, Ontario Ministry of Transportation and Communications, 1201 Wilson Avenue, Downsview, Ontario M3M 1J8, Canada
- Grealy, Philip J., Transportation Training and Research Center, Polytechnic Institute of New York, 333 Jay Street, Brooklyn, N.Y. 11201
- Hajek, J. J., Research and Development Branch, Ontario Ministry of Transportation and Communications, 1201 Wilson Avenue, Downsview, Ontario M3M 1J8, Canada
- Harris, Roswell A., Transportation and Engineering Research, Department of Civil and Environmental Engineering, Vanderbilt University, Box 1569 Station B, Nashville, Tenn. 37235
- Hatano, Mas, Division of Engineering Services, Office of Transportation Laboratory, California Department of Transportation, 5900 Folsom Boulevard, P.O. Box 19128, Sacramento, Calif. 95819
- Higgins, John S., Federal Highway Administration, U.S. Department of Transportation, New Mexico Division, P.O. Box 1088, Santa Fe, N. Mex. 87504
- Iida, Kazuyoshi, Noise and Vibration Control Group, Technical Research Laboratory, Research and Development Division, Bridgestone Corporation, Yokohama, Japan
- Kondoh, Yoshikazu, Noise and Vibration Control Group, Technical Research Laboratory, Research and Development Division, Bridgestone Corporation, Yokohama, Japan
- McShane, William R., Transportation Training and Research Center, Polytechnic Institute of New York, 333 Jay Street, Brooklyn, N.Y. 11201
- Okado, Yasuhiro, Noise and Vibration Control Group, Technical Research Laboratory, Research and Development Division, Bridgestone Corporation, Yokohama, Japan
- Slutsky, Simon, Transportation Training and Research Center, Polytechnic Institute of New York, 333 Jay Street, Brooklyn, N.Y. 11201
- Stahr, Mark T., Office of Environmental Policy, HEV-30, Federal Highway Administration, U.S. Department of Transportation, 400 7th Street, S.W., Washington, D.C. 20590
- Staiano, Michael A., Staiano Engineering, Inc., 1923 Stanley Avenue, Rockville, Md. 20851
- Stusnick, Eric, Wyle Laboratories, 2361 Jefferson Davis Highway, Suite 404, Arlington, Va. 22202

Noise Studies for the San Antonio "Y" Project

GRANT S. ANDERSON

ABSTRACT

Measurements were made in Austin, Texas, of highway traffic noise reflecting from the underside of an overhead roadway to diagnose these reflections and the resulting amplification to the side. Special care was taken to normalize all measurements to the actual emission level of each passing truck. It was determined that reflections from the precast I girders were scattered to the side rather than reflected specularly. An equation was developed that related this scattered sound to the relevant cross-sectional geometry at the two measurement sites. Subsequent measurements at two additional sites verified the scattering equations to within 1 dB, on average. For different cross-sectional geometries in San Antonio, where the proposed structure is a composite wing girder rather than a precast I girder, calculations were made of the sideline amplification caused by the expected specular reflections. Comparison of these calculated (specular) results with the measured (scattered) results in Austin indicates that the San Antonio amplification should be less than that measured in Austin, except when both of the following occur: (a) the receiver is within 50 to 60 ft of the edge of the elevated structure, and (b) the upper roadway curves away from the receiver.

Figure 1 shows a portion of I-35 in Austin, Texas, where the Interstate is split level: half the traffic is depressed and the other half is elevated. Along this portion of I-35 the Texas State Department of Highways and Public Transportation (TSDHPT) had received complaints that the elevated structure was amplifying traffic noise to the side by reflecting sound from its underside. Attempts to measure this possible amplification had been inconclusive.

Of immediate concern was a similar split-level Interstate proposed for San Antonio. Would the proposed San Antonio structure amplify noise levels above what was predicted from the standard FHWA equations? If so, by how much?

Figure 2 shows the two elevated structures for Austin and San Antonio. The Austin structure consists of a precast concrete deck supported on steel I girders. When sound reflects from the underside of such a structure, a portion of it is reflected specularly as from a mirror, where the angle of reflection equals the angle of incidence.

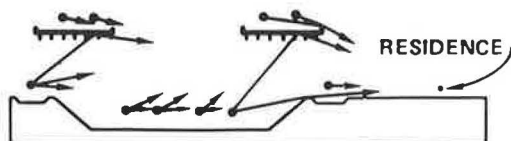
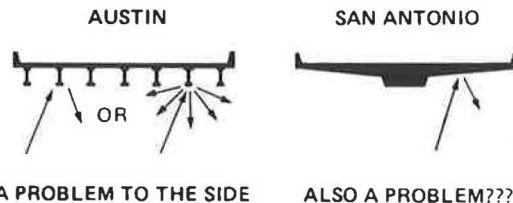


FIGURE 1 Complete measurement geometry in Austin.



A PROBLEM TO THE SIDE ALSO A PROBLEM???

FIGURE 2 The two elevated structures.

Another portion is scattered in all directions on reflection. For the Austin structure, the relative strengths of these reflected components are not obvious.

By comparison, reflection from the San Antonio structure is surely specular. This proposed structure--a so-called composite wing girder--consists of broad expanses of flat concrete devoid of any exposed beams. Because the two structures are so different from an acoustical point of view, amplification to the side in Austin does not necessarily mean similar amplification in San Antonio.

A three-part investigation of this type of amplification is discussed in this paper:

1. Measurement of the amplification in Austin,
2. Diagnosis of the reflected sound in Austin to determine if it is predominantly specular or predominantly scattered, and
3. Application of the Austin results to predict possible amplification in San Antonio.

The results are summarized as follows. Austin amplification was measured to range between zero and 12 dB, depending on receptor distance to the side. The diagnosis clearly indicates that Austin reflections are predominantly scattered. As a result, the Austin measurements are no help in predicting possible amplification in the San Antonio structure.

The amplification of the San Antonio structure was computed by assuming specular reflections from the underside of the elevated structure. The resulting amplifications range between zero and 7 dB, but most are usually between zero and 3 dB.

The remainder of this paper contains details of the Austin measurements and their mathematical analysis, followed by details of the resulting amplifications and diagnosis of the reflected sound. Additional Austin verification measurements are also given. Finally, the predictions of amplification in San Antonio are described.

AUSTIN MEASUREMENTS: AN OVERVIEW

Figure 1 shows the Austin cross-sectional geometry. Two sites were chosen for measurement: one depressed 18 ft and the other depressed 12 ft. The geometrical complexity is obvious from the figure. With this geometry, the component of the sound reflected from the structure may not predominate enough to be measured at all by using the time-averaging descriptor L_{eq} .

To eliminate this complication during diagnosis, peak passby levels were measured for individual heavy trucks on the lower roadway, rather than the

L_{eq} . As long as no other trucks are close by during each peak measurement, the uncontaminated measurement shown in Figure 3 results. In Figure 3 the total level at the microphone consists of two components: a direct component and a reflected component.

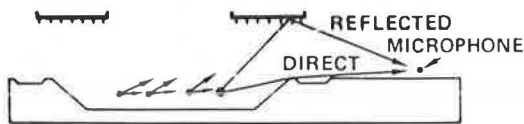
Depressed sections were chosen for measurement so that the reflected component would dominate over the direct component, which is reduced by diffraction over the top edge of the retaining wall. Even though this reflected component dominates, the direct component must still be subtracted from the total at the receptor to precisely determine the reflected component. The only recourse is to compute this direct component.

Errors inherent in this computation will not significantly affect the result of the subtraction as long as the reflected component dominates. The introduction of a computation into the analysis adds another complication, however. Computation of the direct component for an individual truck passby includes an emission-level term. Rather than assume that the noise emission from each vehicle is equal to the national average, precision is maintained by an independent measurement of the emission level of each vehicle as it passes. Measurement of emission level is not straightforward, however, because an uncontaminated measurement 50 ft to the side is impossible. Instead, a surrogate is used for emission level, which is measured at a reference microphone directly above the median and high enough so that essentially no reflected sound reaches it. The resulting geometry is shown in Figure 4. The peak reference level as a truck passes by is a measure of the noise emissions from that vehicle, but upwards at an angle rather than to the side, and not at the standard distance.

In summary, the diagnosis uses measurements of single truck passbys, simultaneously measured to the side and at the reference position. The reference level is used to normalize the entire analysis to the emission level of that particular truck. The (computed) direct component is subtracted from the total level L_T at the microphone to yield the reflected component L_R . It is this reflected component that is then quantified and diagnosed as specular, scattered, or a mixture of the two.

ANALYSIS OF AUSTIN MEASUREMENTS

Two equations are basic to the analysis. The first relates the amplification of the structure to the measured L_{Total} and the computed L_{Direct} :



$$\text{AMPLIFICATION} = \text{TOTAL} - \text{DIRECT}$$

FIGURE 3 Measurement geometry for one lane and receptor pair.

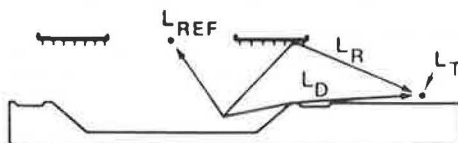


FIGURE 4 Measurement geometry with reference microphone.

$$\text{Amplification} = L_{Total} - L_{Direct} \quad (1)$$

For example, if the direct component is 67 dB(A), this would also be the sound level at the receptor in the absence of the elevated structure. If the measured L_{Total} is 75 dB(A), the structure has amplified the sound level by the simple difference between these two: 8 dB.

The second equation of interest relates the total level to its direct and reflected components:

$$L_{Total} = L_{Direct} \oplus L_{Reflected} \quad (2)$$

The circle around the plus sign signifies decibel addition. For example, if the direct component is 67 dB(A) and the reflected component is 74 dB(A), then the total level at the receptor will be the decibel sum of these two: 75 dB(A). Equation 2 can be rewritten as

$$L_{Reflected} = L_{Total} \ominus L_{Direct} \quad (3)$$

where the circle now signifies decibel subtraction. The example numbers are the same as those previously given:

$$74 \text{ dB(A)} = 75 \text{ dB(A)} - 67 \text{ dB(A)}.$$

Equation 1 is used to derive the amplification from the measured L_{Total} and the computed L_{Direct} . Equation 3 is used to derive the reflected component from these same two quantities.

In energy-like notation (to allow normal arithmetic rather than decibel arithmetic), Equation 3 converts to

$$10^{L_R/10} = 10^{L_T/10} - 10^{L_D/10} \quad (4)$$

Then Equation 4 is normalized by the emission level (L_{EL}) of the vehicle, the maximum passby level 50 ft to the side. Normalization of the first term on the right proceeds in two steps: first to L_{REF} at the reference microphone, and second to L_{EL} :

$$10^{(L_R - L_{EL})/10} = 10^{(L_T - L_{REF})/10} \times 10^{(L_{REF} - L_{EL})/10} - 10^{(L_D - L_{EL})/10} \quad (5)$$

$$10^{(L_R - L_{EL})} = (\text{Term 1}) (\text{Term 2}) - (\text{Term 3}) \quad (6)$$

Equation 6 identifies each of the terms of Equation 5 for easier discussion in the following sections, where each of these terms is discussed in detail.

Basic Data: Term 1 of Equations 5 and 6

Term 1 of Equations 5 and 6 comprises the basic data. This term is measured for each individual truck passby: L_{Total} at the receptor and L_{REF} simultaneously at the reference microphone. Precision is maintained in these simultaneous measurements by calibrating the ballistics of the two sound level meters.

A total of 219 heavy trucks (three or more axles) were measured. These data span a combination of 40 receptor and travel lane combinations, comprised of 10 receptor positions matched with 4 lower-roadway travel lanes.

Next, these data are separated by lane and receptor pairs into 40 subtables, each for a common lane and receptor pair. A standard error of 0.4 dB is typical of all 40 subtables.

In summary, there are 40 term 1's, each corresponding to one of the lane and receptor pairs. Each term 1 is the mean value of one of these 40 subtables divided first by 10, and then exponentiated on 10, as indicated in Equation 5. These 40 terms comprise truck noise levels normalized to the overhead reference microphone. Sufficient trucks are measured for each lane and receptor pair so that the mean is known within ± 1 dB.

Surrogate Term: Term 2 of Equations 5 and 6

Term 2 of Equations 5 and 6 converts the reference measurements to proper emission levels by independent experiment. The experiment is not in Austin, where the overhead roadways provide reflections, but instead at a similar cross-sectional site in San Antonio, where no overhead roadways exist. The reference microphone was supported on a cross-street bridge, as were the reference microphones in Austin. The level to the side was measured at one side position.

Figure 5 shows the cross-sectional geometry. The reference microphone is 35 ft above the travel lanes of the lower roadway and directly above the centerline of the slow travel lane. Because of this all sources extend to the left of this reference microphone position. The distance to the left is designated X. X ranges from zero for the slow travel lane, out to larger values for subsequent travel lanes, and ends at the slow travel lane in the opposite direction.

The side microphone is 5 ft above the pavement and 25 ft from the centerline of the nearest travel lane. Distance to the side microphone varies for each of the travel lanes, and all sideline levels are later converted to 50 ft. A regression equation is desired for the difference between the side and the overhead level as a function of which lane the vehicle is in.

Term 2 is not actually a difference in sound levels but instead is a ratio of energies associated with these sound levels. It is desirable to regress this ratio of energies directly, rather than to regress the differences in the exponent of 10 in these terms.

In addition, term 2 has one more complicating factor to it, as shown in Equation 7:

$$\begin{aligned} \text{Term 2} &= \left(10^{L_{REF}/10}/10^{L_S/10}\right) \left(10^{L_S/10}/10^{L_{EL}/10}\right) \\ &= \left(10^{L_{REF}/10}/10^{L_S/10}\right) [50/(25 + X)]^2 \end{aligned} \quad (7)$$

Term 2 does not just consist of the first factor in Equation 7, which relates the overhead reference microphone to the side level measured in this experiment. The second factor must also be included. This second factor is a distance conversion factor that converts the side microphone measurement to 50 ft (the standard distance for emission levels). This

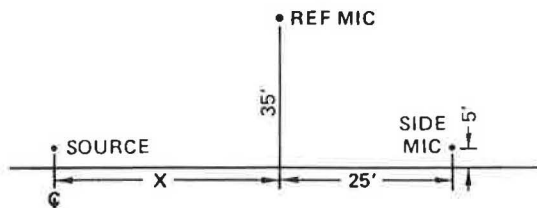


FIGURE 5 Independent experiment geometry to convert reference level to emission level.

entire term 2 is regressed, including the squared ratio term, so that the regression result is the full term 2. The result is

$$\text{Term 2} = 2.133 - 0.05933X + 0.0005371X^2 \quad (8)$$

This is the conversion to emission level from L_{REF} , the surrogate for emission level. It is an average term, averaged over the 69 trucks that passed by in San Antonio.

Computed Direct Level: Term 3 in Equations 5 and 6

Term 3 of Equations 5 and 6 is the computed sound level at the receptor, which ignores reflections from above. This computation proceeds in two steps:

$$\begin{aligned} \text{Term 3} &= \left[10^{(L_D/10) \text{ no barrier}}/10^{L_{EL}/10}\right] 10^{-A/10} \\ &= (50/D)^2 10^{-A/10} \end{aligned} \quad (9)$$

In this equation the first term is the distance correction term from the 50-ft distance of the emission level to the proper distance. The second term corrects for the barrier attenuation, which is a function of geometry.

The barrier-attenuation equations that underlay the FHWA barrier calculations were used. However, also used were the equations for a point source, rather than for a line source, because the peak passby level is the result of a single truck near its closest point of approach.

Note that Equation 9 does not contain vehicle emission level, which has been normalized out of the computation. In essence, this computation is a function only of the propagation between source and receptor.

RESULTING AUSTIN AMPLIFICATIONS

Figures 6 and 7 show the resulting amplifications in Austin. These amplifications follow from the measurements and from Equation 1. The resulting amplifications differ significantly between Austin Site 1 and Site 2. At Site 1 the noise increases are all large and do not drop off with distance from the roadway. At Site 2 the noise increases are smaller and drop off significantly as the receptor moves farther from the roadway.

To explain this site difference, ray-tracing techniques are used to search for a basic difference

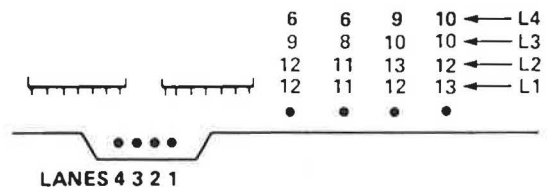


FIGURE 6 Resulting Austin amplifications, Site 1.

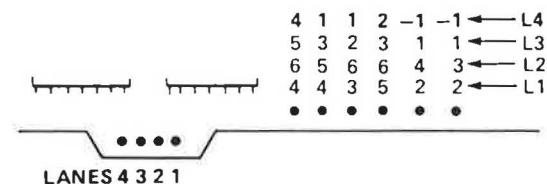


FIGURE 7 Resulting Austin amplifications, Site 2.

between Site 1 and Site 2. Figure 8 shows this basic difference. For Site 1, this figure shows that this site produces a unique triple bounce of truck noise, aimed directly at the receptors. This triple bounce occurs not only from the lane shown, but for all other lanes. It also occurs in several other manners. For example, from the lane shown, it bounces first off the roadway pavement, then to the opposite retaining wall, then to the overhead structure, then back down to the retaining wall, and then to the receptor. In effect, this is a quadruple bounce.

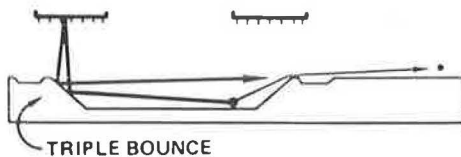


FIGURE 8 Site 1 anomaly.

This triple bounce for Site 1 results in additional paths by which sound can reach the receptors. These paths are quite similar to the direct path (shown lightly in the figure), except for two differences. First, they are longer, and second, they contain reflections.

These reflections are essentially specular because they are from the retaining wall and from the overhead structure, reflected perpendicularly. Because they are essentially specular, they result in a geometry that can be calculated, just as the direct geometry was calculated. This calculation was undertaken for each of the image sources that each receptor would see (i.e., bounced off the opposite retaining wall).

For each possible path, the expected level at the receptor was computed and subtracted from the total. In effect this means that the total sound level had many terms subtracted from it, not only the direct term, which goes directly over the retaining wall toward the microphone, but also each of these image terms. Even after this subtraction, however, Site 1 amplification is significantly more than that at Site 2.

What appears to be happening is the following: Sound generated by traffic and proceeding toward one of the retaining walls is bounced up to the overhead structure and back down to the retaining wall. This aims a significant amount of sound over to the opposite retaining wall, which then bounces it up to the opposite overhead roadway and back down again. In this manner sound is trapped between the two retaining walls, as if they were vertical. In reality they are not vertical, but the nearly 45-degree slopes of the retaining walls, combined with the horizontal overhead structure, in effect produces a vertical retaining wall. This results in a large amount of reverberant energy trapped in this depressed section. Each time the sound bounces off the overhead structure, some of it is scattered sideways by the structure to the receptor. After many bounces, significantly more sound is scattered sideways than would otherwise be there. This additional scattering makes Site 1 very different from Site 2.

Because of this triple-bounce anomaly at Site 1, which will not occur in San Antonio, the amplification results of Site 1 are not considered to be as relevant as those of Site 2. Both sets of results are retained in the analysis, nevertheless.

DIAGNOSIS OF REFLECTED SOUND

Combination of terms 1, 2, and 3 in Equation 5 yields the reflected portion of the sound at each receptor. This reflected portion is determined separately for each of the 40 lane and receptor pairs.

For many of these pairs there is no path by which sound can reflect off the upper roadway directly to the receptor with the angle of reflection equal to the angle of incidence. By pure ray-tracing reasoning, therefore, the sound for these pairs should not be amplified by the overhead structure.

Such pairs without direct specular reflections are as follows: for Site 1, for receptor 2: lanes 1 and 2; for receptor 3: lanes 1-3; and for receptor 4: lanes 1-4; and for Site 2, for receptor 3: lane 1; and for receptors 4-6: all lanes. The receptor numbers increase with distance from the roadway.

Nevertheless, for these lane and receptor pairs, amplification due to the upper roadway did occur. This portion of the amplification must be due to scattering from the upper roadway surface.

Figure 9 shows the reasoning behind the next steps of the analysis. For those lane and receptor pairs that have no chance of specular reflections, a regression analysis was undertaken to determine scattering as a function of the angles of interest. This scattering was subtracted from the other data to determine the residual component that remained. This residual was essentially zero, and therefore the other data were essentially all scattered as well.

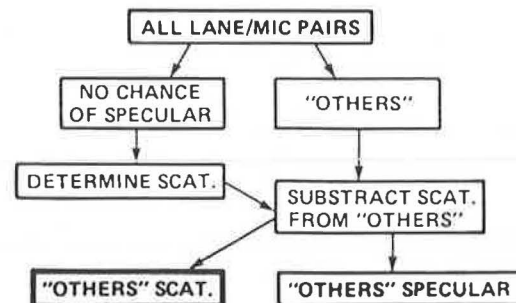


FIGURE 9 Overview of Austin diagnosis of reflected sound.

The scattering geometry is shown in Figure 10. For each lane and receptor pair, a line was drawn directly from the source up to the center of the reflecting surface and then down to the receptor. The two angles shown are the angle of incidence and the angle of scatter. This path has length D , which in general differs from 50 ft, the reference distance. Therefore, the total reflected component, normalized to the reference distance, is

$$10^{(L_R - L_{EL})/10} = (50/D)^2 F(\alpha_{inc}, \alpha_{scat}) \quad (10)$$

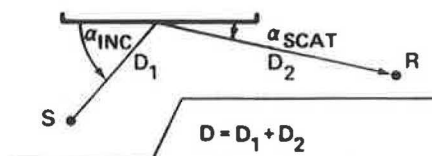


FIGURE 10 Scattering geometry.

In this equation F is the fraction of incident energy that is reflected toward the microphone. This fraction is a function of the two angles of concern, and it is this fraction that is sought.

Because the expression on the left has been previously measured for each of these lane and receptor pairs, and because the distance D is known, this equation can be used to solve for F . This was done for each of the lane and receptor pairs previously given. The average values of F are 0.62, 0.63, and 0.50 for Site 1 and 0.21, 0.34, 0.08, and 0.07 for Site 2.

As is apparent, Site 1 still does not match with Site 2; the scattered energy is far greater. For this reason, an attempt was made to interpret Site 1 data by a higher source height than for Site 2. Justification for this is as follows.

At Site 1 the trucks were coming out from underneath the cross-street overpass and accelerating up a grade of greater than 5 percent. Such acceleration results in two things. First, the emission levels of the trucks are increased. This is accounted for automatically by the reference microphone measurement directly above the truck. Second, most of the energy of an accelerating truck comes from the top of the stack of the truck, rather than from its tires, because the throttle is increased during acceleration. Thus the source height of these trucks is likely to be higher than it is for Site 2, where such upgrade acceleration did not occur.

For this reason all calculations were redone with a source height of 12 ft. The resulting Site 1 values of F were reduced by this increase in source height, but were still much larger than at Site 2.

A quadratic nonlinear fit was attempted on (a) all the data, including Site 1, and (b) on Site 2 data only. The statistics are as follows: On all data, $R^2 = 0.45$, and on the Site 2 data only, $R^2 = 0.73$. These fits are considered satisfactory for use and were retained as the final results. For F at both sites and no direct deflection,

$$F = 0.1435a_{inc} - 0.00171a_{inc}^2 + 0.02422a_{scat} - 2.731 \quad (11)$$

and for F_2 with no direct reflection,

$$F_2 = 0.1469a_{inc} - 0.001697a_{inc}^2 + 0.03225a_{scat} - 3.0709 \quad (12)$$

Equation 11 is later used for Site 1 data, and Equation 12 is used for Site 2 data.

As noted previously, many lane and receptor pairs were left out of this regression analysis. These were left out because, for these pairs, strong single specular reflection is possible.

The next obvious question is how well the regression fit explains the lane and receptor pairs that were not used in its development. In other words, each of the pairs that has a direct specular reflection also has an angle of incidence and an angle of scatter. Therefore, they would probably also have a portion of the excess energy contributed by scattering. In essence, this scattered portion is found by using the regression equations. Then, after subtracting it from the total sound for those pairs, the remainder is the portion that would arrive by way of direct specular reflection.

Results indicate that, except for the first two lane and receptors pairs, the specular reflections have no influence on the measured noise levels. All of the energy arrives by way of scattering. Even for the first two pairs, scattering controls the amplification at the microphone position.

It is concluded from this analysis that all the amplification to the side in Austin is caused by

scattering, and essentially none is caused by specular reflection.

A FINAL CHECK: SPECULAR PREDICTIONS FOR AUSTIN

The specular amplification for the Austin geometry was next predicted for comparison with the measured scattered amplification. In this manner the difference between specular and scattered conditions could be directly determined. The results of the specular calculations are described herein.

The basic equation is

$$L_T = (L_D - A) + (\sum L_R) \quad (13)$$

dB sum, also

This equation states that the total measured noise level is the sum of the direct level (minus the barrier attenuation) and all reflected levels received by reflected paths. All these sums are decibel summations.

The results of this analysis appear as dotted lines in Figures 11 and 12 as a function of distance from the edge of the structure. For comparison, the solid line shows the measured amplification in Austin. The measured amplification significantly exceeds the specular predictions, as is obvious from the figures.

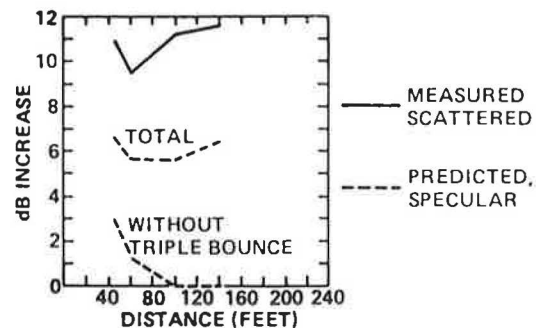


FIGURE 11 Austin comparisons of measured amplification and specular predictions, Site 1.

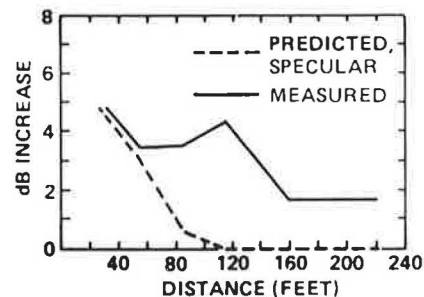


FIGURE 12 Austin comparisons of measured amplification and specular predictions, Site 2.

Figure 11 shows a breakdown of the specular amplification into that produced by the triple bounce and that produced by the remainder of the reflections. As is obvious from Figure 11, most of the amplification is from the triple bounce and little is from the remaining reflections. This check on specular reflections confirms the diagnosis that scattering predominates over specular reflection from the underside of the Austin structure.

VERIFICATION

Overview

The measurements previously cited are best called diagnostic measurements. They involve individual truck passbys, where the lane of travel is known for each passing truck. During the closest point of approach for each such truck, noise from that truck completely dominates the total sound level at the receptor. The measurement then allows diagnosis of the path(s) that this noise has traveled from truck to receptor.

Such diagnostic measurements could not have been made by using the full noise climate at the receptor. This full noise derives from many different vehicles, each with its own emission level, and from vehicles traveling on many different lanes. The propagation situation is simply too complicated for diagnosis.

Another way of looking at the diagnosis is that the diagnostic measurements were of short duration, essentially just a second or less, when an individual truck was registering its maximum noise level at the receptor. During this short duration one noise source dominated. The situation is relatively simple. On the other hand, longer measurements capture many vehicles and much more complexity. These longer measurements do not allow diagnosis.

It was thought desirable, notwithstanding these difficulties, to measure noise during some longer periods to determine if the results of the diagnosis would adequately predict the longer-term noise levels; specifically, the energy-average noise level L_{eq} . For this purpose a series of verification measurements was made.

Verification measurements were made at Site 2, as well as at two additional sites along the elevated sections of I-35 in Austin. These two additional sites are both sites where the lower roadway is at grade. They differ from each other in that the elevated roadway is significantly higher at one than at the other.

Method

At each of these three verification sites a series of 10-min L_{eq} 's was obtained. Simultaneously, the traffic was classified and speeds were measured. In addition, overhead noise levels were measured for each passing heavy truck for later conversion to emission levels. Then, by using these measured data at the site, the L_{eq} 's were predicted for each 10-min period for matching with the measured 10-min L_{eq} 's.

The L_{eq} noise predictions were made in accordance with the current FHWA method (1), as embodied in FHWA's (Texas Instruments) programmable-calculator program. Instead of using the national average emission levels for heavy trucks on the lower roadway, emission levels specific to the measurement period were obtained from the overhead reference levels. These emission levels, specific to I-35 in Austin and specific to the actual 10 min of measurement, were used only for heavy trucks on the lower roadway. The national average emission levels were used in all other cases.

Full traffic classifications were made for the lower roadway, separately by lane, and also for the near frontage road. These classifications were made simultaneously with the noise measurements. Classification on the upper roadway was done only by direction of travel, either before the period of measurement or after it, generally within 2 hr of the

measurement. Although this time displacement for the upper roadway results in only an approximate classification during measurement, traffic from this roadway is shielded from the receptors by the edge of structure. It does not dominate the noise.

Speeds were measured on the lower roadway and the near frontage road by timing a sample of heavy trucks between two fixed points. The average of these sampled speeds was used for computation.

Volumes and speeds on the far frontage road were taken to be identical to those measured on the near frontage road. All barrier calculations were done separately by lane and separately by the three vehicle types: automobiles (all four-tire vehicles), medium trucks (all six-tire vehicles), and heavy trucks (all vehicles with more than six tires). For these barrier calculations, all traffic on the two elevated structures was positioned in the lane nearest the receptor.

The noise calculations were kept separate by lane and by vehicle type for each 10-min period. Before combining them into the total 10-min noise level, the heavy-truck contributions on the lower roadway were adjusted to account for the level difference between the national average emission (ignoring grade) built into the FHWA method and the measured emission levels during the measurement period.

First, the overhead reference levels were converted to sideline emission levels at 50 ft by using the following equation:

$$L_{REF} - L_{EL} = 10 \log(2.133 - 0.05933X + 0.0005371X^2) \quad (14)$$

where X is the horizontal distance between the reference microphone and the centerline of the lane of travel, as before. Then emission levels of all the heavy trucks that passed during the 10-min period were energy-averaged to obtain the average emission level for that measurement period.

A total of 329 heavy trucks were measured over the total of 21, 10-min verification periods, for an average of 16 trucks per period. Note that this number of trucks is not a small sample; it is all the heavy trucks that passed during the measurement periods and comprises the full population of trucks that should be used for emission level adjustment. The heavy-truck emission level adjustments, relative to the national average emission levels, ranged between -7 and +2 dB, averaging -2.1 dB.

Another complication enters here. The overhead reference levels for these trucks were measured at the closest cross-street bridge that passed over the lower roadway. For verification of Site 1 data, which was identical to a diagnostic site, this closest bridge was immediately adjacent, where the lower roadway was fully depressed. For the other two verification sites, however, the nearest cross-street bridge was a distance from the measurement site.

Of most importance here is that the overhead measurement occurred where the trucks were in a depressed section, whereas for the verification the sideline measurement occurred where they were at grade. It is possible that truck drivers use different amounts of throttle for these two different positions along their travel, and it is possible that this throttle change introduces a bias in the computation method.

To check for such a bias and to compensate for it if found, the sideline noise of 51 heavy trucks was measured along I-35 in San Antonio at a location where the cross section alternated between depressed and at grade (similar to Austin). Distinction was made between trucks passing in the two different

directions. For these trucks in San Antonio, the differences in emission levels were

Direction 1: $L_{\text{depressed}} - L_{\text{up-grade}} = 0.3$ dB,
 Direction 2: $L_{\text{depressed}} - L_{\text{up-grade}} = -0.8$ dB, and
 Full average: $L_{\text{depressed}} - L_{\text{up-grade}} = 0.2$ dB.

Within experimental error, this small level difference is not significantly different from zero. Therefore, no adjustment was made to account for the fact that the overhead measurements were not made immediately adjacent to the sideline measurements for verification Sites 2 and 3.

After emission level adjustments were made for all lower-roadway heavy trucks, the contributions from all vehicles on the lower roadway and frontage roads were increased by reflection from the underside of the structure. In total,

$$10^{L_T/10} = 10^{L_R/10} + 10^{L_D/10} \times 10^{-A/10} \quad (15)$$

where A equals the barrier attenuation for this particular lane, vehicle, and receptor combination. Note that L_D is the direct contribution without barrier attenuation. Next,

$$10^{L_R/10} = 10^{L_D/10} (D_D/D_R)^1 F \quad (16)$$

where the distance ratio is taken to the power of unity because the L diverges as a line source. The fraction F is the fraction of energy lost on reflection from the upper surface:

$$F = 0.1469a_{\text{inc}} - 0.001697a_{\text{inc}}^2 + 0.03225a_{\text{scat}} - 3.0709 \quad (17)$$

from the scattering measurements at diagnostic Site 2. Next, the amplification due to reflection is

$$\text{Amp} = L_T - (L_D - A) \quad (18)$$

In total,

$$\text{Amp} = 10 \log \{ [0.1469a_{\text{inc}} - 0.001697a_{\text{inc}}^2 + 0.03225a_{\text{scat}} - 3.0709] (D_D/D_R) + 10^{-A/10} \} + A \quad (19)$$

This equation was used to compute the overhead amplification separately for each lane, vehicle, and receptor combination for a total of 55 amplification computations.

Finally, once these two adjustments were made (emission level and amplification), the contributions from all lanes were summed to the total 10-min L_{eq} .

Results

On average, the predictions agree with measurements within 1 dB, which is better than could generally be hoped. For closeby receptor positions, predictions fall below measurements by 3 to 5 dB; in other words, the predictions are too low. There exists the possibility that the predicted amplification from the structure is too low. This is most likely not the case, however, because the amplification was measured precisely during the diagnostic measurements, which are far more controlled than are these verification measurements. In addition, the verification predictions have many possible sources of bias not connected with the upper structure. Perhaps

the FHWA method under-predicts the noise from the frontage road traffic, which is generally stop-and-go traffic. According to the computations, this frontage road traffic was a significant contributor to the total noise level, especially for the closeby receptor positions, basically because it is so close.

For receptor positions that are farther out, predictions are greater than measurement by 1 to 7 dB; that is, predictions are too high. This is most likely due to shielding, in plan, which intervenes between the receptors and the traffic lanes, both to the right and to the left of the closest point of approach. This shielding was not taken into account in the computations. In addition, the over-prediction could result partly from the assumption of hard ground between source and receptors ($\alpha = 0$ in the FHWA method). This hard-ground assumption is more nearly true, on average, than it would be for the soft-ground assumption because of the street or driveway down which the receptor line was placed, but a significant amount of the intervening ground was grass.

In summary, the verification measurements do not dispute the results obtained from the diagnostic measurements. For this reason, they lead to no changes in the conclusions of the study. The verification measurements are shown in Figure 13.

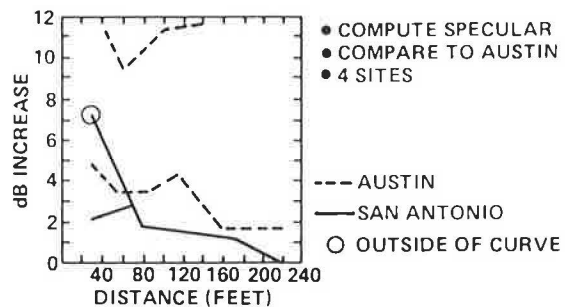


FIGURE 13 Summary of Austin verification measurements.

SAN ANTONIO COMPUTATIONS

Four typical sites were chosen for analysis in San Antonio: depressed, vertical retaining walls; depressed, grassed slopes; flat; and 10-lane elevated. At these cross sections the noise from all vehicles on the lower roadway was computed, assuming specular reflection from above.

These calculations were made with the official FHWA highway noise traffic prediction model embodied in its programmable-calculator form. Therefore, they all assume infinite roadway and infinitely long barriers. Source height assumptions were zero height for automobiles, 2.8 ft for medium trucks, and 8 ft for heavy trucks. These source heights are important to barrier calculations.

Calculations were made for every travel lane and for the three vehicle types at every receptor location. Receptor locations were chosen to be at the closest building lines and 5 ft above the local terrain. At the fourth site an additional receptor location was placed 15 ft above the local terrain to account for noise entering the second story at this site.

In Figure 14 the results are condensed as a function of distance from the edge of the structure, where they are compared with the Austin results. At 30 ft the two sides of the roadway differ appreciably, as shown in the figure.

In conclusion, the noise in San Antonio increases

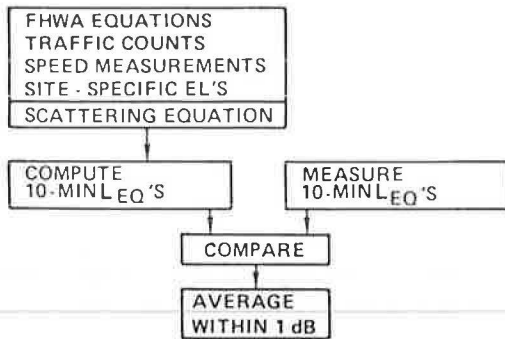


FIGURE 14 Predicted San Antonio amplification compared with Austin measurements.

to the side due to overhead reflections, and it should be less than that measured in Austin, except when both of the following occur: (a) the receptor is within 50 to 60 ft of the edge of the elevated structure, and (b) the upper roadway curves away from the receptor. When the upper roadway curves away from the receptor, its tilted undersurface

tends to aim energy toward the receptor, thereby increasing the noise. The San Antonio values of 2 and 7 dB on the graph occurred at such a roadway curve, on opposite sides of the roadway.

The particular 10-lane elevated section chosen for study in San Antonio is unique. It occurs where the frontage road runs underneath the upper roadway. For most of the 10-lane elevated section there is no roadway underneath to be amplified. For this calculated cross section, where the frontage road is underneath, the upper roadway increases frontage roadway noise to the side by approximately 3 to 4 dB.

REFERENCE

1. Highway Traffic Noise Prediction Model. Report FHWA-RD-77-108. FHWA, U.S. Department of Transportation, Dec. 1978.

Publication of this paper sponsored by Committee on Transportation-Related Noise and Vibration.

Evaluation of T-Profile Highway Noise Barriers

J. J. HAJEK and C. T. BLANEY

ABSTRACT

An acoustical performance evaluation of unique 5-m-high sound-absorbing parallel highway noise barriers, with a horizontal cap to form a T-profile, is presented. The evaluation was done by using (a) direct field measurements, (b) analytical procedures based on the STAMINA 2.0 computer program and the application of geometrical acoustics, and (c) acoustical scale modeling. Noise measurements in the residential area behind the barriers indicated that the addition of a 1-m-wide horizontal cap on top of the barrier had increased its insertion loss by about 1 dB(A). Similar results were obtained by acoustical scale modeling, which also indicated that it is usually acoustically more effective to increase the barrier height rather than to build a T-top.

The objective of this paper is to present the results of an acoustical evaluation of unique parallel highway noise barriers constructed in 1983. The barriers have sound-absorptive layers on both the highway and the residential sides. A 1-m-wide sound-

absorptive cap is mounted horizontally on top to create a T-profile.

The evaluation has been conducted by using direct field measurements, analytical calculations, and acoustical scale modeling. The latter two methods were used to establish their accuracy in relation to the field measurements and to evaluate various design parameters, such as the T-top shape and absorptive treatment of barrier walls, which could not be evaluated effectively in the field.

The barriers are located along both sides of the Queen Elizabeth Way (QEW), east of Cawthra Road in Mississauga, Ontario. At this location the QEW has six traffic lanes, three in each direction, and the barriers are about 36 m apart. On both sides of the QEW there are two-lane service roads. The terrain is flat, gently sloping toward the south (Lake Ontario). Figure 1 shows the general barrier setting, together with the location of T-top and conventional barriers, and the measurement locations used for evaluation.

The photographs in Figures 2 and 3 have been included to illustrate the appearance and aesthetics of T-top barriers. Although opinions in these matters can certainly differ, the addition of the horizontal cap does not appear to degrade the appearance of a conventional type barrier.

Construction of noise barriers at this site had been anticipated during highway construction in 1977. Thus 0.8- to 1.2-m-high New Jersey (NJ) type

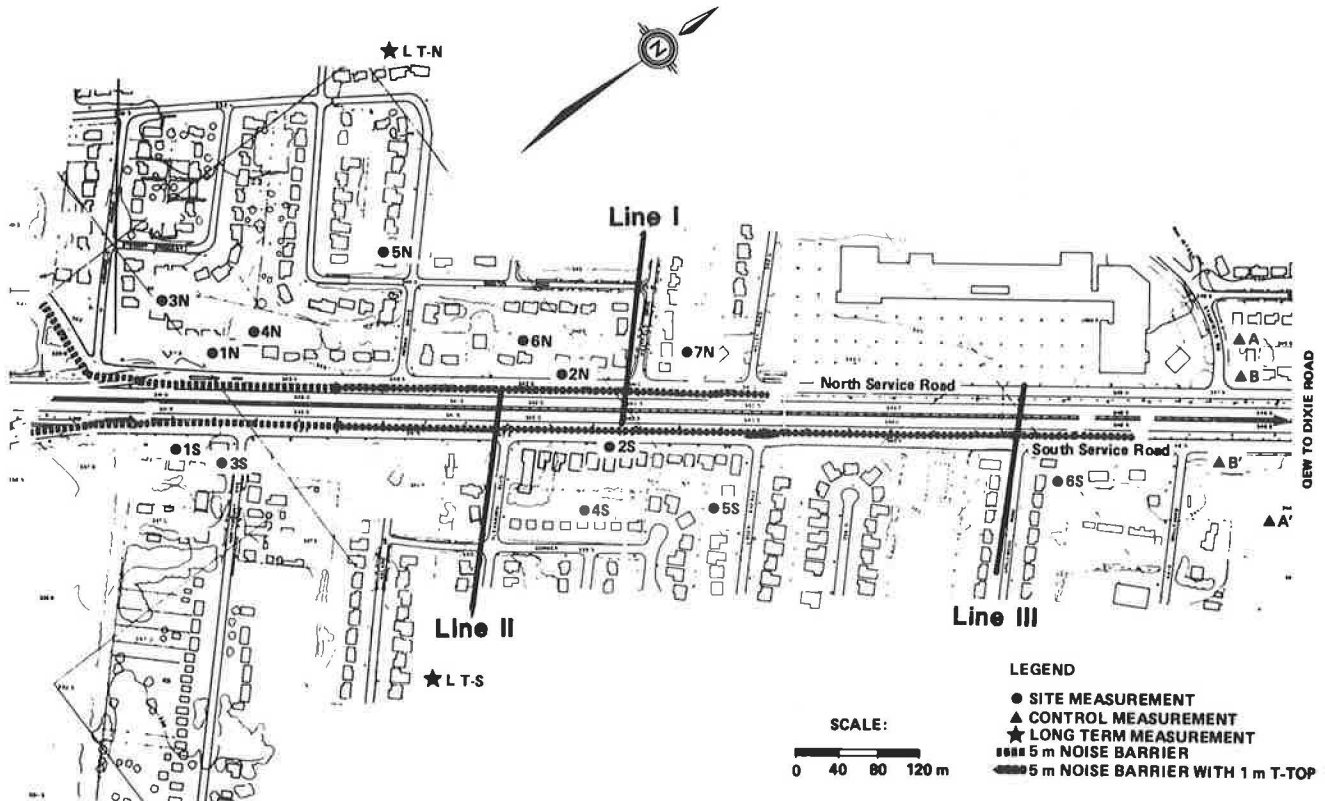


FIGURE 1 QEW, Cawthra to Dixie roads, general setting.



FIGURE 2 Site overview from the pedestrian overpass (North Service Road is on the right).



FIGURE 3 View from the residential side showing T-top and conventional barriers.

walls, which would separate the QEW from the service roads, were designed to serve also as a foundation for noise barriers (Figure 4). Because of the foundation design, the height of possible noise barriers was limited by wind load considerations to 4 m above the NJ walls (i.e., to about 5 m above the pavement elevation). This height restriction placed a limit on performance of the noise barrier (1).

The need for higher insertion loss (than that predicted for 4-m-high barriers mounted on top of NJ walls) without exceeding the total barrier height of 5 m was the main reason why T-top experimental barriers were constructed at this site. Research and development considerations, such as the effect of barrier shape and community acceptance, also contributed to the decision.

PREVIOUS EXPERIENCE

May and Osman (2) conducted a comprehensive acoustical scale-modeling study on different barrier shapes and reported a 3 dB(A) increase in the bar-

rier insertion loss with a 1-m increase in the width of the horizontal cap. This rate compared well with the insertion loss growth rate of about 2 dB(A) per 1-m increase in the height of a conventional barrier found for the same test situation. The study also recommended an absorptive treatment of the horizontal cap on the upper surface.

Although it appears that the present application is the first actual installation of a T-top barrier, two previous full-scale experiments were found. In a report evaluating the Doublewal noise barrier (3,p.27), it was noted that there was no discernible difference in the barrier insertion loss if the barrier was fitted with a 1.5- or 2.4-m-wide T-top. (The thickness of the basic Doublewal unit was about 1.2 m.) On the other hand, it was reported that temporary addition of a 0.75-m-wide horizontal cap, 2 cm thick, to an existing 4-m-high noise barrier had increased its insertion loss by about 1 to 1.5 dB(A) (4).

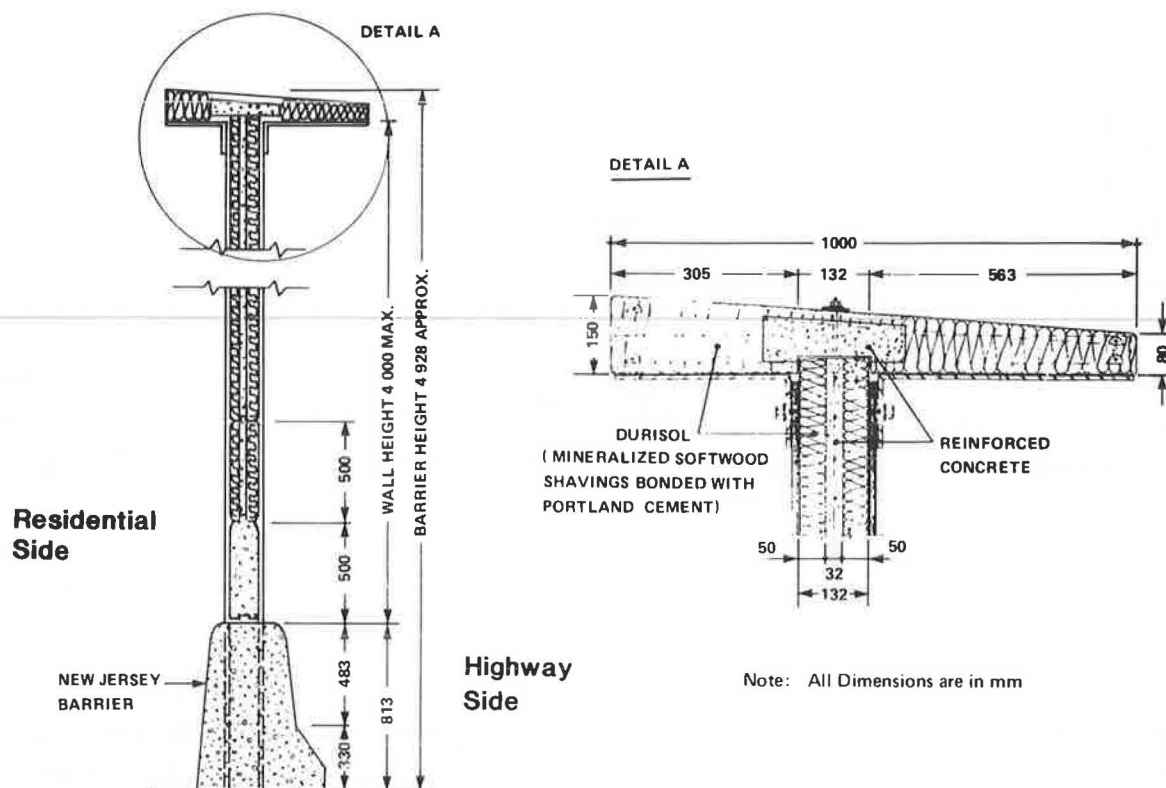


FIGURE 4 Construction details of T-profile noise barrier mounted on NJ wall.

BARRIER DESIGN AND CONSTRUCTION

The design and construction of the Cawthra Road barriers were based on a study by Hajek et al. (1), which recommended a sound-absorptive treatment on the barrier side facing the highway (freeway side) as well as on the side facing the service roads (residential side). The recommendation for the sound-absorptive treatment on the freeway sides was based on the evaluation of multiple reflections caused by parallel barriers, according to a procedure outlined elsewhere (1,5).

The recommendation for a sound-absorptive treatment on the residential side was based on sound levels emitted by traffic on service roads that cannot be attenuated by noise barriers. A 12-hr traffic classification survey, conducted in April 1981, indicated that traffic on the service road was relatively high. Depending on time, the South Service Road traffic volumes represented about 15 to 28 percent of the eastbound QEW traffic, and the North Service Road traffic volumes represented about 12 to 18 percent of the westbound QEW traffic (1). It was feared that if the barriers were sound reflecting on the residential side, they would reflect sound from the service road traffic to the community behind the barrier and amplify it by as much as 3 dB(A).

A typical barrier construction detail, showing the T-top, is shown in Figure 4. Sound-absorptive treatment consisted of a Durisol building material, which is described as a lightweight material (density of about 560 kg/m³) made of chemically mineralized and neutralized softwood shavings bounded together under pressure with portland cement. It is an open-textured material with a noise reduction coefficient (NRC) of about 0.60 for 5-cm thickness when mounted against a rigid backing. The structural support for Durisol was provided by a steel-reinforced concrete core. The complete panels are 3 m

long, 0.5 m high, and 0.132 m thick. The panels are interlocking with tongue-and-groove joints, and the joints between the panels and steel posts are sealed with a rubberized compound. The first panel on top of the NJ walls was an all-concrete panel.

FIELD EVALUATION

The acoustical performance of the barriers was assessed by comparing sound levels measured before the barrier construction with the sound levels measured (a) after the erection of sound-absorptive vertical barriers and (b) after the addition of the horizontal cap. The before-and-after measurements were done on identical locations in the residential community behind the barriers and during similar times of the day.

The measured barrier insertion loss was normalized to remove the effects of source strength and other variations as described in previous studies by the Ontario Ministry of Transportation and Communications (MTC) (4,6), where sound levels were measured behind the barrier and, simultaneously, at a control measurement location unaffected by barrier construction, both before and after barrier erection. In this study the procedure was slightly modified in that two control locations, rather than one, were used to indicate any changes that may occur between the measurements. The first control measurement location was close to the highway (about 40 m from the centerline, 4 m aboveground) and was intended to account mainly for the source strength (traffic) variation. The second control location was farther from the highway (about 90 m from the centerline, 1.2 m aboveground) and was intended to account, in addition to the source strength variation, for weather-related factors (e.g., wind and temperature gradients, wind speed) and ground condi-

tions that were not fully accounted for by the control measurement placed close to the highway. Two control measurements were used on each highway side, as shown in Figure 1.

Altogether four types of acoustical field evaluations were conducted in the area behind the barriers, as described in the following sections.

Measurements at Single Location Sites

At the single location sites, shown in Figure 1, measurements were done in two measurement series: before barrier construction and after the completion of the barrier, including the T-top. The data in Table 1 summarize the measurement results as well as the predicted results described later. Overall, the barrier insertion loss was rather limited; the first row housing receivers attaining about 5 dB(A), and the more distant ones from about 2 to 4 dB(A).

Measurement Lines

The (three) measurement lines (shown in Figure 1) served as the main evaluating tool. The sound level measurements at these lines were done before barrier construction and then at several construction stages (e.g., after barrier construction to a height of 3 m, after its extension to 5 m, and after the T-top was in place). At each stage the measurements were repeated at least two times on different days and were of 20 min duration. Figures 5-7 show average measured results before the barrier construction and after construction of the 5-m barrier without the T-top. The reason why the T-top results are not shown are rather insignificant changes in levels due

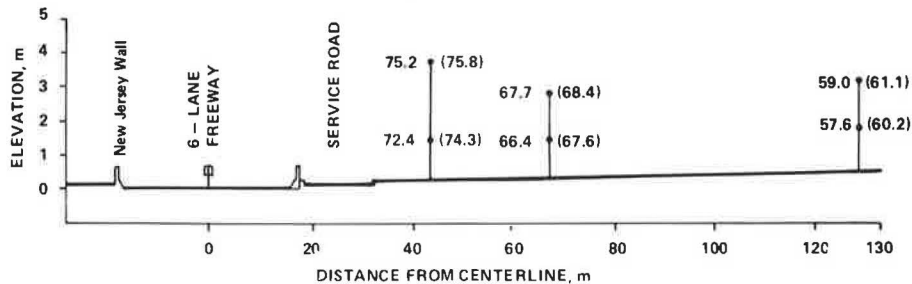
TABLE 1 Comparison of Measured and Predicted Sound Levels

Measurement Location ^a	Sound Levels Before Barrier, L_{eq} [dB(A)]		Barrier Insertion Loss, ΔL_{eq} [dB(A)]	
	Measured	Predicted	Measured ^b	Predicted ^c
Part A: Locations not Shielded by Houses				
1N	74.0	74.7	4.3	5.3
2N	75.4	75.9	5.1	5.7
1S	73.4	74.4	4.4	4.7
2S	74.3	74.5	4.7	5.3
Avg	74.3	74.9	4.6	5.3
Part B: Locations Shielded by One or More Rows of Houses				
3N	62.3	64.4	2.2	2.4
4N	64.9	66.0	3.3	4.1
5N	58.6	59.4	3.5	1.4
6N	62.0	63.7	4.3	4.4
7N	66.1	67.7	4.5	3.2
3S	64.0	66.0	4.7	4.1
4S	60.3	63.1	2.9	2.2
5S	58.6	61.0	4.0	2.7
6S	66.0	67.4	3.7	5.8
Avg	62.5	64.3	3.7	3.4
Part C: Control Measurement Locations				
A	68.2	67.1		
B	77.2	76.5		
A ¹	65.6	66.1		
B ¹	76.3	76.4		
Avg	71.8	71.5		

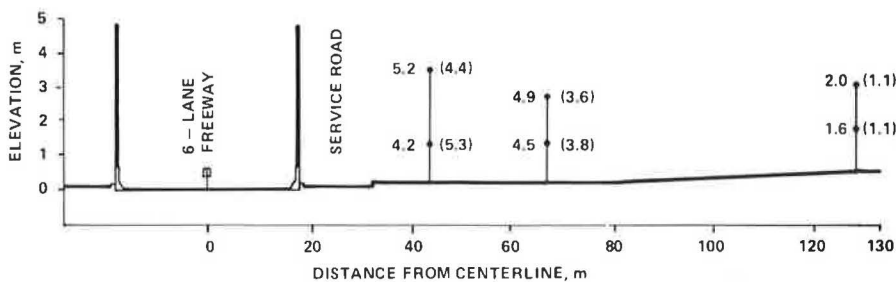
^aMeasurement locations are shown in Figure 1. All measurements were taken 1.2 m aboveground and were of 20-min duration.

^bMeasured insertion losses have been adjusted for traffic and other variations by using control measurements. The insertion loss measurements were done after the construction of the T-top.

^cThe effect of the T-top was not included in the calculations.



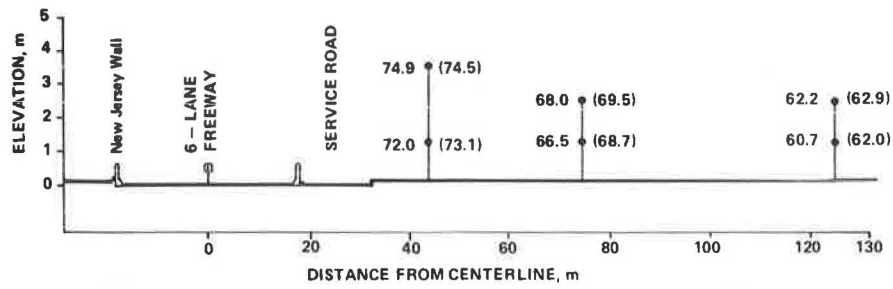
a) Average Sound Levels Measured (and Predicted) Before Barrier Construction, L_{eq}
Includes New Jersey Walls



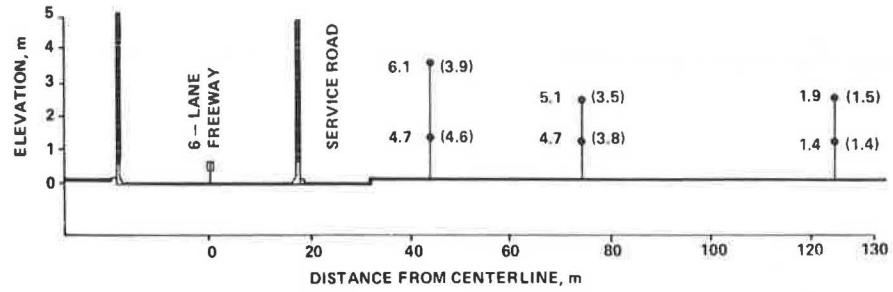
b) Average Insertion Loss Measured (and Predicted) After Barrier Construction, L_{eq}
Includes New Jersey Walls and Barriers

LEGEND 75.2 Measured Level
 (75.8) Calculated Level
 ● Microphone Location

FIGURE 5 Comparison of measured and predicted sound levels, Line I.



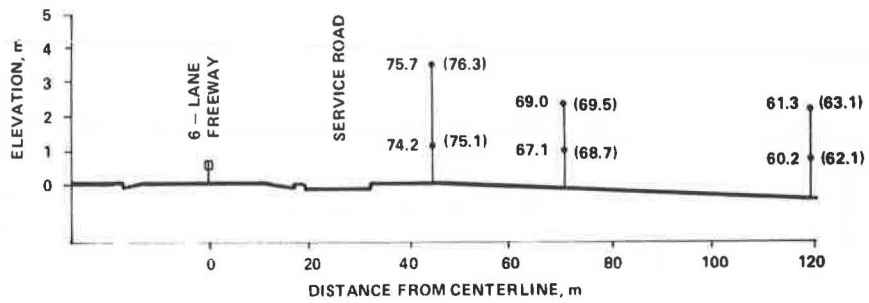
a) Average Sound Levels Measured (and Predicted) Before Barrier Construction, L_{eq}
Includes New Jersey Walls



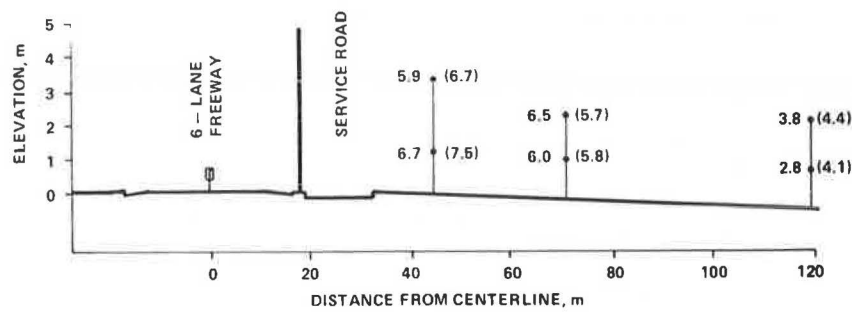
b) Average Insertion Loss Measured (and Predicted) After Barrier Construction, L_{eq}
Includes New Jersey Walls and Barriers

LEGEND 74.9 Measured Level
 (74.5) Calculated Level
 ● Microphone Location

FIGURE 6 Comparison of measured and predicted sound levels, Line II.



a) Average Sound Levels Measured (and Predicted) Before Barrier Construction, L_{eq}



b) Average Insertion Loss Measured (and Predicted) After Barrier Construction, L_{eq}

LEGEND 75.7 Measured Level
 (76.3) Calculated Level
 ● Microphone Location

FIGURE 7 Comparison of measured and predicted sound levels, Line III.

to the T-top. This, together with the calculated results also shown in the figures, are discussed later.

Direct Comparison of Conventional and T-Top Barriers

A direct comparison of the conventional versus T-top barriers was done at the western end of the site where these two barrier types were constructed side-by-side (Figure 1). Measurements were done by using, simultaneously, four type 1 sound level meters (7), two located behind the conventional barrier at various distances and heights aboveground, and the other two located behind the T-top barrier at the same distances and heights as their conventional barrier counterparts. Because all variables at the two measurement sites were the same (e.g., traffic, weather-related variables, height of the barrier not including the thickness of the horizontal cap, distance behind the barrier), with the exception of the T-top, the differences between the two sets of measurements were attributed to the influence of the T-top only.

Based on extensive measurements, the contribution of the T-top was rather limited and amounted to only about 1 dB(A) if the effect of service road traffic was eliminated during the measurements. The contribution was less than 1 dB(A) if the traffic on service roads was included. A similar limited influence of the T-top was measured at the measurement lines.

Long-Term Monitoring

In order to evaluate long-term changes in sound levels associated with the construction of parallel barriers, a separate measurement procedure was con-

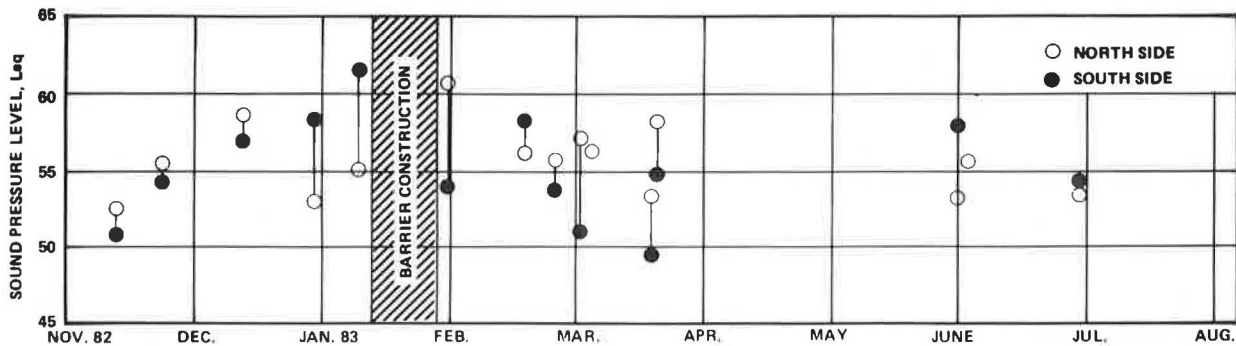
ducted. Also, the MTC has received a number of complaints from residents (often living several hundred meters behind highway noise barriers) that noise has actually increased after barrier construction.

Two locations, approximately 350 m from the highway centerline, were selected, one on each side of the highway (see Figure 1). At these locations five 24-hr sound level measurements were conducted before barrier construction and eight to ten 24-hr measurements were conducted after construction. The results, summarized in Figure 8, show a considerable day-to-day variation in sound levels. No statistically significant difference between the before-and-after sound levels, or between the north side and south side sound levels (Figure 8a), was obtained. The influence of weather-related variables on the measured sound levels was studied, but it was difficult to quantify because of the transient nature of these variables. The nighttime sound levels were about 6 dB(A) lower than the daytime levels (Figure 8b) both before and after barrier construction.

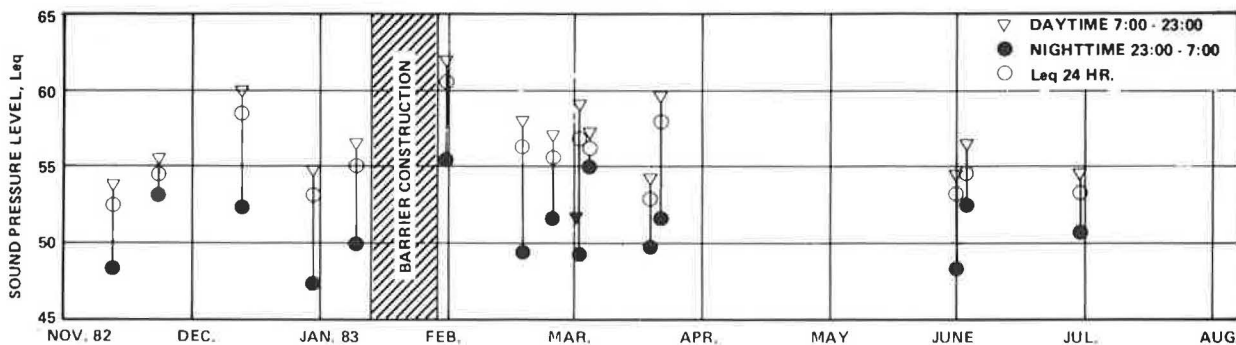
ANALYTICAL EVALUATION

In addition to the field measurements, the barriers were also evaluated analytically by using the STAMINA 2.0 computer program (8). To account for the effect of multiple reflections off parallel barrier walls, a number of image roadways were constructed by using principles of geometrical acoustics and were included in the program input. The procedure is explained elsewhere (9). Alternatively, the calculations can be performed more easily by using a computer program developed by Bowlby and Cohn (10).

The reasons for the analytical evaluation of the completed barriers were three-fold:



(a) 24 Hour Leq, North and South Sides



(b) Daytime and Nighttime Leq, North Side

FIGURE 8 Long-term (24-hr) measurements at distant locations (approximately 350 m from centerline) before and after barrier construction.

1. To verify the accuracy of the prediction procedure and its applicability to a parallel barrier situation with barrier surfaces partly sound absorbing,

2. To quantify the effectiveness of the sound-absorptive treatment used at this site, and

3. To evaluate the effectiveness of alternative designs that may be required for different barrier sites.

The measured and predicted results are compared in Table 1 and in Figures 5-7. In general, there was satisfactory agreement between the measured and predicted sound levels and insertion losses. This reflects well on both the STAMINA 2.0 program and on the procedure used to account for the parallel barrier situation. However, sound levels at locations shielded by one or more rows of houses were consistently over-predicted by about 1 or 2 dB(A). This may be attributed to rather subjective selection of housing shielding factors or to the prediction procedure. At any rate, it appears that the overall accuracy of the predictions is adequate and that the prediction methodology can be used with confidence for alternative designs.

The predicted insertion losses for the existing and alternative barrier designs are given in Table 2 for three typical receiver types:

1. Receivers unshielded by houses (front yard receivers),
2. Receivers shielded by one row of houses (receivers in the back yards of the first housing row), and
3. Receivers shielded by two or more rows of houses.

Row 3 in Table 2 indicates that the predicted insertion loss provided by NJ walls alone ranges from 0.2 to 0.7 dB(A). It should be stressed that the measured results, reported in Table 1 and in Figures 5 and 6, indicate only the insertion losses caused by the erection of the noise barriers on top of the NJ walls. The total insertion loss, including that predicted for the NJ walls, is thus 0.2 to 0.7 dB(A) higher.

Based on the predicted data given in row 4 of Table 2, the insertion loss of the existing barriers would have been reduced by 1.1 to 2.6 dB(A) if sound-reflecting barriers (NRC = 0.05) were built instead. If the barriers were fully sound absorptive (NRC = 1.00), the insertion loss of the existing barriers (NRC = 0.60) would have been increased by 1.7 to 3.4 dB(A) (row 5, Table 2). It may be noted that the additional insertion loss from the absorp-

tive treatment increases with the distance from the barrier. For example, the additional insertion loss for the north-side receivers is 1.7 dB(A) for unshielded receivers, and increases to 3.4 dB(A) for receivers shielded by two or three rows of houses.

The last row in Table 2 indicates that the existing absorptive treatment on the residential side had only a limited effect. The reason is that the first 1.5 m of the barrier structures are made of concrete (NJ wall plus the first barrier panel) and are sound reflecting. Based on the principles of geometrical acoustics and considering receivers close to the ground, the sound-absorptive treatment above the height of 1.5 m is beneficial only for noise emitted by heavy trucks. The absorptive treatment on the residential side should have extended as low to the ground as possible, but it did not have to reach to the top of the barrier. Because the degradation effect of multiple reflections between the barriers exceeds that of a single reflection off the residential side, and because of the different reflection geometries involved, the amount and the placement of the absorptive treatment on the two barrier sides should be optimized to achieve maximum acoustical effectiveness at the lowest cost.

SCALE-MODELING EVALUATION

In addition to the field and analytical evaluations, a congruent acoustical scale-modeling study was conducted at the MTC scale-modeling facility. The equipment and materials used were described by Osman (11,12) and have been used extensively (4,13). The use of scale modeling provides a rapid and inexpensive way to evaluate a number of alternative designs and situations (e.g., T-profile dimensions and materials, and the source, barrier, and receiver geometry) that would be impractical or impossible to evaluate in any other way. The objective of the scale-modeling study was to verify the accuracy of scale modeling and to determine optimal design parameters of T-profile barriers.

A 1:16 scale model was used for both spatial variables and the A-weighted traffic noise spectra. However, all dimensions quoted in the following paragraphs are full-scale equivalents. The sound-absorptive properties of the model materials (such as grassland, barrier surfaces, and pavements) were tested to ensure that they appropriately modeled the actual materials on the 1:16 scale. The acoustical hardware consisted of a high voltage spark as a noise source, a 0.125-in. microphone, filtering and processing instrumentation, and an oscilloscope.

TABLE 2 Insertion Loss Prediction for Different Barrier Alternatives

Row	Alternative Barrier Arrangement	Receivers Unshielded by Houses (front yard)		Receivers Shielded by One Row of Houses		Receivers Shielded by Two or Three Rows of Houses	
		North Side	South Side	North Side	South Side	North Side	South Side
1	Insertion loss of existing barriers, including insertion loss provided by NJ walls	6.1	5.7	4.0	3.5	1.4	1.6
2	Insertion loss of existing barriers, not including insertion loss provided by NJ walls	5.5	5.0	3.5	3.1	1.2	1.4
3	Insertion loss provided by NJ walls alone	0.6	0.7	0.5	0.4	0.2	0.2
4	Reduction in insertion loss of existing barriers if sound-reflecting barriers on both sides (NRC = 0.05) were built instead	1.2	1.1	1.9	1.4	2.6	1.5
5	Increase in insertion loss for existing barriers if fully sound-absorptive barriers (NRC = 1.00) were built on both sides instead	1.7	2.7	2.6	3.4	3.4	3.4
6	Reduction in insertion loss for existing barriers if the residential sides only were changed to be sound reflecting (NRC = 0.05)	0.1	0.1	0.1	0.1	0.1	0.1

Note: Results are averaged over a number of points (site measurement points and line measurements, see Figure 1). All locations were 1.2 m aboveground behind the parallel barrier corridor. Calculation assumes a conventional barrier (no T-top). NRC = noise reduction coefficient.

The source, barrier, and receiver geometry used, shown in the lower portions of Figures 9 and 10, was selected to model the Cawthra Road site. For simplicity, the majority of tests were done by using a point source only. Some of the single-point source tests were repeated by using an incoherent line source, created by moving a point source at small intervals along a line. The results indicated that although the absolute insertion loss values were smaller for the incoherent line source, the point source was sufficient to indicate the relative performance of different barrier shapes. Consequently, only the point-source results are reported here.

A number of different horizontal caps, mounted on top of 4- to 5-m-high conventional barriers, were evaluated. The T-tops differed in width (from 1 to 2 m), thickness (from 3 to 25 cm), shape (sharp-edged and rounded), their position relative to the barrier center (larger or smaller overhang toward the source), and material (reflective, $NRC = 0.05$; absorptive, $NRC = 0.75$). However, with the exception of the T-top width, these variables, within the ranges defined, had a small, hardly measurable influence on the insertion loss.

The addition of a 1-m-wide T-top to a 5-m-high barrier increased the insertion loss (e.g., 40 m behind the barrier, 1.2 m aboveground) by about 1 dB(A) (Figure 9). This is the same increase measured in the field. The addition of a 2-m-wide T-top to the identical barrier increased its insertion loss by about 2 dB(A) (Figure 10). A similar 2 dB(A) increase was obtained by increasing the barrier height by 2 m.

T-Top Versus Increased Barrier Height

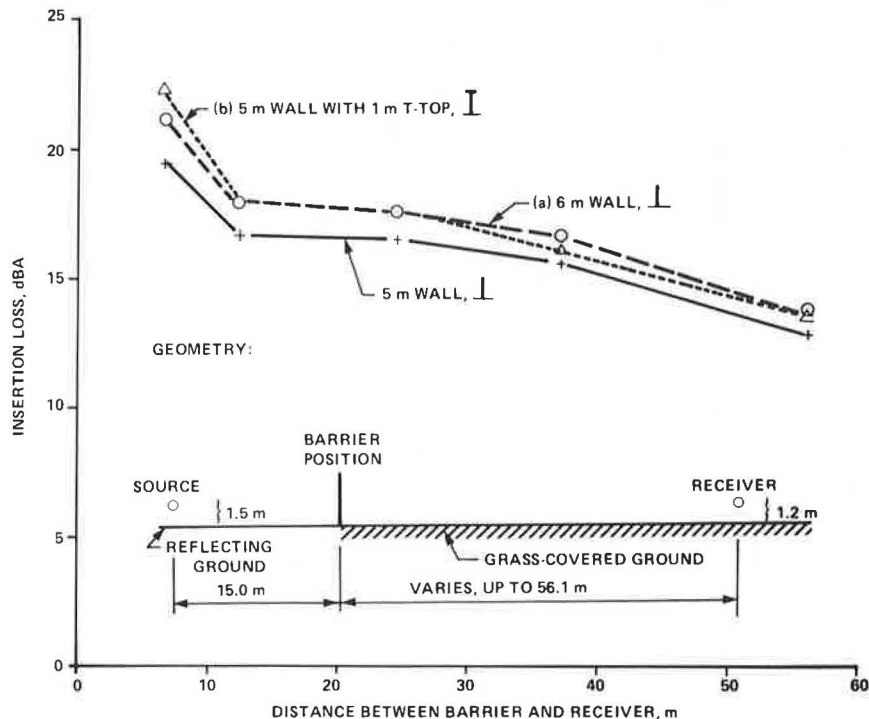
The insertion loss of barriers with the T-top is also compared in Figures 9 and 10 with that of barriers that have increased heights equal to the T-top

width (vertical cap). According to these figures, at short distances behind the barrier (10 to 20 m), the T-top provides a higher insertion loss than its vertical cap counterpart. At larger distances behind the barrier (30 to 40 m), the vertical cap provides a somewhat larger insertion loss. These results apply only for the source, barrier, and receiver geometry shown in Figures 9 and 10.

A more extensive comparison of horizontal and vertical barrier extensions, covering many receiver positions, is shown in Figure 11 by means of isodecibel lines or, in regions where isodecibel lines were difficult to define, by single measurement points. According to Figure 11a, the addition of the T-top provides the greatest insertion loss increase for receivers just behind the barrier, close to the ground. The addition to the barrier height (Figure 11b) is most effective for receivers also close behind the barrier, but higher above the ground. Figure 11c shows that the 1-m vertical addition provides higher insertion loss than the 1-m T-top for all receivers more than about 20 m behind the barrier. Only at distances less than 10 m behind the barrier is the T-top addition better than the vertical one. It appears that given a choice and the same amount of material, it is acoustically more effective to increase barrier height rather than to build a T-top.

Discussion of Results

The beneficial effect of T-profile was theorized by May and Osman to be "due to the limited opportunity for pressure doubling to occur at the point that the incident wave impinges on this barrier at the end of the T" (4). Incidentally, this was the main reason why the T-top was positioned to overhang more on the freeway side (main source side) than on the residen-



Note: The horizontal top overhang on the source side is about twice that on the receiver side. Results are obtained by acoustical scale modeling.

FIGURE 9 Change in insertion loss of 5-m-high barrier due to (a) increase in barrier height by 1 m and (b) addition of 1-m-wide horizontal T-top.

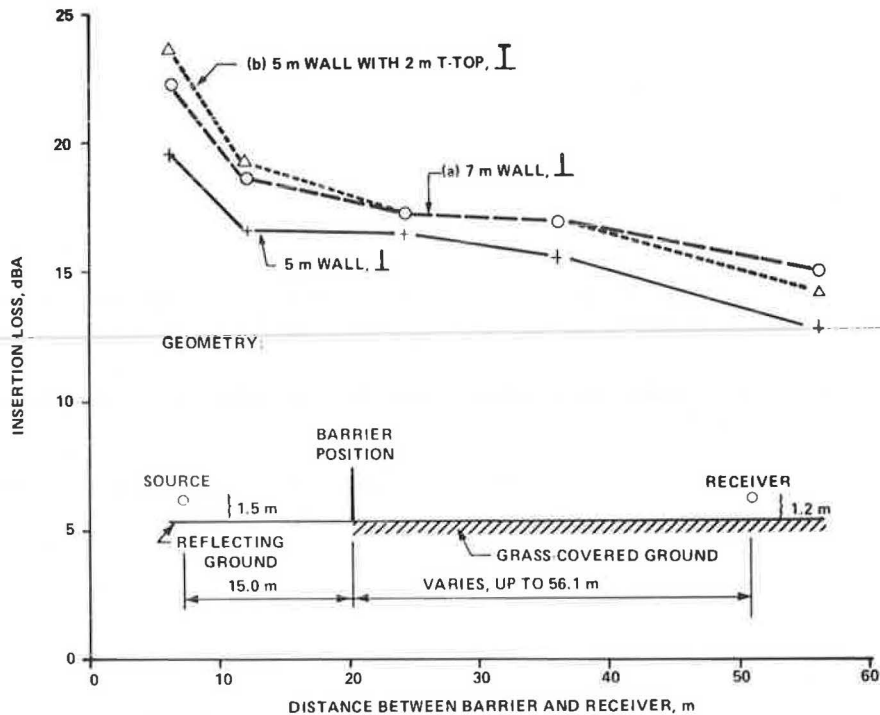


FIGURE 10 Change in insertion loss of 5-m-high barrier due to (a) increase in barrier height by 2 m and (b) addition of 2-m-wide horizontal T-top.

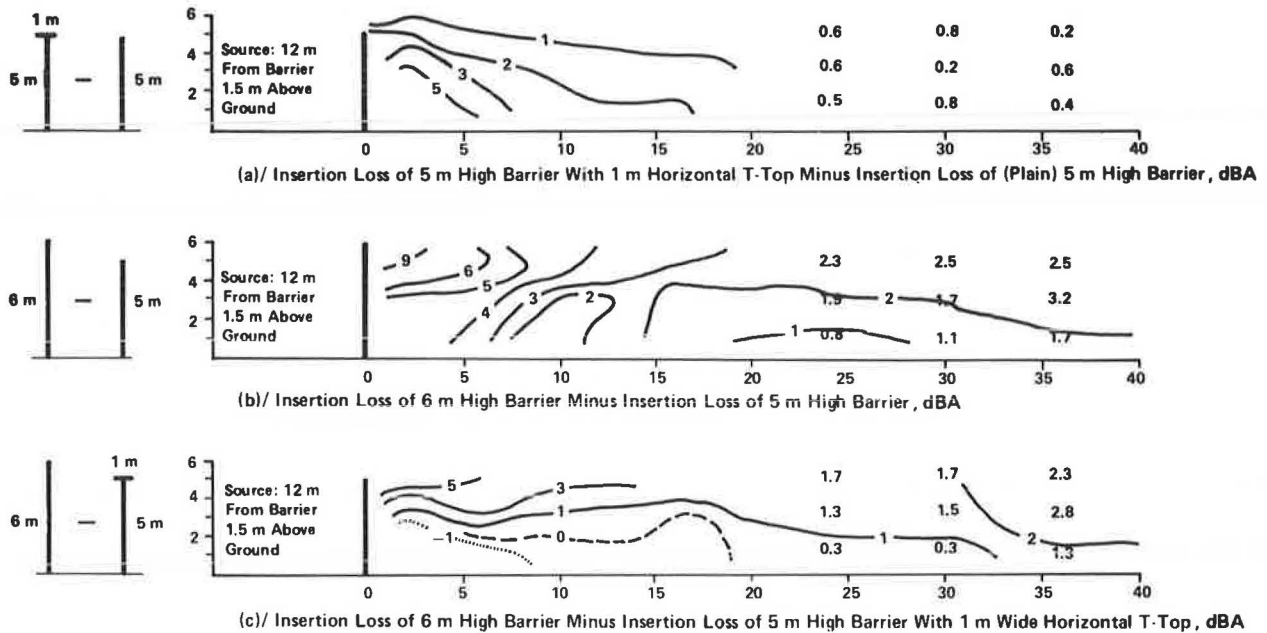


FIGURE 11 Comparison of insertion losses (obtained by scale model measurements) for 5-m-high barrier, with and without 1-m-wide horizontal T-top and 6-m-high barrier.

tial side (Figure 4). Even though the T-top has not produced the expected results [as based on data by Mays and Osman (4)], the increase in the insertion loss due to the T-top was still somewhat larger than that predicted for the change in the path-length difference alone. This additional increase may be

attributed to the pressure doubling effect previously described or to the effect of double diffraction or, perhaps, to other causes. At any rate, when the effect of the T-top is compounded with other effects of outdoor sound propagation, such as refraction and scattering in the atmosphere, it

appears that only limited acoustical benefits can be expected from sophisticated barrier shape designs similar to the T-top.

CONCLUSIONS AND RECOMMENDATIONS

1. Based on noise measurements in the residential area behind the barrier, the addition of a 1-m-wide T-top to a 5-m-high barrier has increased the barrier insertion loss by about 1 dB(A). Similar results were obtained by using acoustical scale modeling.

2. To increase barrier insertion loss, it is usually more effective to increase barrier height by a certain amount rather than to add a T-top of the same size.

3. Good agreement was obtained between measured and calculated sound levels. This tends to verify the applicability of the prediction procedure, based on the STAMINA 2.0 computer program and the application of geometrical acoustics, for parallel barrier calculations.

4. Based on calculations, the sound-absorptive treatment on the residential side provides only a limited benefit because it does not extend to the ground. The amount and the placement of the absorptive treatment on the freeway and residential sides should be optimized to achieve maximum acoustical effectiveness.

5. Sound levels at locations about 350 m from the highway centerline were unaffected by the barrier construction.

6. Aesthetically, the addition of a T-top does not appear to degrade the appearance of the conventional barrier.

ACKNOWLEDGMENTS

The authors gratefully acknowledge the assistance they received from J. Egan and J. Walsh, Experimental Testing Laboratory, in conducting field measurements, and from R.W. Krawczyniuk, Research and Development Branch, in predicting sound levels. The authors also acknowledge the support given for this field trial by the Highway Design Office, in particular, J.R. Wear.

REFERENCES

1. J.J. Hajek, F.W. Jung, and M.R. Hunter. Highway Noise Barrier Options: Q.E.W. East of Cawthra Road. Report AE-81-06. Research and Development Branch, Ontario Ministry of Transportation and Communications, Downsview, Ontario, Canada, June 1981.

2. D.N. May and M.M. Osman. Highway Noise Barriers: New Shapes. *Journal of Sound and Vibration*, Vol. 71, No. 1, 1980, pp. 73-101.
3. F.A. Prah, M.M. Myles, and L.E. Witting. Noise Attenuation Measurements on a Doublewall Noise Barrier. Report 3740. Bolt Beranek and Newman, Inc., Cambridge, Mass., Jan. 1978.
4. D.N. May and M.M. Osman. The Performance of Sound Absorptive, Reflective, and T-Profile Noise Barriers in Toronto. *Journal of Sound and Vibration*, Vol. 71, No. 1, 1980, pp. 65-71.
5. J.J. Hajek and L. Kwan. Effect of Parallel Highway Noise Barriers. *Proc., Inter-Noise 80*, Dec. 1980, pp. 595-598.
6. J.J. Hajek. Performance of Parallel Highway Noise Barriers, Yonge St. to Bayview Ave., Toronto. Report AC-80-01. Research and Development Branch, Ontario Ministry of Transportation and Communications, Downsview, Ontario, Canada, 1980.
7. Specification for Sound Level Meters. Report ANSI S1.4-1971. American National Standards Institute, New York, April 1971, p. 8.
8. W. Bowlby et al., eds. Noise Barrier Cost Reduction Procedure STAMINA 2.0/OPTIMA: User's Manual. Report FHWA-DP-58-1. FHWA, U.S. Department of Transportation, April 1982.
9. J.J. Hajek. Effects of Parallel Highway Noise Barriers. In *Transportation Research Record 937*, TRB, National Research Council, Washington, D.C., 1983, pp. 45-52.
10. W. Bowlby and L.F. Cohn. IMAGE-3: Computer-Aided Design for Parallel Highway Noise Barriers. In *Transportation Research Record 937*, TRB, National Research Council, Washington, D.C., 1983, pp. 52-62.
11. M.M. Osman. MTC Scale Model Facility for Transportation Noise Problems: Materials Choice and Validation for Scale Modelling. Report AC-77-04. Research and Development Division, Ontario Ministry of Transportation and Communications, Downsview, Ontario, Canada, June 1977.
12. M.M. Osman. MTC Scale Model Facility for Transportation Noise Problems: Instrumentation Manual. Report AC-77-03. Research and Development Division, Ontario Ministry of Transportation and Communications, Downsview, Ontario, Canada, June 1977.
13. J.J. Hajek. Are Earth Berms Acoustically Better than Thin-Wall Barriers? In *Transportation Research Record 896*, TRB, National Research Council, Washington, D.C., 1982, pp. 60-67.

Publication of this paper sponsored by Committee on Transportation-Related Noise and Vibration.

Noise-Compatible Development: A Pilot Demonstration Project

MARK T. STAHR

ABSTRACT

Recently FHWA initiated a pilot demonstration project in noise-compatible development. Site visits were made to two locations (Oakdale, Minnesota, and Bradenton/Manatee County, Florida) to offer technical assistance in both estimation of future noise levels and consideration of noise in land use planning and development decisions. Based on local data of traffic, speed limits, and the percentage of truck travel, noise contours were produced for all major highway facilities in both areas. In addition, planning techniques for considering noise were discussed, as were the legal aspects regarding noise and zoning. Based on these pilot projects, it was concluded that the information provided was useful to the local communities, and that technical assistance from the federal and state levels is critical to the effectiveness of noise-compatible development.

For a number of years FHWA has been interested in the subject of noise-compatible development for several reasons. First, while state and local noise barrier programs along major highways have had many successful applications, the percentage of highway right-of-way on which barriers can be placed is fairly small because of topography, the nature of development, cost, aesthetics, or the inability to install a continuous barrier without breaks. Second, it is generally not practical to erect barriers along the thousands of miles of highways where there is currently no development because it is not known when and where development will take place or what type of development it will be. For these reasons FHWA has a policy of not funding barrier construction on undeveloped lands. Third, it is clear that traffic noise will continue to be an issue because of projected long-term increases in automobile and truck travel, and because of anticipated development along major highways.

Until recently, FHWA involvement in noise-compatible development had been in the production and distribution of pamphlets and audio-visual materials alerting local communities to the need for noise-compatible development. Although these were generally well-accepted materials, it also became evident that they were not meeting all of the needs of local communities with little or no experience in analysis or mitigation of traffic noise, or incorporation of noise as a factor into local land use planning activities. As a result, during the past year FHWA initiated a pilot demonstration project in noise-compatible development. Site visits were made to two locations to offer technical assistance in both estimation of future noise levels and consideration of noise in land use planning and development deci-

sions. The purpose of this paper is to report on the results of these site visits.

DESCRIPTION OF PILOT DEMONSTRATION

The three basic aims of the pilot demonstration were as follows.

1. Develop noise contours for major highway facilities in a local area. The FHWA STAMINA 2.0 noise model was used, making several simplifying assumptions appropriate to the community-wide (instead of site-specific) nature of the analysis. These assumptions will be discussed.

2. Provide local personnel with simple techniques that can be used to produce additional noise contours. The techniques provided and discussed were a nomograph method published by the U.S. Department of Housing and Urban Development (HUD) (1) and the FHWA programmable-calculator method (2).

3. Discuss with the local personnel different techniques that they may use to incorporate noise considerations into the land use planning or subdivision approval processes. A packet of information was provided in which zoning techniques for noise, subdivision approval considerations, site design issues, and so forth were discussed. Legal issues regarding noise and the ability to plan for it were discussed, and informational pamphlets that could be provided to local decision makers or interested citizen groups were also included.

Choosing the Sites

Before setting up a more formalized means of technical assistance, it was decided to try this at two pilot sites to make sure that FHWA would have something meaningful to provide to local communities, and that there is a demand for this type of assistance. In choosing the pilot sites, three screening criteria were used; these criteria would apply to any future technical assistance as well:

1. Local officials consider highway traffic noise to be an issue in their community and are motivated to initiate a noise-compatible development program;

2. Local agencies have not yet developed an expertise in noise-compatible land use planning, but are interested in doing so; and

3. There is right-of-way along major facilities not yet developed but which will be developed in the next few years; this recognizes that the ability to plan for noise is much greater where the land has not yet been fully developed.

Through the FHWA field offices, communities in California, Florida, Minnesota, Nevada, and Pennsylvania were submitted as candidate sites.

The communities chosen for the pilot demonstration were Oakdale, Minnesota, and Bradenton/Manatee County, Florida. Before the demonstration, preliminary site visits were made to collect data to de-

velop noise contours and to investigate the structure of local land development activities. The demonstrations that took place at each site are covered in the following sections.

Oakdale

Oakdale is a suburban community of 12,000 people located in the Twin Cities (Minneapolis-St. Paul) area in Minnesota. It is primarily residential in character, with a small amount of light industry and commercial property. Although much of the land is still undeveloped, the Beltway around the Twin Cities (I-694) runs through Oakdale, and its good accessibility has increased pressure for development. In addition to the Interstate facility, there are several major arterials where traffic noise is also a potential issue.

The community was incorporated as a municipality in 1972. The single planner on the city staff is responsible for a number of functions, and relies on the state and consultants for much of the traffic planning and engineering work. The demonstration consisted of several hours of discussion with the city planner, plus a brief presentation on the purpose of the demonstration to the Oakdale City Council.

For input into the FHWA STAMINA model to produce noise contours, 1982 and 2000 traffic estimates were provided by the city's consultants, speed limits were provided by the Oakdale Sheriff's Department, and the percentage of truck travel was supplied by the Minnesota Department of Transportation (MinnDOT). With this information, L_{eq} noise contours were produced for major highway facilities, giving the distance from the centerline of the roadway to levels of 75, 70, 67, 65, and 60 dB(A). In addition, the packet of materials given in Table 1 was presented and discussed, and a slide and tape presentation entitled "Sound Planning" was shown. Meetings were also held at MinnDOT and the League of Minnesota Cities to summarize the demonstration in Oakdale.

At the meeting in Oakdale, the community's interest in traffic noise was discussed, as well as general thoughts on the course of future development. The two primary motivations to addressing noise issues were the desirability of quality development (i.e., a pleasant living environment) and the need to meet Federal Housing Administration/Veterans Administration (FHA/VA) standards on noise so that developments could qualify for mortgage guarantees.

Bradenton/Manatee County

The city of Bradenton (population 121,000) and Manatee County (population 148,000, including Bradenton) are located on Florida's Gulf Coast in a rapidly developing area just north of Sarasota and south of the Tampa/St. Petersburg area. A major Interstate (I-75) goes through the area, and a number of US and state roads also carry heavy traffic. There is considerable truck traffic associated with the citrus industry in certain parts of the county.

There is a city planning staff that covers activities within the Bradenton city limits, and a county staff that covers the remainder of the county. Most of the city is currently developed, so virtually all of the rapidly developing areas are the responsibility of the county staff. Presentations were made to a planner on the city staff and a planner on the county staff.

The year-2000 traffic estimates were available from projections made by the Sarasota/Manatee Area Transportation Study (SMATS). Truck percentages were estimated from counting programs of both the Florida Department of Transportation and Manatee County. Speed limits were assembled by county staff. From this, the L_{eq} contours were produced, and because the state and county use the L_{10} descriptor, a discussion was given on the relationship between L_{eq} and L_{10} . The packet of material in Table 1 was discussed. As in Oakdale, the desire for a pleasant living environment and the desire to meet HUD standards were both reasons to be concerned about noise.

EVALUATION OF PILOT DEMONSTRATIONS

It is difficult to come up with an ultimate measure of success for a program like this because the most likely (and possibly the most desirable) outcome would be for local planning staffs to use the contours and zoning and subdivision information in informal discussions with developers. However, the pilot demonstrations can be evaluated for how well they transmitted useful information to local area planners, and what limitations the information may have had. The technical and policy aspects of the demonstration are discussed in the following sections, and an attempt is made to interpret the information from a local point of view.

Assembling Data

The three major data items needed to be able to

TABLE 1 Noise-Compatible Development Materials Distributed to Localities

Publication	Use
Policy on Land Use and Source Control Aspects of Traffic Noise Attenuation. AASHTO, Washington, D.C., 1980.	Demonstrates AASHTO support for noise-compatible development
Guidelines for Considering Noise in Land Use Planning and Control. Federal Interagency Committee on Urban Noise, June 1980; available from FHWA, U.S. Department of Transportation.	Discusses federal agencies' policies and standards for noise
W. J. Gallaway and T. J. Schultz. Interim Noise Assessment Guidelines. Office of Policy Development and Research, U.S. Department of Housing and Urban Development, Dec. 1980.	Provides nomograph techniques for estimating noise impacts from transportation sources on a development
M. J. Meshenberg. The Administration of Flexible Zoning Techniques. Planning Service Report 318. American Society of Planning Officials, Chicago, June 1976.	Discusses newly developing techniques for zoning to be able to consider a wider range of issues
M. T. Stahr. Reducing Noise Impacts of Motor Vehicles: A Problem With Diffused Solutions. Unpublished; submitted for a course at George Washington University, March 1983.	Discusses where noise-compatible development may be appropriate and how it may be accomplished
The Audible Landscape: A Manual for Highway Noise and Land Use. FHWA, U.S. Department of Transportation, Aug. 1976.	Suggestions for incorporating noise into land use and site design decisions
Highway Noise and Compatible Land Use. FHWA, U.S. Department of Transportation, May 1979.	Five case histories
Highway Traffic Noise and Future Land Development Can be Compatible. FHWA, U.S. Department of Transportation, 1979.	Pamphlet promoting noise-compatible development

produce noise contours are traffic forecasts, speed data, and the percentage of truck travel. In both communities all these data were available, and the contours could be produced by making certain assumptions. For Oakdale, the year-2000 traffic projections were given as a range by the consultant [average daily traffic (ADT) of 46,000 to 55,000], recognizing the uncertainty associated with travel forecasts. The midpoint of this range was used for traffic data. For Bradenton, the SMATS travel forecasts were used. These forecasts were from an unrestrained traffic assignment process, and because Bradenton is a rapidly developing area, the projected volumes in some cases exceeded the roadway capacity. In those cases the capacity of the roadway was chosen rather than the projected volume.

The speeds used in estimating contours were the current speed limits on facilities in both areas. Two potential drawbacks of using current speed limits are that the limits may change in the future, and that as future volumes approach capacity, actual speeds will decrease. The decrease in speed, however, may be offset by the noise associated with acceleration and deceleration in congested traffic. Therefore, the use of current speeds was thought to be a reasonable assumption.

Highway noise-prediction models are sensitive to the percentage of truck travel because heavy trucks are much noisier than passenger cars. In both communities (and probably in most other areas as well) there was no breakdown available for every arterial and freeway on truck travel. Also, most truck counting figures do not divide the percentages into heavy versus medium trucks, and the noise models require both. For both Oakdale and Bradenton, the states had collected truck data for major facilities, and in addition, Manatee County (Bradenton) had estimates for some additional facilities. With this information, the percentage of trucks could also be assigned to other facilities of the same type. The breakdown of medium versus heavy trucks was derived from national average data obtained from an FHWA Technical Advisory (3).

Developing Contours

Once the data were assembled, the development of contours was a straightforward matter. The FHWA STAMINA 2.0 model was used. Receptors were located perpendicular to the roadway at 50-ft intervals, and from the output it was possible to interpolate to develop the contours. A sample of the contours developed is given in Table 2. Assumptions used in the STAMINA runs were as follows.

1. National average data by city size from NCHRP Report 187 (4) were used to develop peak-hour factors from ADT. Peak-hour L_{eq} noise contours were developed.
2. Flat sites with no barriers were assumed.
3. Soft sites were assumed.
4. The nighttime percentage of ADT was assumed at 15 percent, thus making the L_{eq} (FHWA measurement) and L_{dn} (HUD measurement) comparable.
5. Each segment of roadway was modeled separately, assuming an infinite length, and distance from the centerline was measured. Segments were not modeled separately for each direction of travel. Distances were rounded to the nearest 10 ft.
6. Shielding by houses was not accounted for.

Although these assumptions were reasonable in each community and simplified the use of STAMINA compared with a project-specific analysis, there is still a lot of analysis involved. This is because

TABLE 2 Sample of Contours Developed During Pilot Demonstration Project

Facility	Contour, L_{eq} [dB(A)]	Distance from Centerline (ft)	
		2000	1982
I-694, between TH-120 and TH-36	75	100	60
	70	200	140
	67	320	220
	65	420	280
	60	900	600
I-694, between TH-36 and 40th Street north	75	100	60
	70	250	130
	67	375	200
	65	500	270
I-694, between 40th Street north and TH-5 (does not take into account barriers)	60	1,100	550
	75	110	60
	70	240	130
	67	360	200
	65	500	270
I-694, between TH-5 and I-94	60	1,050	550
	75	130	70
	70	270	150
	67	430	230
	65	580	310
TH-120, between I-694 and 50th Street north	60	1,300	650
	75	-	-
	70	-	-
	67	60	45
	65	80	60
TH-120, between 50th Street north and 40th Street north	60	200	140
	75	-	-
	70	50	-
	67	90	60
	65	120	70
TH-120, between 40th Street north and Stillwater	60	250	160
	75	-	-
	70	70	50
	67	110	80
	65	160	110
TH-120, between Stillwater and 10th Street north	60	350	230
	75	-	-
	70	60	-
	67	90	60
	65	120	90
	60	270	190

each time the ADT, speed limit, or percentage of truck travel changes on a facility, a separate analysis must be done on that link. On a community-wide basis, a large number of analyses may have to be run.

The contours were easy to explain to local staffs not familiar with noise. It was also easy to explain that these were only approximate distances; the local planners were comfortable with that. It was a little more confusing to describe the different noise descriptors (L_{eq} , L_{dn} , L_{10}) and their application because neither community had significant experience in noise measurement. The relationship between L_{eq} and L_{dn} was particularly important in both areas because HUD uses the L_{dn} description for the noise standard for FHA mortgage guarantees and other HUD programs.

Planning and Legal Aspects

The packet of materials discussed (Table 1) consisted both of informational brochures outlining the traffic noise problem and suggesting land use solutions, and more detailed booklets on how noise impacts may be successfully incorporated into the land use planning and subdivision approval processes. In zoning, several options were discussed, with the most promising appearing to be definition of a noise overlay zone. The overlay zone, which has typically been used previously in defining flood plains, would put high noise areas into a special zone (based on the contours), which would be in addition to whatever zoning the property would al-

ready have, and would thus require mitigation. Conditioning subdivision approvals on proper consideration of noise impacts would have the same purpose, but would place consideration later in the development process. The legal issues relating to both liability for noise and zoning for noise were also covered.

Planners in both communities rated these materials "very useful" or "somewhat useful." The underlying sentiment appeared to be that although these were helpful as guidance documents, neither community intended to extensively revamp their zoning process to incorporate noise because of the sensitive political nature of making any changes in the zoning process. Instead, the materials would be used in discussions with developers on a case-by-case basis.

CONCLUSIONS

In evaluating the success of these pilot demonstrations and considering setting up a continuing program of technical assistance, three basic measures of success need to be examined: whether it is technically feasible to supply noise contours, whether there is an identifiable demand for this type of assistance, and whether local areas have enough information to continue to work in noise-compatible development after the demonstration project.

1. Technical feasibility: The two pilot demonstrations have shown that it is possible to provide contours to a local community with a quick turnaround time. Some of the assumptions made about being able to provide this quick turnaround would not be considered acceptable for a project-specific analysis [for use in an environmental impact statement (EIS), for example], but they were thought to be reasonable for community-wide estimates. The necessary data were obtainable in both communities without a major level of effort. The issue of how defensible the contours are and whether they can be successfully used to determine the use of individual parcels of land remains unresolved. If it is assumed that the contours developed are accurate to within ± 3 dB(A), this still leaves considerable latitude as to the true location of the contour. A developer may argue that if the contour is 3 dB(A) too high, he will be unfairly prevented from using a large parcel of his land. Although this is an issue to be concerned about, it need not prevent the use of contours in development decisions. As evidence, a parallel situation has existed for years in many communities: Developers have been required to pay for road improvements (widening, turning bays, and so forth) on the basis of imperfect traffic forecasts. The main concerns from both a legal and equity standpoint should be that noise contours be developed by using a rational process and best available data, and that the standards be applied equally to everyone.

2. Demand: There were several other communities that expressed an interest in being pilot sites besides the two chosen, and wider advertisement should increase interest. The total demand is unknown because noise is still not considered a critical issue in most communities. However, for cities

and counties expecting growth, planning for noise ahead of time ought to avoid a lot of homeowner dissatisfaction in later years.

3. Continuation of the process: From a technical standpoint, the HUD nomograph procedure provided to both areas should allow them to easily update contours if circumstances change. It was also apparent from the pilot demonstrations, however, that the support of the state is critical to the continuation of these activities. The involvement of state department of transportation experts in noise in both these demonstrations was a major factor in the overall credibility of the demonstration. Local planners in both communities were more at ease in dealing with noise knowing there was someone in the state they could call on for general guidance, technical assistance, and data. Depending on the knowledge and experience available in the local community, help could be needed from federal and state governments in the following areas: traffic forecasts, truck forecasts, noise contours, fundamental concepts of traffic noise, fundamental concepts of noise description, experiences in other communities, and zoning and legal issues. In terms of policy guidance offered to the communities, the pilot programs showed that the handouts appeared to be appropriate and useful. The documents were seen as somewhat vague in terms of specific solutions, however. A "cookbook" approach would be more desirable, but this is not feasible because each local community will differ in its treatment of zoning, relationship with developers, and so forth.

In general, it can be concluded that (a) there is a need for consideration of noise in the land use planning and subdivision approval process, (b) local areas will have to follow through because they are responsible for land use decisions, (c) it is necessary for federal and state governments to offer assistance to local governments on this subject, and (d) the pilot demonstration projects were a reasonable example of how all this may be accomplished.

REFERENCES

1. W.J. Gallaway and T.J. Schultz. Interim Noise Assessment Guidelines. Office of Policy Development and Research, U.S. Department of Housing and Urban Development, Dec. 1980.
2. Hand-Held Calculator Listings for the FHWA Highway Traffic Noise Prediction Model. FHWA Technical Advisory T5040.5. FHWA, U.S. Department of Transportation, Sept. 5, 1978.
3. Vehicle Types for Environmental Design Methodologies. FHWA Technical Advisory T5040.1. FHWA, U.S. Department of Transportation, Feb. 16, 1978.
4. A.B. Sosslau, A.B. Hassam, M.M. Carter, and G.V. Wickstrom. Quick-Response Urban Travel Estimation Techniques and Transferable Parameters: User's Guide. NCHRP Report 187. TRB, National Research Council, Washington, D.C., 1978, 229 pp.

Publication of this paper sponsored by Committee on Transportation-Related Noise and Vibration.

Determination of Reference Energy Mean Emission Level in Georgia

ROSWELL A. HARRIS

ABSTRACT

In conducting any detailed noise impact analysis and subsequent barrier design, it is always desirable to calibrate the noise prediction model (STAMINA) with measured noise levels at the site in question. The model does not always yield noise levels acceptably close to those measured in the field, often for no apparent reason. It is suggested in this paper that the reference energy mean emission curves published by FHWA may cause the model to significantly overpredict noise levels in the vicinity of major highways. New emission data are offered and then used to compare the results of the noise prediction model with field measurements. This comparison reveals significantly closer agreement between the noise levels calculated by STAMINA, using the new emission curves, than was obtainable with the FHWA curves.

The presence of high noise levels adjacent to major highways continues to be a major problem to state transportation agencies throughout the United States. The primary mandate of these agencies is to provide the citizens of their respective states with a safe and efficient highway network. As a result, efforts to improve existing facilities and construct new facilities are causing significant increases in ambient noise levels in established residential areas. Many states are thus committing substantial sums of money to noise-abatement barriers in an attempt to minimize increases in existing noise levels along their highway systems.

Acoustic design of these noise barriers is accomplished through a computer model that calculates anticipated future noise levels and the insertion loss provided by a given barrier configuration. It is suggested in this paper that the state-of-the-art model may significantly overpredict expected noise levels for any given highway design. Although this may not pose a serious problem along an existing highway where present noise levels can be easily measured, a significant lack of confidence in the predicted noise levels could occur on a new location or project. A transportation agency will naturally be less likely to commit funds for noise abatement when the engineer cannot express a high level of confidence in his noise impact analysis.

PROBLEM STATEMENT

The author's past experience with STAMINA 1.0 and STAMINA 2.0 has indicated a tendency of the model to overpredict noise levels adjacent to Interstate highways. At first it was unclear if the error was related to the user's choice of the ground absorption (alpha) factor. Although there is ample evi-

dence to support the use of 0.0 for acoustically reflective ground cover and 0.5 for absorptive cover, topographic characteristics vary from site to site; thus the choice of an alpha factor requires good judgement by the user based on prior experience. Even though this step does introduce a possible source of error for users not familiar with the model, experience should provide the necessary guidance in selecting the proper alpha factor.

Traffic volume and speeds are easily measured or can be closely estimated by an experienced observer, thus minimizing errors of this type. The calibration process should include noise measurements at a location free of terrain influence, thus eliminating any excess attenuation error. In short, the experienced user should be able to keep input data errors to a minimum, and expect the calculated noise levels from the model to agree closely with measured noise levels. If the calculated and measured noise levels do not agree within desired limits for the calibration sites, the user typically cannot find a logical explanation for the discrepancy.

Because the reference energy mean emission levels published by FHWA were gathered by the Four-State Noise Inventory (1) conducted in 1975, the question was raised on whether these data were valid for the state of Georgia. Accordingly, tests were begun to develop emission level curves for highway traffic in Georgia and then compare that data with the FHWA emission level curves. The results of that study are presented herein.

EMISSION LEVEL METHODOLOGY

The study was conducted in accordance with procedures established by FHWA (2). Only a brief discussion of the procedure will be presented here because a detailed description is available from the report.

All test sites were chosen to be level and free of extraneous terrain influence. The microphones were placed at 50 ft from the centerline of the near traffic lane, with a clear line of sight to the roadway and an unobscured arc of at least 150 degrees at the microphone. All roadways had a grade of less than 2 percent and consisted of dry, smooth asphalt or concrete pavement.

Measurement sites were chosen to minimize potential contamination of each sample by noise from other vehicles. This was done by choosing locations with wide, tree-covered medians, or locations with low traffic volumes. The sound level meter was carefully watched while the observer physically listened for interference from other vehicles. Careful application of this procedure ensured that these emission level samples were not contaminated by noise from other sources.

Wind speed, temperature, and humidity were checked at a local National Oceanic and Atmospheric Administration (NOAA) office to ensure that meteorological conditions were within acceptable limits for the time of the sample. It was assumed that humidity and temperature did not vary significantly at the measurement sites from that reported at the NOAA

station, a reasonable assumption for middle Georgia during the summer months. Measurements were halted if the wind began gusting or if the constant wind speed was suspected of approaching 12 mph.

A Metrosonics db-602 Sound Level Analyzer was used to record the maximum A-weighted noise level from each vehicle passby. This equipment was field calibrated before and after each measurement session to ensure accuracy. The speed of each sample vehicle as it passed the microphone was measured with a hand-held radar unit, which was also calibrated before and after each measurement session.

Traffic was classified into three groups: (a) automobiles, which included light trucks with four tires; (b) medium trucks, which consisted of trucks with two axles and six tires; and (c) heavy trucks, which consisted of trucks with three or more axles and all tractor-trailer combinations. An estimated number of vehicles to be sampled from each classification was obtained from Figure 1 (2) for a desired confidence interval of ± 1 dB(A) at a 95 percent confidence level. Samples were grouped into a speed range of ± 3 mph, with midpoints ranging from 30 to 58 mph.

EMISSION LEVEL RESULTS

All samples greater than 48 mph were gathered on the Interstate highway system outside the Atlanta area. Because the vast majority of noise problems occur along this type of facility, it is significant to note that these routes are heavily used by interstate travelers. Thus the results of this study are influenced by traffic (all classifications) from states other than Georgia. The remaining samples of heavy and medium trucks were obtained from local roads in the vicinity of several interstate trucking terminals in south Atlanta. Consequently, the emission curves developed in this paper should be indic-

ative of noise emissions from vehicles in other states as well.

The statistical tests used in the validation procedure all assume the data are normally distributed. In order for this assumption to be used with confidence, all the data for each vehicle classification were tested to determine if they were from a normal population. The tests for normality were accomplished by use of a statistical computing package (MINITAB) developed by the Statistics Department at Pennsylvania State University and modified for use on the DECsystem-10 at Vanderbilt University. A normal probability plot for each vehicle classification was produced (Figure 2). If the sample is from a normal population, the points on the plot will fall roughly on a straight line. As can be seen from Figure 2, all plots are reasonably straight. MINITAB also calculates a correlation coefficient that measures the straightness of each plot. Each set of data proved to be from a normal population based on a 95 percent level of confidence.

After the final number of samples of each vehicle classification was collected, the actual confidence interval for a 95 percent level of confidence (3) for each speed range within each vehicle classification was calculated according to the following equation:

$$\bar{x} - t_{0.025, n-1} / (S/\sqrt{n}) < \mu < \bar{x} + t_{0.025, n-1} / (S/\sqrt{n}) \tag{1}$$

where

- \bar{x} = sample average emission level,
- t = Student's t-test distribution,
- s = sample standard deviation, and
- n = actual number of samples.

The actual number of samples for each vehicle classification within each speed range is given in Table 1. Also included is the confidence interval as

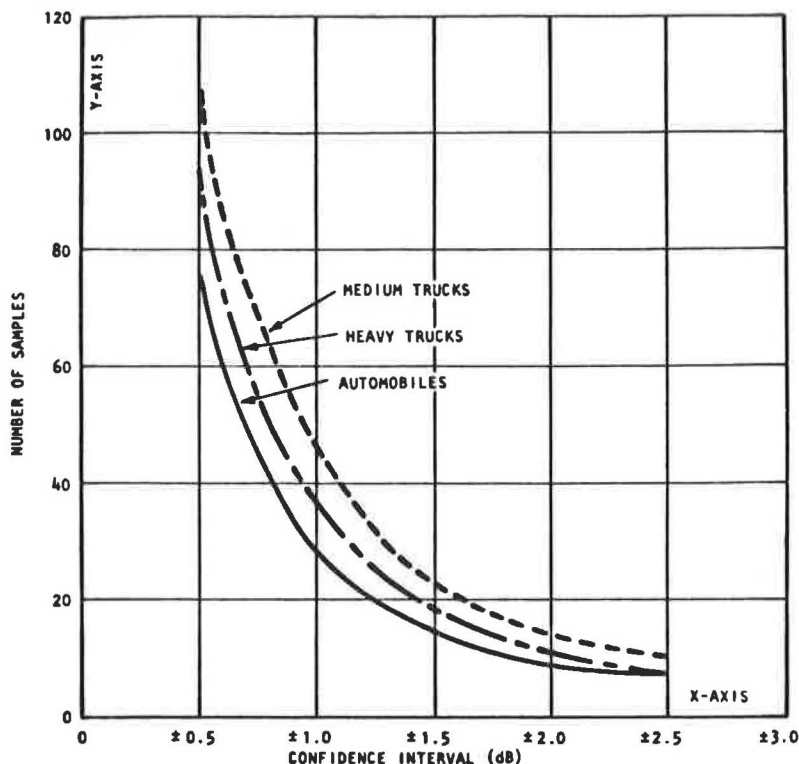


FIGURE 1 Estimated number of samples (2).

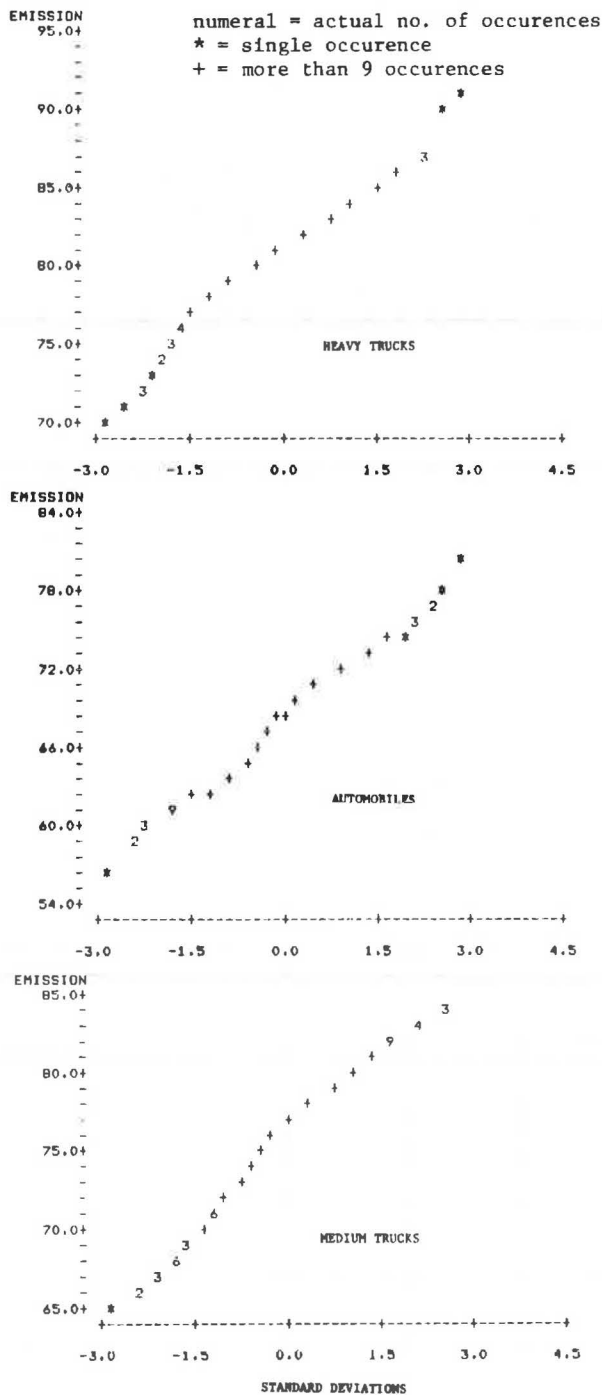


FIGURE 2 Normal distribution plot, all vehicle classifications.

calculated by Equation 1 for a 95 percent confidence level.

As illustrated by the data in Table 1, the larger the number of samples, the smaller the error limits. It is significant to note that because the vast majority of noise problems occur on facilities with high traffic speeds and volumes, all data at speeds greater than 40 mph were within the desired error limit of ± 1.0 dB.

The reference energy emission level for each speed range within each vehicle classification was then calculated according to Equation 2:

$$(\bar{L}_o)_{Ei} = (\bar{L}_o)_i + 0.115 (s)_i^2 \quad (2)$$

where

$(\bar{L}_o)_{Ei}$ = reference energy mean emission level for the *i*th vehicle class for a single speed range,

$(\bar{L}_o)_i$ = arithmetic average sound level of the *i*th vehicle class for a single speed range, and

$(s)_i$ = sample standard deviation of the emission levels of the *i*th vehicle class for a single speed.

The arithmetic average sound level for the *i*th vehicle class $[(\bar{L}_o)_i]$ is calculated according to Equation 3:

$$(\bar{L}_o)_i = (1/n) \cdot \sum_{k=1}^n (\bar{L}_o)_{ki} \quad (3)$$

where $(\bar{L}_o)_{ki}$ is the *k*th measured emission level for the *i*th class of vehicles for a single speed, and *n* is the number of measured emission levels for the *i*th class of vehicles for a single speed range. The sample standard deviation $(s)_i$ of the *i*th vehicle class is calculated according to Equation 4:

$$(s)_i = \sqrt{[1/(n-1)] \sum_{k=1}^n [(L_o)_{ki} - (\bar{L}_o)_i]^2} \quad (4)$$

Once these calculations were completed, it was desired to find the mathematical equation that best described the relationship between the reference energy mean emission level and speed for each vehicle classification. This was accomplished through a regression analysis by the method of least squares. The values of the regression constants were obtained in this calculation, as well as the coefficient of determination (r^2). The value of r^2 will lie between 0 and 1 and will indicate how closely the equation fits the experimental data (the closer r^2 is to 1, the better the fit).

The data in Table 2 give the mean sound level, the standard deviation, and the reference energy mean emission level for each speed range and vehicle classification.

TABLE 1 Actual Number of Samples and Confidence Interval for 95 Percent Confidence Limit

Vehicle Class	Item	Speed Range (mph)				
		27-33	34-40	41-47	48-54	55-61
Automobiles	No. of samples	28	54	61	76	96
	Confidence interval (dB)	± 1.0	± 0.7	± 0.7	± 0.5	± 0.4
Medium trucks	No. of samples	46	47	46	56	71
	Confidence interval (dB)	± 1.2	± 1.1	± 0.8	± 0.6	± 0.6
Heavy trucks	No. of samples	38	65	58	60	78
	Confidence interval (dB)	± 1.2	± 0.8	± 0.8	± 0.7	± 0.5

TABLE 2 Data Summary

Vehicle Class	Parameter	Emission Level as a Function of Speed [dB(A)]				
		27-33 mph	34-40 mph	41-47 mph	48-54 mph	55-61 mph
Automobiles	(L ₀)	63.8	64.4	65.6	70.8	71.6
	s	2.64	2.69	2.63	2.35	2.03
Medium trucks	(L ₀) _E	64.6	65.3	66.4	71.5	72.1
	(L ₀)	73.3	73.3	76.9	77.8	78.5
Heavy trucks	(L ₀) _E	75.1	75.0	77.7	78.5	79.2
	(L ₀)	80.7	80.8	81.1	81.1	81.6
	s	3.66	3.18	3.08	2.75	2.38
	(L ₀) _E	82.3	81.9	82.2	81.9	82.2

The mean emission level from Table 2 was used with the midpoint of each speed range in a regression analysis to calculate the following equations, where V is vehicle speed in miles per hour:

Automobile: $(\bar{L}_0)_E = 28.19 \text{ Log}(V) + 21.91 \text{ dB(A)}$ ($r^2 = 0.89$) (5)

Medium truck: $(\bar{L}_0)_E = 16.36 \text{ Log}(V) + 50.41 \text{ dB(A)}$ ($r^2 = 0.90$) (6)

Heavy truck: $(\bar{L}_0)_E = 81.1 \text{ dB(A)}$ (7)

Figure 3 is a graphic comparison of the data collected in Georgia with the FHWA emission level curves. There is a dramatic difference in the higher

speed emission levels for both medium and heavy trucks, with relatively little change in the curve for automobiles. It is interesting to note that the emission level for heavy trucks is independent of speed, which is similar to the emission level applied to all trucks by NCHRP Report 117 (4) in 1971.

VALIDATION METHODOLOGY

STAMINA 2.0 was modified (5,6) by replacing the FHWA emission level curves with the curves defined in this paper, and a validation study was conducted in accordance with FHWA procedures (2). Four sites were chosen for this study.

Noise measurements were made with an equipment system provided by FHWA. The system consisted of a computer-controlled GenRad real-time analyzer modified to permit simultaneous A-weighted sampling from several microphones. GenRad 1962 0.5-in. electret microphones, powered by GenRad preamplifiers, send signals through shielded coaxial cables to a mobile laboratory. There the signal passes through Ithaco 451 amplifiers to an A-scale filtering modified GenRad 1925 multi-filter. The A-weighted signal is then sent to a GenRad 1926 rms detector, which, for this study, was set to sample the noise level eight times per second. These data are then sent through a Telecom 5141 interface to a Hewlett-Packard 2100S computer. The computer then analyzes the data and computes the Leq at the desired location.

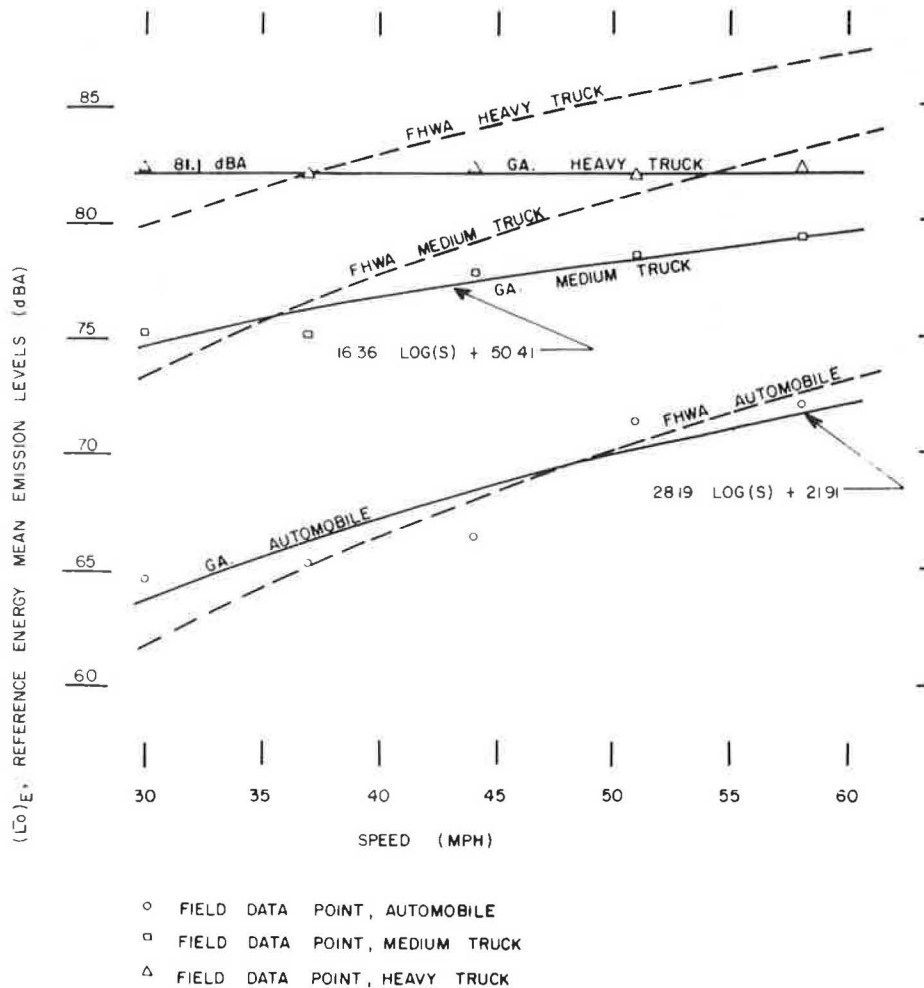


FIGURE 3 Reference vehicle sound emission levels.

Carefully controlled field measurements were then compared with STAMINA 2.0 output by first using the FHWA emission curves and then using the emission curves developed in this paper.

VALIDATION RESULTS

A comparison of the measured and calculated noise levels for each site is given in Table 3.

TABLE 3 Calculated Versus Measured Noise Levels

Site	L _{eq} [dB(A)]			Difference [dB(A)]	
	FHWA	Georgia	Measured	FHWA - Measured	Georgia - Measured
	1	80.1	78.1	79.1	1.0
	80.1	78.1	77.4	2.7	0.7
	80.1	78.1	78.7	1.4	-0.6
2	74.3	72.8	73.0	1.3	-0.2
	73.9	72.5	72.1	1.8	0.4
3	70.7	69.1	69.2	1.5	0.1
	71.0	67.6	68.0	3.0	-0.4
4	77.1	74.6	75.1	2.0	-0.5

As the data in Table 3 indicate, STAMINA 2.0 consistently overpredicts by 1 to 3 dB when using the FHWA emission curves. By using the same input data but with the Georgia emission curves, STAMINA predictions were all within the desired ± 1.0 dB tolerance limit. The input data used in this comparison are given in Table 4.

It was then necessary to determine if the difference between measured and calculated noise levels was significant in either case. The Student's t-test for paired data was applied to the mean difference in measured and calculated noise levels (3) for both conditions. A mean difference of 1.84 dB(A) was obtained by using the FHWA data and -0.19 dB(A) was obtained by using the Georgia emission data. At a 95 percent level of confidence, there is a significant difference between the model results, using FHWA emission data, and measured noise levels at the modeled location. On the other hand, there was no significant difference between calculated and measured noise levels using the Georgia emission data.

CONCLUSIONS

The data presented in this paper suggest that the FHWA emission level data for medium and heavy trucks (1) may have changed over the years, or the data from that study may simply not be representative of the noise emission levels of the vehicles in states other than those sampled. Specifically, the following can be concluded.

1. The energy mean emission level for heavy trucks was found to be 81.1 dB(A), independent of speed. At 55 mph this is approximately 5.2 dB(A) lower than the speed-dependent value suggested by FHWA.

2. The energy mean emission level for medium trucks was found to be speed dependent. However, at 55 mph the Georgia emission level data produce a noise level 3.4 dB(A) lower than the FHWA emission level data.

3. At low speeds the Georgia emission level data are slightly higher than the FHWA emission level data for all three vehicle classifications.

4. Validation measurements at four sites indicate that calculated noise levels, using the Georgia emission level data, were not statistically different from measured noise levels at the modeled location at a 95 percent level of confidence. The same measurement data revealed a statistically significant difference in the calculated and measured noise levels using the FHWA emission data.

RECOMMENDATIONS

Atlanta is recognized as the major transportation hub in the southeast. As such, it is reasonable to state that the radial Interstate system through the city is well traveled by vehicles of all classifications from a large number of states. It therefore follows that the emission level data presented in this paper may also be representative of vehicles in other states as well.

It is suggested that other state transportation agencies may want to develop their own emission level data. An alternative would be for FHWA to develop regional emission level data based on measurements in a number of states in each region. This could be accomplished in a cooperative effort with

TABLE 4 STAMINA 2.0 Input Data Summary

Location	Automobiles		Medium Trucks		Heavy Trucks	
	No.	Speed (mph)	No.	Speed (mph)	No.	Speed (mph)
Site 1, all 3 runs						
I-285 NBL	4,518	58	178	57	203	57
I-285 SBL	5,094	61	200	56	229	58
Frontage Road	36	52	5	40	1	40
Site 2, run 1						
I-285 NBL	3,360	54	144	49	152	51
I-285 SBL	3,272	60	176	56	164	56
Site 2, run 2						
I-285 NBL	2,828	54	144	49	152	47
I-285 SBL	2,404	57	208	56	164	57
Site 3, run 1						
I-20 EBL	740	58	36	58	40	65
I-20 WBL	604	56	16	58	48	53
Frontage Road	76	45	1	30	4	41
Site 3, run 2						
I-20 EBL	564	62	24	59	36	59
I-20 WBL	528	58	60	59	72	59
Frontage Road	36	45	0	0	0	0
Site 4, run 1						
I-75 NBL	743	61	59	58	141	55
I-75 SBL	713	59	57	58	135	55

Note: NBL = northbound lane, SBL = southbound lane, EBL = eastbound lane, and WBL = westbound lane.

the state transportation agencies and would add reliability to the predictions of the model nationwide. Verification of the emission level data will not only give the user more confidence in his analysis, but it also has the potential for providing more cost-effective noise barrier designs.

REFERENCES

1. Highway Noise Measurements for Verification of Prediction Models. Report DOT-TSC-OST-78-2/DOT-TSC-FHWA-78-1. FHWA, U.S. Department of Transportation, Jan. 1978.
2. Sound Procedures for Measuring Highway Noise: Final Report. Report FHWA-DP-45-IR. FHWA, U.S. Department of Transportation, Aug. 1981.
3. W.W. Hines and D.C. Montgomery. Probability and Statistics in Engineering and Management Science. Wiley, New York, 1980.
4. C.G. Gordon, W.J. Galloway, B.A. Kugler, and D.L. Nelson. Highway Noise: A Design Guide for Highway Engineers. NCHRP Report 117. HRB, National Research Council, Washington, D.C., 1971, 79 pp.
5. Noise Barrier Cost Reduction Procedure, STAMINA 2.0/OPTIMA: Program Maintenance Manual. Report FHWA-DP-58-2. FHWA, U.S. Department of Transportation, June 1982.
6. Noise Barrier Cost Reduction Procedure, STAMINA 2.0/OPTIMA: User's Manual. Report FHWA-DP-58-1. FHWA, U.S. Department of Transportation, April 1982.

Publication of this paper sponsored by Committee on Transportation-Related Noise and Vibration.

Rumble Strip Noise

JOHN S. HIGGINS and WILLIAM BARBEL

ABSTRACT

The Illinois Department of Transportation (IDOT) placed rumble strips near the north end of the Edens Expressway to alert drivers that they were approaching a signalized intersection. The intersection was a high-accident location, and previous safety measures were not significantly effective in lowering the number or severity of the accidents. Many complaints about noise were received from adjacent property owners after the strips were placed. When a berm that was placed between the residents and the strips did not reduce the complaints, IDOT requested assistance from the Demonstration Projects Division of FHWA to study berm effectiveness and rumble strip noise. Two types of strip construction were compared, the formed and the cut types. Several different configurations were also analyzed. Outside measurements were taken at three sites, and inside noise measurements were taken from the tractor of a semitrailer unit. Vibration measurements were taken from the steering column of the truck. The results indicated that the formed type of strip provided better driver perception than did the cut type at all speeds tested. Outside noise did not significantly vary with the different types and configurations of the rumble strips. The strips appear to have reduced the number and severity of accidents at the Edens Expressway location.

Rumble strips have been used by highway agencies as a safety feature to alert drivers to some impending change in the traffic flow (i.e., an upcoming toll booth on an expressway, and construction zones). Typically, the strips are used in conjunction with a visual stimuli, such as warning signs or lights. When the strips are crossed over, a driver feels the vibration and hears the noise. This causes the driver to become more alert and, on seeing the visual stimuli, to take the appropriate action.

The strips are usually made by cutting, or forming, transverse grooves or ridges in the pavement approximately 1 to 2 cm (0.5 to 1 in.) deep. The width, distance between, and the number of grooves (or ridges) vary. A set of grooves or ridges becomes a rumble strip. Typically, three strips are used with a length of untreated pavement in between each strip.

The Illinois Department of Transportation (IDOT) placed a set of rumble strips to warn drivers of the terminus of the Edens Expressway at Clavey Road in Highland Park. This intersection, which is signalized, has a high-accident history, the most severe being rear-end collisions. The abrupt change from a limited-access facility to a major arterial was the cause of these accidents. IDOT had tried several improvements to alleviate the problem, such as signs and warning lights. The effectiveness of these improvements has not been significant (1).

Public pressure became so great that rumble strips were placed to help warn the drivers of the upcoming signal. Immediately, complaints about noise from the rumble strips were received from the neighboring homeowners. IDOT attempted to reduce the noise from the rumble strips by constructing a 3.2-m

(10-ft) berm. When the complaints continued, IDOT requested assistance from the Demonstration Projects Division of FHWA in analyzing the noise being generated from the rumble strips and the effectiveness of the berm.

Another problem that IDOT wished to investigate was the vibration inside the vehicle as it passed over the rumble strip. IDOT testing indicated that the vibration inside automobiles was felt, but in large trucks it was not noticeable.

THE STUDY

The study had three objectives:

1. To measure the noise amplitude and frequency of the strip at various distances from the highway,
2. To measure the vibration inside a semitrailer tractor as it passes over the strips, and
3. To analyze how selected strip configurations affect both outside and inside vehicle noise and vibration when the tractor passes over it.

SITE DESCRIPTION

At the first three sites noise and vibration were analyzed from existing rumble strips. At the fourth site strips with different configurations were temporarily placed for analysis.

1. Site 1, East-West Toll Road at Toll Plaza No.

61: The strips are located in concrete pavement on the westbound lanes. Figure 1 shows the general configuration, and Table 1 gives the specific dimensions of the strips. Note that the grooves are rounded, which eliminate any sharp edges. The terrain slopes gradually upward from the roadway. These strips are of the formed type.

2. Site 2, Edens Expressway at Clavey Road: The strips are located in the northbound lanes, and their configuration is shown in Figure 2 (the dimensions are given in Table 1). These grooves were cut into the concrete pavement. Note that these strips have sharp edges rather than the rounded ones at Site 1. A 3.2-m-high (10-ft) berm separates the roadway and the neighboring property owners.

3. Site 3, US-12, south of Volo, Illinois: Four sets of strips, each with a different configuration, were cut into the concrete in the southbound lanes. The general configurations are shown in Figure 2, and the specific dimensions are given in Table 1. Note that strip A has a 10-degree tilt from normal. The terrain near the highway was generally flat, open fields.

4. Site 4, Tri-State Tollway at Toll Plaza No. 21: This site is similar to Site 1, only the grooves are slightly deeper and have been filled with a small lift of asphalt. (Refer to Figure 1 and Table 1 for the dimensions.) Only internal truck vibration and noise measurements were taken at this site.

Outside measurements were taken by using up to eight microphones, a real-time analyzer, and a computer (equipment from FHWA Demonstration Project No.

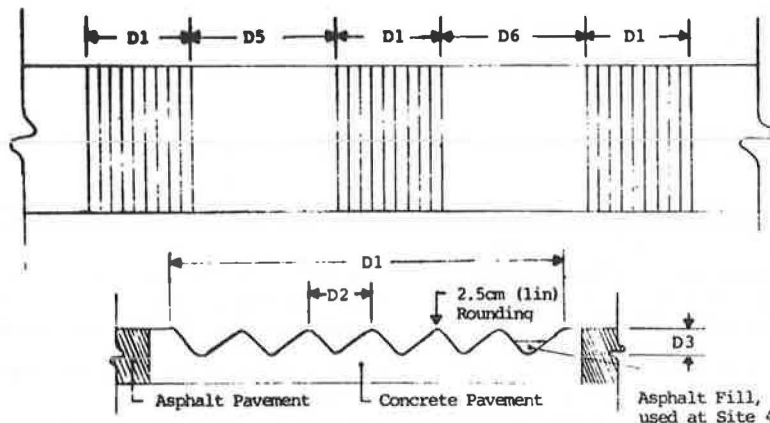


FIGURE 1 Strip layout: Site 1, East-West Toll Road, and Site 4, Tri-State Tollway.

TABLE 1 Rumble Strip Dimensions

Site	Length of One Strip, D1 (m)	Type of Strip	No.	Center-to-Center Distance of Grooves, D2 (cm)	Depth, D3 (cm)	Width, D4 (cm)	Distance Between Strips (m)	
							1-2 (D5)	2-3 (D6)
1	6.4	Formed ^a	42	15	0.8	NA	32.2	29.4
2	6.1	Cut	21	32	1.6	10	30	30
3								
Strip A	3.6	Cut ^b	13	30.5	1.3	10	30 ^c	
Strip B	3.6	Cut	13	30.5	1.9	10	30	
Strip C	6.1	Cut	21	30.5	1.3	10	30	
Strip D	2.4	Cut	13	20.3	1.3	10	30	
4	6.4	Formed ^d	42	15	1.7	NA	29.5	30.8

Note: 1 m = 3.28 ft, 1 cm = 0.39 in., and NA = not applicable.

^aGrooves formed with 2.5-cm rounding, thus eliminating all sharp edges.

^bGrooves cut on a 10-degree tilt, thus creating a 0.6-m offset from one end to the other.

^cOnly two strips were cut.

^dGrooves similar to those at Site 1; however, an asphalt lift was used in the groove to flatten the bottom.

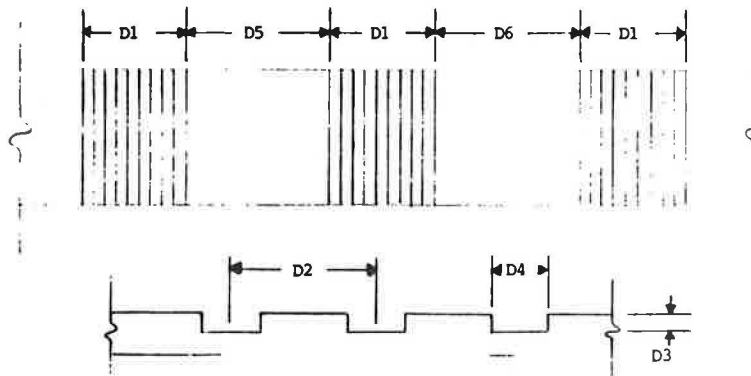


FIGURE 2 Strip layout: Site 2, Edens Expressway, and Site 3, US-12.

45, Highway Noise Analysis). Simultaneous measurements were taken at all microphones, with a sampling rate of 0.125 sec. A frequency distribution was obtained from various microphones at each site. Several measurement periods, each 15 min long, were conducted at Sites 1 and 2. A 1-min period was used at Site 3.

A Digital Acoustics 607 portable sound analyzer recorded the peak noise levels from vehicles crossing the center rumble strip. The duration greater than a threshold value of 75 dB(A) was also recorded.

MICROPHONE PLACEMENT

At Site 1 three microphones [channels (Ch) 43, 46, 47] were placed 15 m (50 ft) from the centers of the three strips. Another was placed as far as possible from the strips, while still maintaining the 15-m distance from the roadway (Ch 42). Three other microphones (Ch 44, 45, 48) were placed at various distances from the center strip in an attempt to measure the drop-off rate. The 607 was placed 15 m from the center strip (near Ch 47). Figure 3 shows the layout of the site. Traffic volumes and speeds were recorded for each vehicle classification (i.e., cars).

At Site 2 the microphones were placed to measure the barrier insertion loss at various locations on the neighboring properties (Ch 42, 44, 46). Measurements were taken in the bedrooms of two of the affected homes (Ch 45, 49), with the windows open and

closed. Frequency measurements were obtained from the top of the berm (Ch 43), in the backyard (Ch 44), and in the bedroom (Ch 45, windows open) of house 226. A microphone (Ch 47) was placed in the front yard of house 242 to measure the neighborhood noise levels. Figure 4 shows the layout of the site. Traffic volumes and speed were also measured at this site.

At Site 3 microphones were placed 15 m from the center of each set of rumble strips (Ch 42, 43 for strips A and C; Ch 46, 47 for strips B and D). Microphones were also placed at various distances away from the highway to measure the drop-off rate (Ch 44, 45 for strips A and C, Ch 48, 49 for strips B and D). Frequency distributions were obtained from the microphones 15 m away from the strips (Ch 43, 46). The 607 was placed 15 m from the center of strips A and C only (near Ch 43). The only noise measured at this site was from the test semitrailer traveling at speeds of 56, 65, 73, 81, and 88 km/h (35, 40, 45, 50, and 55 mph), and a automobile at speeds of 56, 73, and 88 km/h (35, 45, and 55 mph) only. Figure 5 shows the layout of the site, and microphone placement at the strips is given in Table 2.

MEASUREMENT AND PREDICTION PROCEDURES

Outside measurements were conducted in accordance with the guidelines set forth in an FHWA report (2). Both FHWA noise prediction models (STAMINA 1.0 and STAMINA 2.0) (3,4) were used to obtain predicted

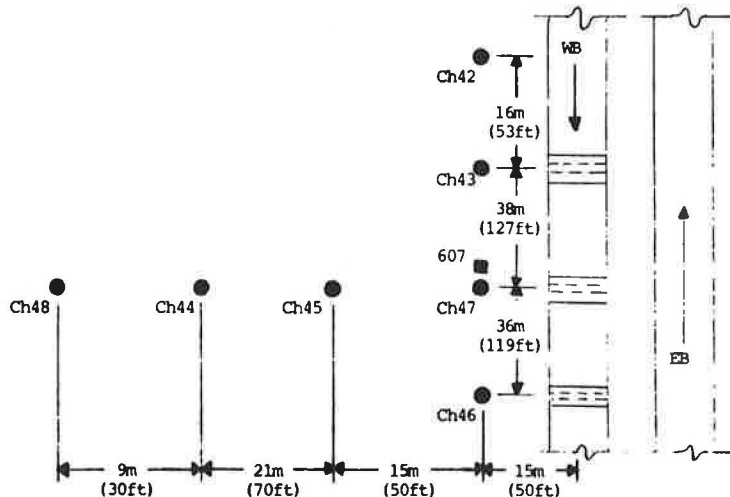


FIGURE 3 Site 1 microphone placement.

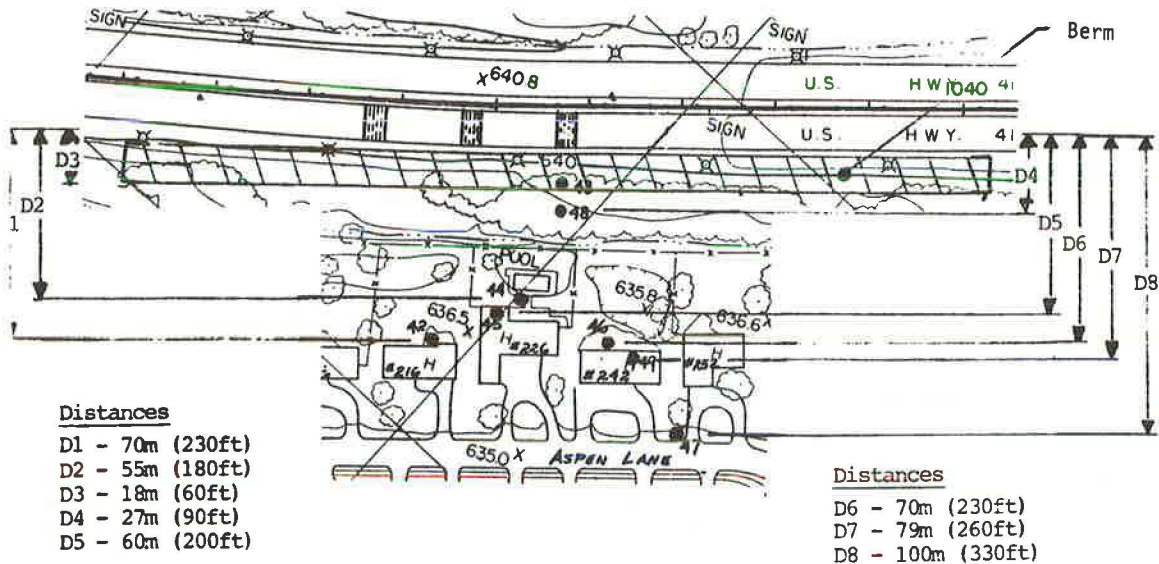


FIGURE 4 Site 2 microphone placement.

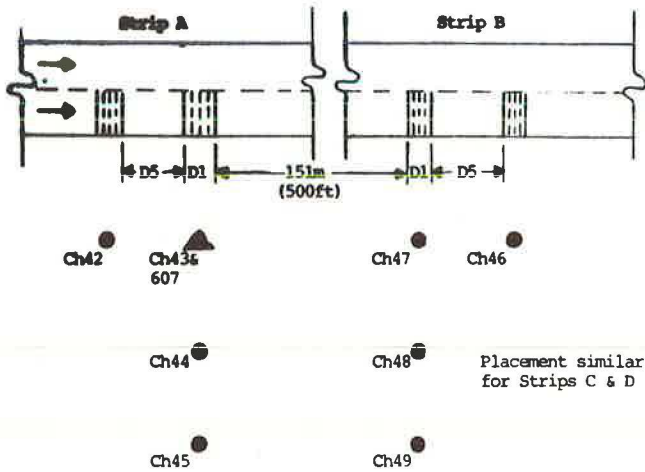


FIGURE 5 Site 3 microphone placement.

TABLE 2 Microphone Locations for Site 3

Strip	Distance (m) From Center of Rumble Strip by Channel							
	42	43	44	45	46	47	48	49
A	15	15	45	90 ^a	-	-	-	-
B	-	-	-	-	15	15	45	79 ^b
C	15	15	45	75 ^{a,b}	-	-	-	-
D	-	-	-	-	15	15	45	105

Note: 1 m = 3.28 ft.

^aOffset slightly because of electrical interference.

^bMaximum cable length reached.

sound levels and frequency distributions at each microphone location from traffic traveling on normal pavement conditions. The predicted values provide a comparison between the expected no-rumble strip condition and the rumble strip condition at each site. The models were used only at Sites 1 and 2.

Internal noise measurements were done by using a B&K impulse sound level meter. Vibrations from the steering column were obtained by using a B&K accelerometer. The vehicle steering column was chosen to measure the vibration because of the direct vi-

bration transmission from the tires, through the steering assembly, to the driver's hands. Data were recorded on a B&K FM data tape recorder. Speeds for which the noise and vibration data were taken at were 56, 65, 73, 81, and 88 km/h (35, 40, 45, 50, and 55 mph). Data were only taken up to 73 km/h (45 mph) at Site 2 because the speed limit was 65 km/h (40 mph). Data were analyzed by running the data through a B&K narrow band fast Fourier transformation (FFT) analyzer and HP chart recorder. Vibration charts were plotted by using millivolts versus frequency (hertz). Internal noise measurements were expressed in sound level [dB(A)] versus frequency (hertz).

To obtain driver perception of the vibration caused by passing over the strip, the vibration from the pavement just before going over the rumble strip was compared with that when the vehicle was on the strip. The frequency of most concern is 2 to 5 Hz, because it is the most sensitive for passenger comfort. Most vehicle suspension systems are designed to resonate at frequencies slightly higher--5 to 20 Hz (5,6).

RESULTS

Site 1, East-West Toll Road

Although three measurement periods were conducted, only two periods of data are available because of an overflow during one period. The noise levels for each channel are shown in Figure 6. The noise levels at each location are similar between the two periods. The L_{eq} at the 15-m (50-ft) microphones (Ch 43, 46, 47) was 78 dB(A), with peak noise levels ranging from 84 to 114 dB(A). The duration above the threshold level ranged from 0.5 to 2 sec. The average peak level was 90 dB(A), which lasted for 0.75 sec. The L_{eq} at the microphone placed near the untreated pavement (Ch 42) was 3 to 4 dB(A) lower than those near the strips.

The frequency distribution from 15 m away from the center strip (Ch 47) is shown in Figure 7. The A-weighted noise level is shown by the bar and numerical value next to 8-A. The bars and numerical values next to lines 14-40 show the distribution of the noise for each frequency band. In both periods the dominant frequencies were in the 80 to 160 Hz

PERIOD NO. 1

CHANNEL NO	I	LEG	L ₁	L ₅	L ₁₀	L ₅₀	L ₉₀	L ₉₉
42	I	73.7	88.0	83.0	79.0	66.0	56.0	53.0
43	I	79.7	92.0	87.0	81.0	66.0	56.0	53.0
44	I	63.9	73.0	70.0	68.0	58.0	52.0	50.0
45	I	69.0	80.0	76.0	73.0	61.0	56.0	54.0
46	I	70.0	91.0	86.0	82.0	67.0	57.0	53.0
47	I	70.6	91.0	86.0	82.0	66.0	56.0	53.0
48	I	61.7	72.0	68.0	65.0	57.0	50.0	50.0

PERIOD NO. 2

CHANNEL NO	I	LEG	L ₁	L ₅	L ₁₀	L ₅₀	L ₉₀	L ₉₉
42	I	74.7	87.0	82.0	77.0	64.0	55.0	51.0
43	I	78.4	92.0	85.0	78.0	63.0	53.0	52.0
44	I	63.1	73.0	70.0	66.0	57.0	51.0	50.0
45	I	68.2	80.0	75.0	72.0	60.0	56.0	55.0
46	I	77.6	91.0	85.0	80.0	63.0	56.0	53.0
47	I	77.3	90.0	84.0	80.0	64.0	55.0	52.0
48	I	61.2	73.0	67.0	64.0	55.0	50.0	50.0

FIGURE 6 Noise levels at Site 1.

and 315 Hz ranges. The fundamental frequency was calculated to be 161 Hz at 88 km/h (55 mph). The measured values show the fundamental frequencies as well as the harmonics.

The STAMINA 1.0 model predicted noise levels, with normal pavement, of 2 to 6 dB(A) less than the measured values. The dominant frequency range was computed to be 500 to 1,000 Hz, which was considerably higher than the measured values.

Inside the test truck, peak noise levels ranged from 75 to 92 dB(A), depending on the speed when the truck passed over the strips; the average value was 87 dB(A). The fundamental frequency was seen in both the interior noise levels and the vibration when the truck passed over the first set of grooves. A significant difference in the vibration displacement amplitude, in the 1 to 20 Hz range, was measured between the pavement just before the rumble strip and when the truck was passing over the strip. Figure 8 (6) presents this difference for the truck at 65 km/h (40 mph). A similar difference was found for all speeds tested.

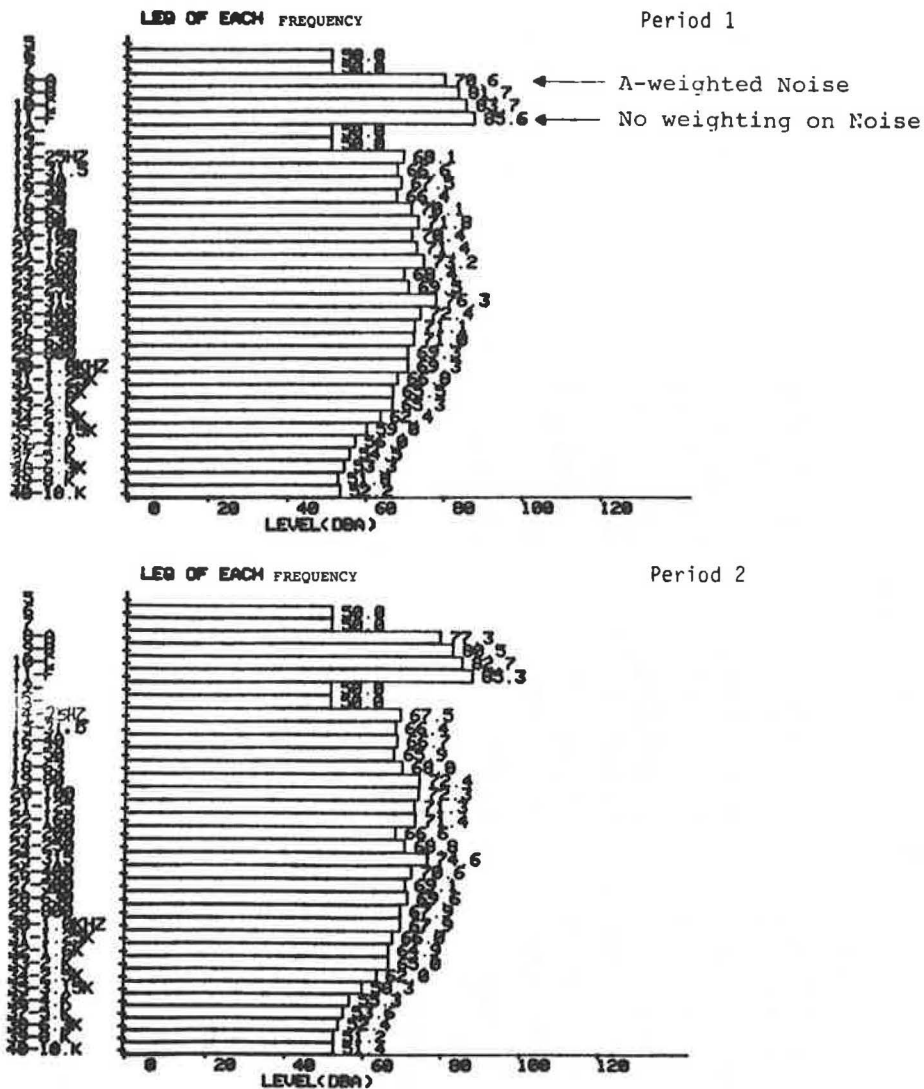


FIGURE 7 Frequency distributions (Ch 47) at Site 1.

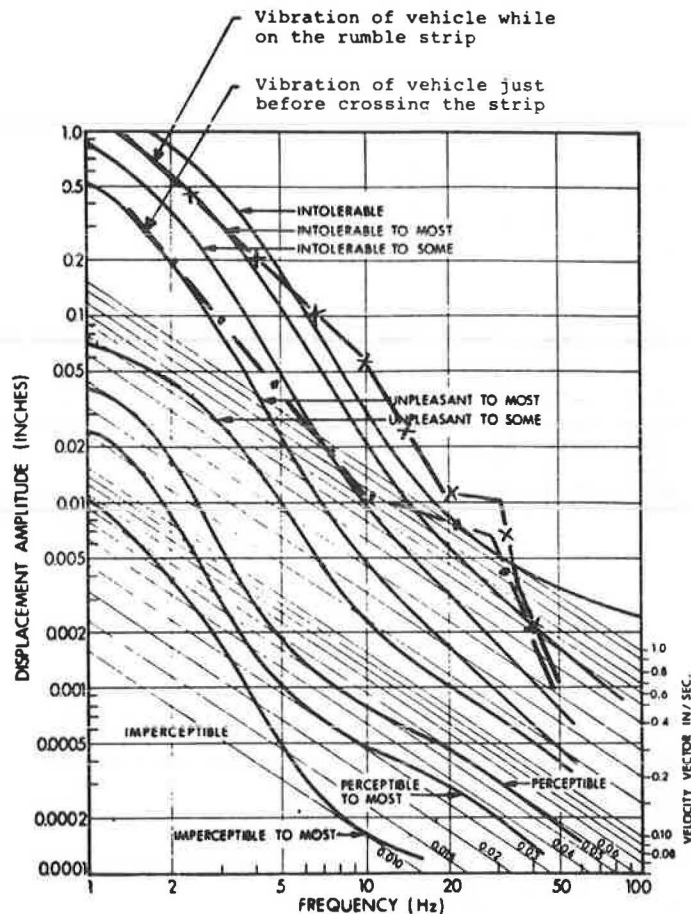


FIGURE 8 Vehicle vibration at Site 1 at 65 km/h (40 mph) (6).

PERIOD NO. 1

CHANNEL NO.	I	LEQ	L 1	L 5	L 10	L 50	L 90	L 99
42	I	61.7	67.0	66.0	65.0	61.0	56.0	54.0
43	I	79.0	88.0	85.0	83.0	75.0	68.0	63.0
44	I	61.6	67.0	65.0	64.0	61.0	58.0	56.0
45	I	58.0	58.0	58.0	58.0	58.0	58.0	58.0
46	I	61.7	69.0	65.0	64.0	60.0	57.0	55.0
47	I	58.7	64.0	61.0	60.0	58.0	56.0	55.0
48	I	58.9	67.0	64.0	62.0	58.0	52.0	50.0
49	I	58.0	58.0	58.0	58.0	58.0	58.0	58.0

Windows closed

Windows closed

PERIOD NO. 2

CHANNEL NO.	I	LEQ	L 1	L 5	L 10	L 50	L 90	L 99
42	I	62.1	68.0	66.0	65.0	61.0	57.0	54.0
43	I	79.0	87.0	85.0	83.0	76.0	68.0	63.0
44	I	62.1	68.0	66.0	64.0	61.0	58.0	56.0
45	I	56.7	62.0	59.0	58.0	56.0	53.0	54.0
46	I	61.0	68.0	65.0	64.0	61.0	57.0	55.0
47	I	58.9	68.0	64.0	62.0	58.0	56.0	55.0
48	I	58.7	67.0	64.0	63.0	58.0	53.0	50.0
49	I	54.2	59.0	58.0	57.0	53.0	50.0	50.0

Windows Open

Windows Open

PERIOD NO. 3

CHANNEL NO.	I	LEQ	L 1	L 5	L 10	L 50	L 90	L 99
42	I	61.9	67.0	66.0	65.0	61.0	57.0	55.0
43	I	79.2	88.0	85.0	83.0	76.0	68.0	61.0
44	I	61.7	66.0	65.0	64.0	61.0	57.0	55.0
45	I	57.3	62.0	59.0	58.0	56.0	54.0	53.0
46	I	61.6	66.0	65.0	64.0	61.0	57.0	55.0
47	I	61.9	67.0	62.0	61.0	59.0	57.0	56.0
48	I	59.1	65.0	63.0	62.0	58.0	52.0	50.0
49	I	54.6	60.0	58.0	57.0	54.0	50.0	50.0

Windows Open

Windows Open

FIGURE 9 Noise levels at Site 2.

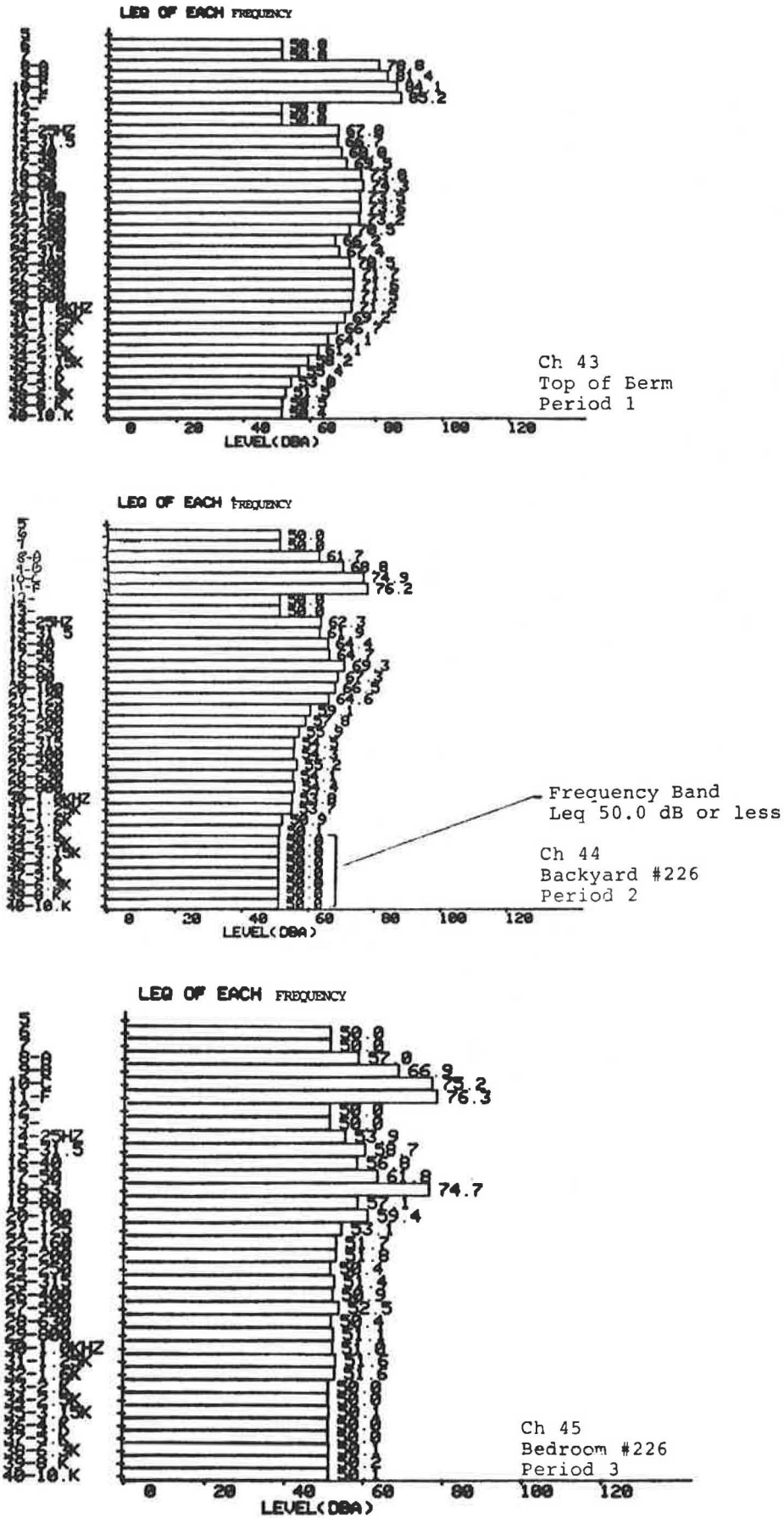


FIGURE 10 Frequency distributions at Site 2.

Site 2, Edens Expressway

Three measurement periods were successfully completed at Site 2. The noise levels at each location were consistent over the three periods; they are shown in Figure 9. The measured L_{eq} in the backyards (Ch 42, 44, 46) was in the low 60s. In the bedrooms (Ch 45, 49) with the windows opened the L_{eq} was in the high 50s; with the windows closed the L_{eq} was less than 50 dB(A). By using the FHWA procedure (2), the berm insertion loss was computed at 10 dB(A), which agrees well with computations by IDOT and an independent consultant.

The frequency measured on top of the berm (Ch 43) was in the ranges of 63 to 160 Hz and 500 to 1,000 Hz. In the backyard (Ch 44) the berm effectively reduced the high frequency noise but did little to the lower frequency noise. In the bedroom (Ch 45, windows open), the low frequency noise was the most significant contributor (75 dB). Taking into account the A-weighted scale, the noise would be 50 dB(A), enough to disturb a person sleeping. Figure 10 shows the frequency distribution at the three locations.

The STAMINA 1.0 model predicted noise levels, with normal pavement, of 2 to 7 dB(A) less than were measured, with the majority of the noise occurring in the 250, 500, and 1,000 Hz octave bands.

Inside the semitrailer the peak noise ranged from 80 to 86 dB(A). The fundamental frequency that was calculated for this set of strips ranged from 53 to 84 Hz, depending on vehicle speed. Many harmonics were created as the vehicle passed over the strips, but they were not as distinct as those created by

the strips at Site 1. The vibration created by the pavement just before the strips was similar to that found while on the strips. There was not a significant change in the displacement amplitude between the two in the 1 to 20 Hz range for the speeds tested. Figure 11 (6) shows this difference for the truck at 65 km/h (40 mph).

Site 3, US-12

All outside measurements were completed satisfactorily. No inside vibration or peak noise levels were available because of an equipment malfunction. The peak noise levels measured from the truck (Ch 42, 43, 46, 47) ranged from 78 to 84 dB(A), depending on speed. Figure 12 shows the average peak noise levels from the semitrailer at 15 and 45 m (50 and 150 ft) from the rumble strips. The average peak noise levels measured by the 607 were approximately 1 to 2 dB(A) higher than those measured by the computer and had an average duration above the threshold [75 dB(A)] of 2 sec. The test automobile had peak noise levels about 3 dB(A) less than those of the truck, and the duration greater than the threshold was about 0.5 sec.

Frequency measurements were conducted on strips A and C. The dominant frequency range at strip A was measured in the 63 to 84 Hz range, depending on vehicle speed. The calculated fundamental frequency ranged from 50 to 80 Hz. The dominant frequency range at strip C was measured in the 50 to 100 Hz range, depending on vehicle speed. The calculated

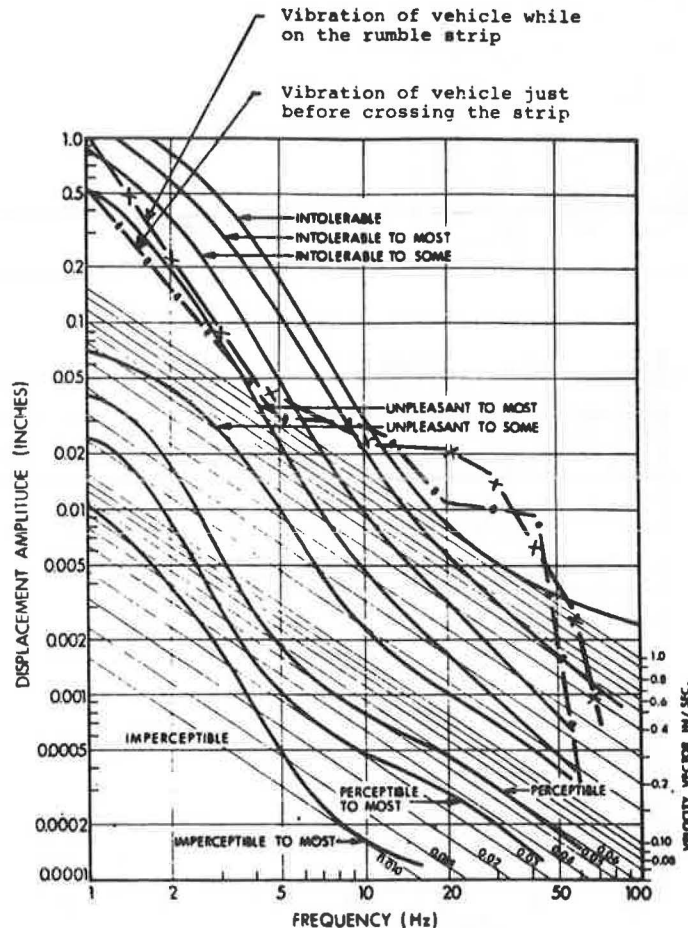


FIGURE 11 Vehicle vibration at Site 2 at 65 km/h (40 mph) (6).

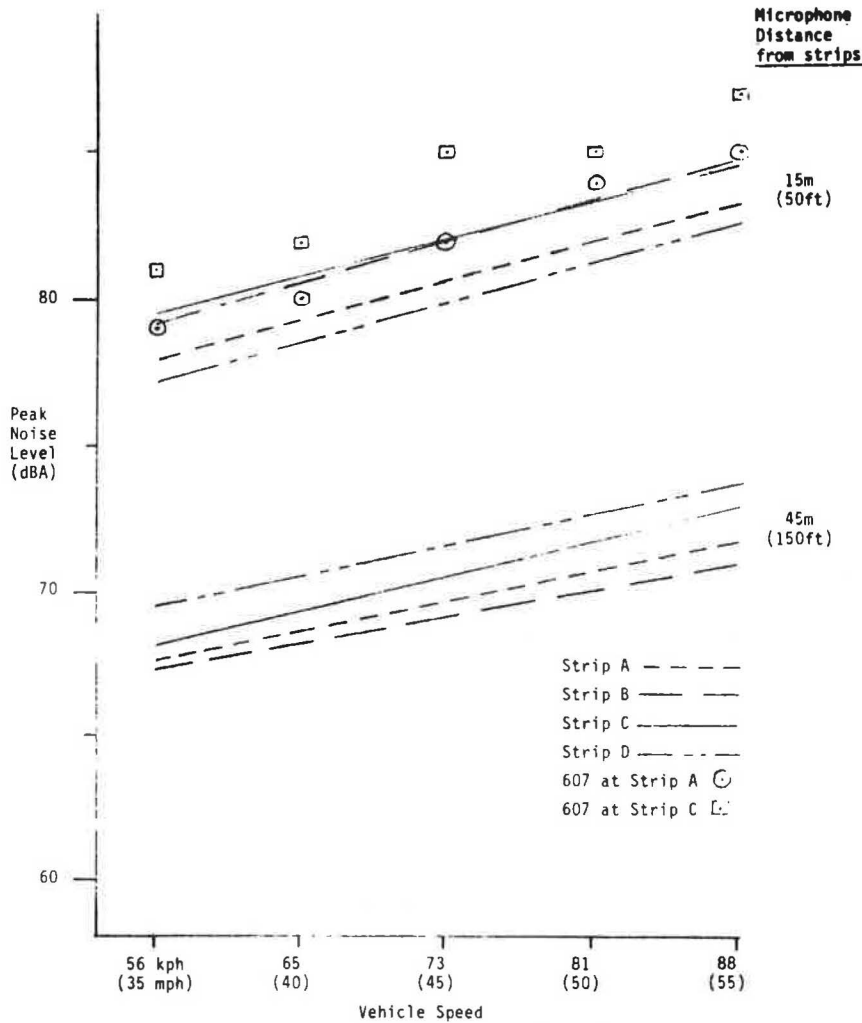


FIGURE 12 Average peak noise levels at Site 3.

fundamental frequency range is the same as that for strip A.

Although the inside equipment malfunctioned, the record level meter settings and the subjective responses from the driver and passengers indicated that strip C produced significant driver perception at the lower speeds tested [56, 65, and 74 km/h (35, 40, and 45 mph)], and strip D produced significant perception at the higher speeds tested [80 and 88 km/h (50 and 55 mph)].

SUMMARY AND CONCLUSIONS

Although this study was limited, enough information was obtained to establish that rumble strips create a noise that is different from normal traffic noise. Because of this, the highway designer should be aware of strip placement when near a residential area.

The following is a list of other conclusions reached in this study.

1. A rumble strip produces a low frequency noise that can increase the L_{eq} noise levels by up to 6 or 7 dB(A) over noise levels produced by traffic on normal pavement.

2. A berm can significantly reduce high frequency noise, but it is not effective in reducing

low frequency noise, such as that produced by a vehicle passing over a rumble strip.

3. A rumble strip that is formed rather than cut into the pavement creates better driver perception.

4. The groove center-to-center distance has some effect on driver perception. Smaller center-to-center distances appear to be more effective on vehicles traveling at higher speeds.

5. The outside noise, which adjacent property owners will hear, does not significantly vary with strip configuration.

6. The outside noise created by an automobile passing over a strip is slightly less than that created by a truck passby. The duration of the noise is much shorter than the duration of a truck.

7. The addition of rumble strips on the Edens Expressway appears to have reduced the number and severity of accidents.

REFERENCES

1. Task Force Report: U.S. Route 41 at Clavey Road. Illinois Department of Transportation, Springfield, June 1983.
2. W. Bowlby, ed. Sound Procedures for Measuring Highway Noise: Final Report. Report FHWA-DP-45-1R. FHWA, U.S. Department of Transportation, Aug. 1981.

3. F.F. Rudder, D.F. Lam, and P. Chueng. User's Manual: FHWA Level 2 Highway Traffic Noise Prediction Model, STAMINA 1.0. Report FHWA-RD-78-138. FHWA, U.S. Department of Transportation, May 1979.
4. W. Bowlby et al., eds. Noise Barrier Cost Reduction Procedure, STAMINA 2.0/OPTIMA: User's Manual. Report FHWA-DP-58-1. FHWA, U.S. Department of Transportation, Aug. 1981.
5. F.F. Rudder. Engineering Guidelines for the Analysis of Traffic-Induced Vibration. Report

FHWA-RD-78-166. FHWA, U.S. Department of Transportation, Feb. 1978.

6. D.T. Wright and R. Green. Human Sensitivity to Vibrations. Report 7. Department of Civil Engineering, Queen's University, Kingston, Ontario, Canada, Feb. 1959.

Publication of this paper sponsored by Committee on Transportation-Related Noise and Vibration.

Examination of the Dependence of Diesel-Electric Locomotive Noise Emission on Speed, Rated Power, and Age

ERIC STUSNICK

ABSTRACT

A statistical analysis was conducted of an FRA data base of locomotive passby noise levels to determine the dependence of diesel-electric locomotive noise emission on speed, rated power, and age. Although a statistically significant dependence on locomotive speed was determined, the data set did not indicate a significant dependence on rated horsepower or age. Reasons for this finding are discussed.

Federal noise emission standards for moving locomotives in line-haul service limit the maximum A-weighted passby sound level at 100 ft to 96 dB for locomotives manufactured before December 31, 1979, and to 90 dB for locomotives manufactured after that date (40 CFR Part 201). Most existing locomotives meet this standard.

Recent efforts to improve fuel economy are leading the diesel-electric locomotive manufacturing industry to design diesel engines with higher rated power than is currently used. There is some concern that locomotives with such engines will not be able to meet the federal noise emission standard. At the time of the development of the noise emission standards, fuel economy was not an important issue.

In addition, there is concern that the noise emissions of a diesel-electric locomotive may increase as the unit ages. If this occurs, then a locomotive that just meets the standard when new may not meet the standard when older.

In order to put some of these concerns in perspective, a study was carried out to examine the

dependence of diesel-electric locomotive noise emission on locomotive speed, rated power, and age.

SOUND LEVEL AS A FUNCTION OF SPEED

The data base used in this study was a computerized listing of locomotive passby sound levels measured by the Office of Safety of the FRA during the period from September 1978 to June 1981. It contained measurements of maximum A-weighted sound levels at 100 ft for 379 single- and multiple-locomotive passbys. Figure 1 shows the distribution of sound levels, which ranged from 69 to 97 dB (1).

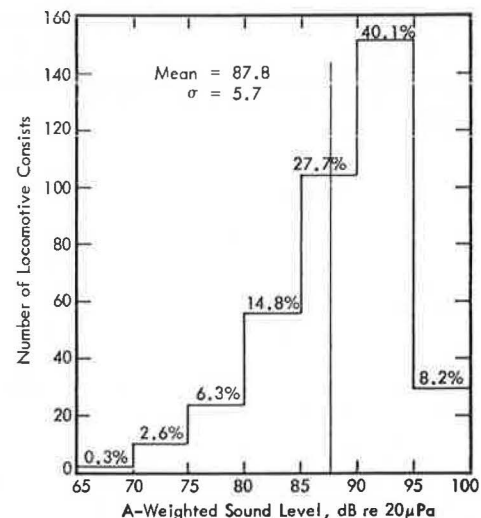


FIGURE 1 Distribution of sound levels for moving locomotive consists.

The data in Table 1 give the range, mean value, and standard deviation of these sound levels as a function of the number of units in the consist. The sound level does not increase with the number of units in the consist, as might be expected. However, note that many of the variables that affect noise emission, such as the power settings of the units, are unknown in these samples. These uncontrolled variables presumably play a more important role in determining the peak sound level than does the number of units.

TABLE 1 Range, Mean Value, and Standard Deviation of A-Weighted Sound Levels of Moving Locomotive Consists

Number of Units In Consist	Number of Samples	A-Weighted Sound Level At 100 Feet (dB re 20μPa)			
		Min.	Max.	Mean	σ
1	153	70	96	88.1	4.8
2	97	70	96	87.4	6.0
3	82	70	96	88.6	5.7
4	30	69	97	85.9	7.6
5	9	74	94	84.8	7.4
6	8	83	96	87.8	5.7
ANY	379	69	97	87.8	5.7

Figure 2 shows the relationship between the maximum A-weighted passby sound level (L_A) and the logarithm of the locomotive speed (V) for a 260-element subset of the FRA data base for which the locomotive speed was known. The corresponding linear regression curve, the standard error of estimate (σ), and the correlation coefficient (r) are also given. A correlation coefficient of +1 or -1 indicates an exact linear relationship between the two variables. A correlation coefficient of zero indicates that no relationship between the two variables exists.

Because the correlation coefficient indicated in the figure is an estimate (based on the 260 sets of measurements) of the actual correlation coefficient that would be found if an infinite number of sets of measurements could be examined, a statistical test must be used to judge whether it is reasonable to assume that the two variables are independent. One such test (2) compares the estimated correlation coefficient with a critical value, which is a function of both the number of sets of measurements and the degree of confidence desired. For 260 sets of measurements and a confidence level of 95 percent, Table A-30a in the work by Dixon and Massey (2) indicates the critical value of the correlation coefficient to be 0.12. Because the observed correlation coefficient of 0.520 exceeds this critical value, a statistically significant dependence of L_A on $\log_{10}V$ is indicated.

In examining Figure 2 note that the scatter of points about the regression line is quite large. Assuming this scatter to be normally distributed, 95 percent of the measurements lie within ± 9.8 dB (2σ) of the regression line. Thus the measured points essentially occupy a 20-dB-wide band.

SOUND LEVEL AS A FUNCTION OF RATED POWER AND AGE

To investigate the dependence of maximum passby sound level on rated power and age, a 40-element subset of the FRA data base was selected. It con-

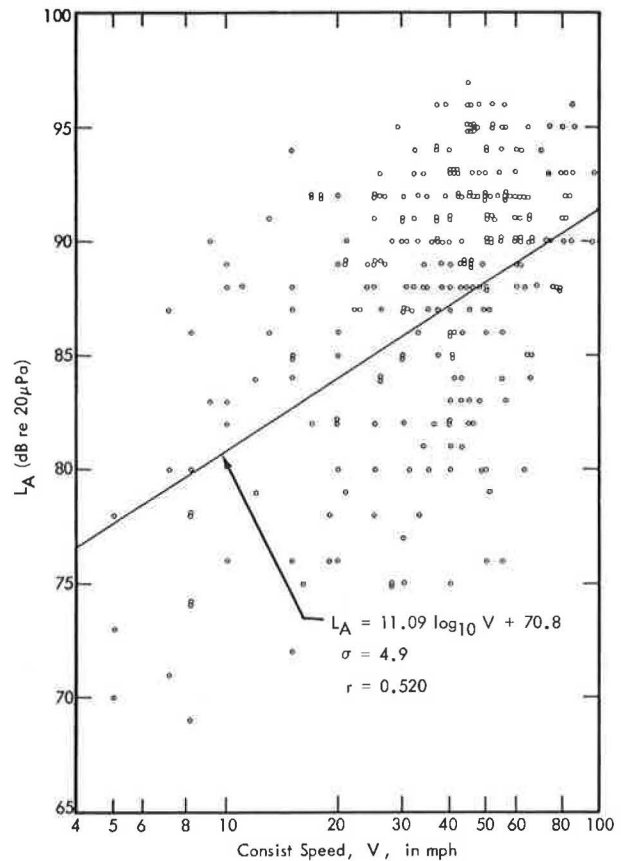


FIGURE 2 Maximum A-weighted sound level of locomotive consist passbys as a function of locomotive speed (V) (measurements at 100 ft).

sisted of single locomotive passbys for which both locomotive speed and identification were known. The rated power and year of manufacture of each locomotive were obtained from the railroad company that owned the locomotive.

Linear regressions were carried out considering the passby sound level as a function of the two independent variables--rated power (P) and age (A)--and as a function of the two derived variables-- $\log_{10}V$ and $\log_{10}P$. The correlation coefficient for each regression is given in Table 2.

TABLE 2 Correlation Coefficients of L_A with Locomotive Speed (V), Rated Power (P), and Age (A)

Independent Variable	Correlation Coefficient
P	0.23
A	-0.11
$\log_{10} V$	0.36
$\log_{10} P$	0.23

As described in the previous section, these correlation coefficients can be used to test for the independence of L_A on each of the dependent variables. For 40 sets of measurements and a confidence

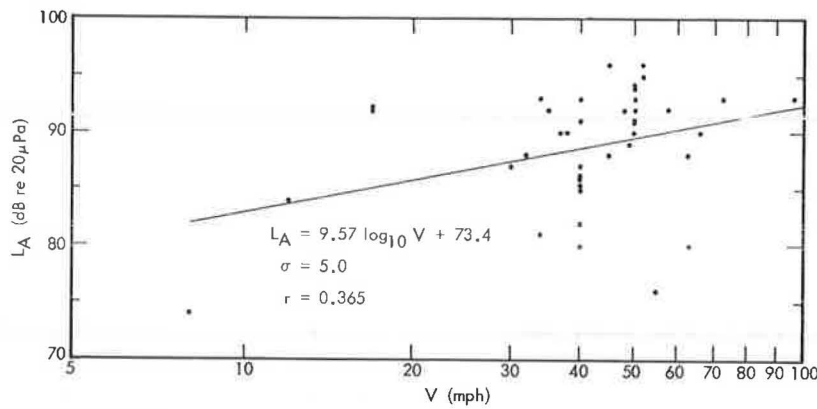


FIGURE 3 Maximum A-weighted sound level of single locomotive passbys as a function of locomotive speed (V) (measurements at 100 ft).

level of 95 percent, Table A-30a (2) indicates the critical value of the correlation coefficient to be 0.31. Applying this criterion to the values in Table 2, it is seen that, at the 95 percent confidence level, L_A is only dependent on the $\log_{10}V$ variable.

The linear regression of L_A with $\log_{10}V$ for the subset of single locomotive passbys is shown in Figure 3. The corresponding regression equation, the

standard error of estimate (σ), and the correlation coefficient (r) for this subset of the data are also given. The dependence on $\log_{10}V$ is similar to that obtained in Figure 2 for the overall data base. The scatter of the data about the regression line is also similar.

Regressions of L_A with P and of L_A with A are shown in Figures 4 and 5, respectively. It is clear from the figures why dependence of the two variables cannot be statistically justified. The large scatter of data points coupled with the small slope of the regression curves cannot preclude a zero slope, which would indicate independence of the two variables.

Note that in Figure 5 the regression line indicates a decrease of passby sound level with increasing locomotive age. This is contrary to what might be expected; however, further examination of the data indicates a possible explanation. The correlation coefficient between rated power and locomotive age is 0.70, so that in this data set these two variables are not independent. Figure 6 shows the linear regression between these two variables. The older locomotives in this data set have lower rated power than do the newer locomotives. If indeed noise emission does increase with rated power, then it would be expected that this data set would indicate a decrease in passby level with age, because most of the older locomotives have lower rated power than the newer ones.

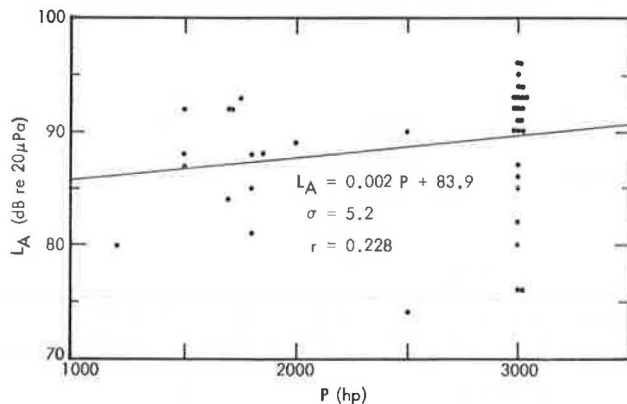


FIGURE 4 Maximum A-weighted sound level of single locomotive passbys as a function of rated power (P) (measurements at 100 ft).

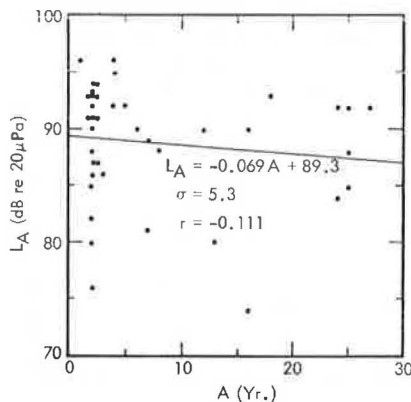


FIGURE 5 Maximum A-weighted sound level of single locomotive passbys as a function of locomotive age (A) (measurements at 100 ft).

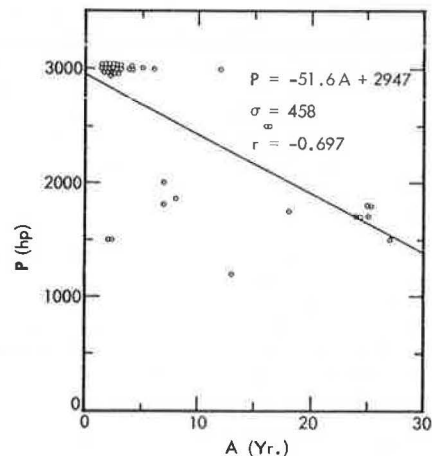


FIGURE 6 Linear regression of rated horsepower (P) with locomotive age (A) for subset of data used in this analysis.

These single-variable analyses ignore the fact that the sound level may be a function of several variables. To consider this case, a multiple linear regression was carried out by using $\log_{10}V$, P , and A as three independent variables. The results of this analysis are given in Table 3. Note that the multiple correlation coefficient (0.42) is larger than any of the values in Table 2, thus indicating a slightly better fit to the data.

TABLE 3 Multiple Linear Regression of L_A as a Function of the Logarithm of Speed, Rated Power, and Age

Regression Equation:			
$L_A = 10.15 \log_{10} V + 0.0022 P + 0.157 A + 65.6$			
Independent Variable	Regression Coefficient	Standard Error of Reg. Coefficient	t-Value
$\log_{10} V$	10.15	4.50	2.26
P	0.002	0.002	1.25
A	0.157	0.138	1.14
Multiple Correlation Coefficient: 0.42 Standard Error of Estimate: 5.0			

In Table 3 the associated standard error and t-value for each regression coefficient are also given. The standard error is a measure of the uncertainty in the regression coefficient; the t-value is a related parameter that can be used to test the hypothesis that the fitted variable (L_A in this case) is independent of the indicated independent variable. By using a procedure similar to that which was described for correlation coefficients, the computed t-value for each independent variable is compared with a critical value that depends on the number of sets of measurements, the number of independent variables in the best-fit equation, and the degree of confidence desired (2). In this case Table A-5 (2) indicates the critical t-value at a 95 percent confidence level to be 2.02.

The data in Table 3 also indicate that only the $\log_{10}V$ variable has a t-value exceeding this critical value. Thus, as in the single-variable analysis, there is only statistical justification (at the 95 percent confidence level) for identifying $\log_{10}V$ as the variable on which L_A depends.

Even though there is no real statistical justification shown in this data base for assuming a dependence of L_A on rated power, it is interesting to note that the best-fit regression equations for P in both the single variable (Figure 4) and the multiple variable (Table 3) analyses indicate an increase in L_A of 0.2 dB with each 100 hp increase in rated power. The standard error in this regression coefficient is of comparable size; thus there is a 95 percent probability that the rate of change of L_A with P is between -0.2 and 0.6 dB per 100 hp.

CONCLUSIONS

A statistically significant dependence on locomotive

speed of the maximum A-weighted sound level during a single locomotive passby has been found. No statistically significant dependence on rated power or age was found for the data set studied.

In interpreting these data, the analyst should be careful to avoid concluding that there is no dependence of locomotive sound level on rated power or on age. Rather, it is more correct to say that this data set has not indicated that there is such a dependence. Because of the necessity to consider only single locomotive passbys (most measured passbys are of multiple-locomotive consists), the data set is quite small. In addition, many variables that may affect the measured sound level, such as throttle setting, load, and the existence of turbocharging, were not considered in the regression. Finally, the normal unit-to-unit variation of sound level for the same locomotive model adds a certain amount of dispersion to the data.

For example, 15 of the 40 measurements in the data set were of different units of the same locomotive model. These 15 units were each rated at 3,000 hp and were each manufactured in 1979. The sound levels of seven of the units were measured while the locomotive was moving at 40 mph; that of seven others were measured at 50 mph. The standard deviation of the measurements at 40 mph was 4.6 dB, and that of the measurements at 50 mph was 1.6 dB. Such large variations in sound level for the same conditions of speed, rated power, and age are indicative of dependences on other unconsidered variables.

In order to further test the dependence of maximum A-weighted passby sound level on the rated power and age of the locomotive, it is necessary to obtain a data base of such sound levels in which throttle setting, load, and turbocharging are also accounted for, as well as speed, rated power, and age.

ACKNOWLEDGMENTS

The statistical analysis of the overall FRA data base was carried out as part of the preparation of a handbook on railroad noise for the Transportation Systems Center, U.S. Department of Transportation, and sponsored by the FRA. The analysis of the single-locomotive subset of this data base and the preparation of this paper was supported by the Association of American Railroads.

REFERENCES

1. E. Stusnick, M.L. Montroll, K.J. Plotkin, and V.K. Kohli. Handbook for the Measurement, Analysis, and Abatement of Railroad Noise. Report DOT/FRA/ORD-82/02-H. FRA, U.S. Department of Transportation, Jan. 1982. NTIS: PB 83-166173.
2. W.J. Dixon and F.J. Massey, Jr. Introduction to Statistical Analysis. McGraw-Hill, New York, 1957, pp. 196-200.

Publication of this paper sponsored by Committee on Transportation-Related Noise and Vibration.

Noise Impact of Rail Passenger Service

MAS HATANO

ABSTRACT

The California Department of Transportation (Caltrans) petitioned the California Public Utilities Commission (PUC) to allow the National Railroad Passenger Corporation (Amtrak) to increase their train speed limit from 65 to 90 mph between Los Angeles and San Diego. The city of Montebello, which had recently constructed a noise barrier that allegedly reduced the train noise from 95 to 75 dB(A) at the adjacent residences, protested the increase because of the belief that the increase in train speed would negate part of the benefit provided by the barrier. Caltrans performed noise measurements behind and beyond the end of the barrier in Montebello. Measurements were also made in an open area near Galivan in Orange County, where the Amtrak train could travel at 90 mph. Conclusions from this study indicated that the noise barrier in Montebello provided about 13 dB(A) attenuation. An increase in train speed from 65 to 90 mph would increase the noise from 74 to 78 dB(A) behind the barrier. However, the exposure time would decrease from 6 to 3 sec at the higher speed. Twelve Amtrak passenger trains operate between 7:30 a.m. and 9:05 p.m. through Montebello. Other noise from sources such as switching of freight cars on nearby tracks, and operation of freight trains and engines, motorcycles, airplanes, and delivery trucks ranged from 71 to 82 dB(A). The highest train whistle recorded was 99 dB(A). These noise levels were all measured behind the noise barrier. Discussions with residents behind the barrier indicated they were bothered by noises previously mentioned that occurred on a regular basis at night. The noise from the Amtrak train was a small part of the noise environment. The PUC granted Amtrak permission to operate at 90 mph between Los Angeles and San Diego based on the information presented in this study.

The work described in this paper was initiated by the Division of Mass Transportation, California Department of Transportation (Caltrans), which was responding to a request of the California Public Utilities Commission (PUC). The Caltrans Office of Transportation Laboratory (TransLab), in turn, was requested to measure passenger train noise and determine any impact when passenger train speeds are increased.

Information concerning noise impacts created by increasing train speeds from 65 to 90 mph was requested by the city of Montebello. The city had recently constructed a noise wall next to the railroad tracks along Sycamore Street, and there was concern that the efforts might be negated if the noise increased significantly because of the increased speed.

Noise measurements were made of the rail pas-

senger service operating between Los Angeles and San Diego. Test sites were located in Montebello along Sycamore Street to evaluate the noise wall and near Galivan in Orange County to evaluate the effects of speed (Figure 1).



FIGURE 1 Location map of Montebello and Galivan sites.

All noise measurements were made on the A scale and denoted as dB(A). This means that the measured noise level is comparable to that perceived by the normal human ear. Noise is expressed in terms of peak levels.

INSTRUMENTATION

The following types and quantities of equipment were used in conducting the measurements used in this study:

1. Two B&K 2206 type 1 sound level meters (SLMs),
2. Two B&K 2203 graphic level recorders (GLRs),
3. One B&K 4230 calibrator,
4. Two foam windscreens,
5. Two radar speedometers (Decatur Electronics), and
6. One wind measuring set (Belfort Instrument Company).

The calibrator, SLMs, and GLRs were checked at TransLab before they were taken to the field. Calibration checks on the SLM and GLR systems were made periodically during the measurement periods. (Records of calibration for all sound instruments are on file at TransLab.) The radar speedometers were also calibrated periodically in the field by using tuning forks.

Noise measurements are affected by wind speeds greater than 12 mph. A wind measuring set was used to periodically ensure that speeds were less than this level.

GALIVAN LOCATION

An open area near Galivan, in the vicinity of Mission Viejo in Orange County, was selected to determine changes in noise levels caused by increasing the passenger train speeds from 65 to 90 mph. The site was an area without vegetation and included an old two-lane concrete highway. There is one main

track of jointed-rail construction for through traffic in this area and one track that serves as a siding for meeting and passing trains. Current regulations permit passenger trains to travel 90 mph at this location.

SLMs were located 50 and 100 ft from the centerline of the tracks at an elevation of 4 ft above the top of rails. The purpose of the two meters was to determine the decrease in noise due to an increase in distance. These data were used to analyze noise levels at varying distances from the noise source at speeds between 65 to 90 mph, where the terrain is comparable to that in Montebello.

Measurements were made on February 14, 1979. The weather was clear, except for some scattered clouds. The temperature was estimated at 60° to 70°F. Wind speeds were measured at 2 to 5 mph.

All peak noise levels were taken from the graphic level recordings and reported to the closest 0.5 dB(A). Figure 2 shows example graphic level recordings from the Galivan location.

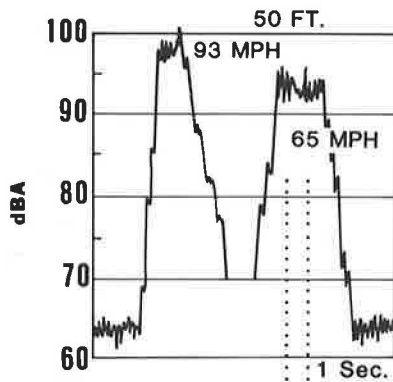


FIGURE 2 Noise level variation with speed.

Train speeds were determined by using two radar speedometers for reliability. The data are given in Table 1 and are plotted in Figure 3.

A regression line was drawn to approximate the estimated increase in noise caused by changes in speed at 50 and 100 ft from the tracks. The data indicate a noise decrease of 4.5 dB(A) as the distance is doubled from 50 to 100 ft. Also, the noise increases 4.5 dB(A) from 65 to 90 mph.

The ambient noise level in this area ranged from 60 to 73 dB(A). This noise was produced by the I-5 freeway near, and due east of, the measurement site. Occasional noise was produced by vehicles using the old highway.

An examination and analysis of the graphic level recordings indicated the peak noise reached a maximum and continued for approximately 6 sec. This

TABLE 1 Decreases in Noise Levels with Distance

Time of Day	Train Speed (mph)	Train Length (cars)	Noise Level [dB(A)] at	
			50 ft	100 ft
8:30 a.m.	72	6	98	92
9:43 a.m.	93	4	101	96
10:00 a.m.	84	4	100	96
11:40 a.m.	65	4	95	92
2:28 p.m.	63	4	96	90
2:44 p.m.	90	5	99	93
Avg	78		98	93

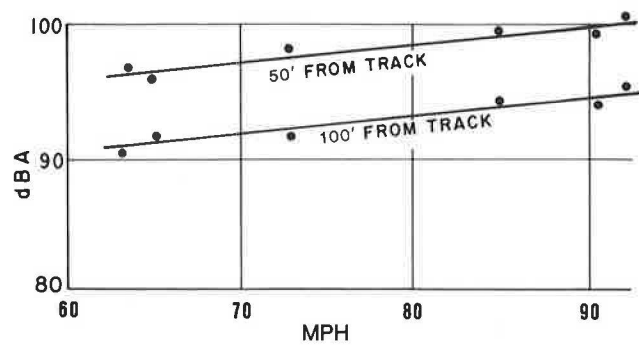


FIGURE 3 Level versus train speed.

occurred when the train speed was 65 mph and the distance from the SLM to the train was 100 ft. The maximum levels were reached and remained for approximately 3 sec at a speed of 90 mph.

MONTEBELLO LOCATIONS

Locations were selected behind the noise wall in Montebello. Two of the locations are shown on the map in Figure 4. Figure 5 shows a typical cross section of the sites behind the noise wall. These sites were far enough from the end of the wall to minimize the noise coming from beyond the end of the wall. There are two main tracks (northbound and southbound) in this area that are of continuously welded rail construction.

Measurements were made at Sycamore and Spruce streets on February 13, 1979. The weather was clear, except for scattered clouds. The temperature was

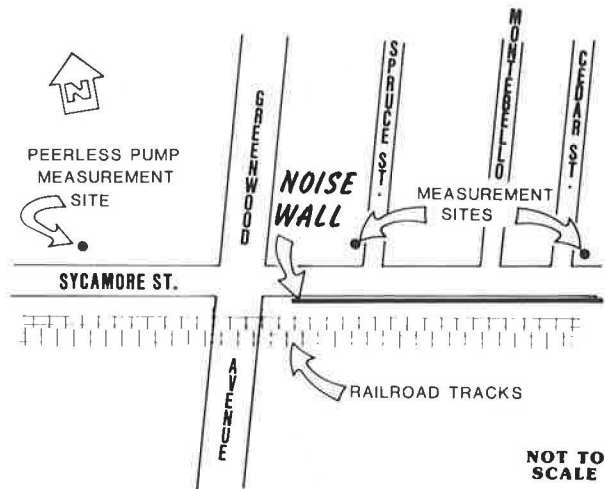


FIGURE 4 Plan of measurement sites in Montebello.

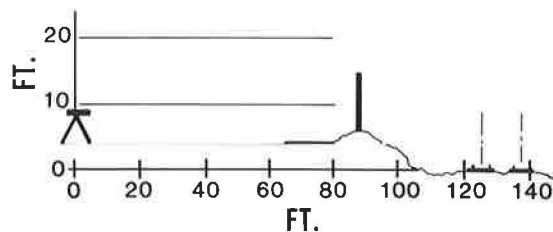


FIGURE 5 Cross section of Montebello site.

estimated at 60° to 70°F. Wind speeds were measured at 2 to 5 mph.

Supplementary measurements were made at Sycamore and Cedar streets on February 15, 1979. Weather conditions were approximately the same as February 13.

A third location was selected in an open area in front of the Peerless Pump Company facility on Sycamore Street north of Greenwood Avenue (Figure 4). There are four sets of tracks in this area, and the main tracks are of continuously welded rail construction. Two other tracks serve as sidings. The measurements at this location also were made on February 13, 1979.

The purpose of the measurements at the three locations was to assess the ambient noise level, passenger train noise, other train noise, noise attenuation because of the sound wall, and any increase in noise from trains traveling at 90 mph. The test data for the various Montebello sites are given in Table 2.

TABLE 2 Montebello Noise Wall Attenuation of Passenger Train Noise

Time of Day	Train Speed (mph)	Train Length (cars)	Noise Level [dB(A)]		
			Behind Wall	Open Area	Attenuation
8:50 a.m.	66	4	74	88	14
9:15 a.m.	67	6	95 ^a	-	-
			74	86	12
10:50 a.m.	63	4	74	87	13
11:50 a.m.	66	4	92 ^a	-	-
			76	85	9
3:15 p.m.	63	4	73	88	15
4:05 p.m.	64	4	74	89	15
Avg	65		74	87	13

Note: Distance from sound level meter to train averaged 127 ft.

^aWhistle.

The following table gives data that compare the noise levels at the Orange County site and the open area site in Montebello:

	Train Speed (mph)	100-ft Noise Level [dB(A)]
Open area in Orange County (Galivan)	64	91
Open area in Montebello	65	87

Adjustments to the noise level in Montebello were made based on a 4.5 dB(A) drop-off for a doubling of distance.

The slightly lower levels in Montebello were caused by the continuously welded rail construction of the track. These data reinforced the assumption that the noise level without the wall along Sycamore Street would be about the same as the noise level at the adjacent open area [87 dB(A)]. Because the measured noise levels behind the wall were about 74 dB(A), the attenuation provided by the wall is approximately 13 dB(A).

OTHER MEASUREMENTS BEHIND THE NOISE WALL

Noise measurements were also taken at Sycamore and Spruce streets on February 13 to assess the neighborhood environmental noise. The data are given in the following table:

Noise	Noise Level [dB(A)]
Automobile	70
Jet aircraft	73
Delivery Truck	77
Freight train	82
Train whistle	99

The noise levels represent the maximum levels recorded between the passing of passenger trains. These and other noise sources intermittently disturbed the quiet of the neighborhood, but they were usually lower than the maximum values shown.

DISCUSSION OF RESULTS

There are currently 12 National Railroad Passenger Corporation (Amtrak) passenger trains operating Monday through Friday between Los Angeles and San Diego (6 in each direction). The first leaves San Diego at 11:05 p.m. All 12 Amtrak trains pass through Montebello between 7:30 a.m. and 9:05 p.m. On weekends, one less train per day is operated.

Passenger train noise measurements at the Galivan site in Orange County indicated an increase of 4.5 dB(A) as the speed increased from 65 to 90 mph. The increase in noise in Montebello behind the wall should be less than 4.5 dB(A) because the trackage is of continuously welded rail construction. This increase, however, will generally occur during the nonsleeping hours and will be about equal to and a part of the neighborhood environmental noise (as shown in the preceding table).

An increase of 2 to 3 dB(A) would hardly be noticeable to most people when the change occurs from one day to the next. An increase of 10 dB(A) doubles the noise level as perceived by the human ear. An increase of 4.5 dB(A) would probably be noticeable.

The engine and rail noise are the primary noise sources from a passenger train. Usually the engine is noisier, but this was not confirmed because the Amtrak passenger train was traveling at high speeds and was pulling only four to six cars. The two noise sources could not be separated or detected on the graphic recordings.

Subjectively, the measurement team could not clearly ascertain if the noise level at 90 mph was significantly louder than at 65 mph. This probably was due to the train whistle, which was the dominant noise source that affected the perception of the lower level engine and rail noise. The engineer blew the whistle whenever he saw anyone near the tracks or when he approached a grade crossing of a street or highway.

The train whistle is not affected by speed. Based on the previous discussion, it appears that the whistle will continue to dominate neighborhood noise in Montebello behind the noise wall.

One resident living near Sycamore and Spruce streets indicated that the noise wall helped keep the noise level down. He noted, however, that the most annoying and loud noise occurred at night during the sleeping hours when the freight cars were being coupled, uncoupled, and switched.

CONCLUSIONS

The following conclusions are reached as a result of this study.

1. The passenger train noise increased approximately 4.5 dB(A) when train speeds increased from 65 to 90 mph over jointed rails.
2. At a train speed of 65 mph, the noise level

at 100 ft reached a maximum level and remained constant for approximately 6 sec.

3. At a train speed of 90 mph the noise level at 100 ft reached a maximum level and remained constant for approximately 3 sec.

4. The noise level behind the noise wall in Montebello was 74 dB(A) when the passenger train speed was 65 mph.

5. Because of continuously welded rail construction of the trackage in Montebello, the noise level is expected to increase less than 4.5 dB(A) if the speed is increased to 90 mph.

6. The noise wall in Montebello along Sycamore Street provides approximately 13 dB(A) attenuation.

7. Other noise from sources (such as switching of freight cars, freight trains, and engines; passing cars; motorcycles; delivery trucks; and airplanes) ranged from 71 to 82 dB(A). The highest train whistle noise recorded was 99 dB(A). These levels were measured behind the wall at the intersection of Spruce and Sycamore streets in Montebello.

Publication of this paper sponsored by Committee on Transportation-Related Noise and Vibration.

Synthesis of Disc Brake Squeal Quieting Experience

MICHAEL A. STAIANO

ABSTRACT

Disc brake squeal produced by Washington Metropolitan Area Transit Authority transit cars precipitated a number of on-car and laboratory tests. The results of these tests are summarized along with the experience of other investigators in both the transit and automotive fields. Experience indicates that some brake systems are prone to squeal while others are not, and that the benefit of system modifications varies dramatically for different disc brake systems. Modifications that hold the most promise for reducing the propensity of a brake system to squeal are sufficiently damping the brake pad backplate, disc rotor, or caliper; altering disc rotor stiffness, caliper mass, or caliper stiffness; reducing (if possible) the brake pad friction coefficient; and, possibly, eliminating brake pad grooves.

The existence of brake squeal has been recognized as a problem for some time primarily because of its occurrence in highway vehicle drum and disc brake systems. Rail transit cars have also exhibited brake squeal from their tread and disc brakes. In the United States three transit systems use disc brakes: the San Francisco Bay Area Rapid Transit District (BART), the Chicago Transit Authority (CTA), and the Washington Metropolitan Area Transit Authority (WMATA). Of these, only WMATA has experienced problems due to brake squeal. The squeal propensity of the WMATA brake system has limited the options available for replacement friction pad materials, and at one point squeal sound levels became so severe that a considerable public outcry ensued. The purpose of this paper is to document the experience

gained in attempting to reduce the brake squeal on WMATA cars and to place this experience in the context of other work.

WASHINGTON METRORAIL EXPERIENCE

The disc brake assembly used by the WMATA Metro cars is similar in configuration to automotive caliper disc brakes with ventilated rotors (Figure 1). The disc is 20 in. in diameter and 3.6 in. thick and weighs 137 lb (1). The kidney-shaped brake pads are actuated by two side-by-side pistons. The brake system was designed by the Abex Corporation with two assemblies fitted per axle for a total of eight assemblies per car. (Author's note: Equipment sup-

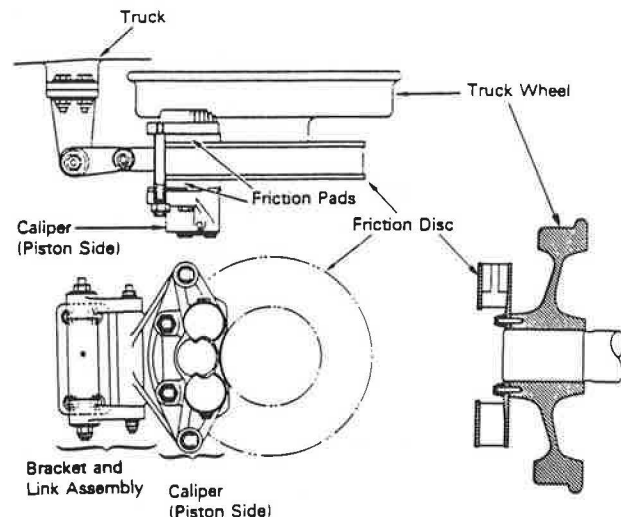


FIGURE 1 WMATA/Abex disc brake system.

pliers are identified in this paper for clarity of presentation. Their reference constitutes neither endorsement nor criticism.)

From the time WMATA initiated rail service, its brake system exhibited a propensity to squeal (2). The BART brake system with similar design parameters, on the other hand, has never exhibited squeal

(1). The squeal experienced early in the Metrorail history was occasional in nature and relatively low in amplitude and frequency (Figure 2a). However, when the original asbestos-bearing Abex 45109 friction pads were replaced with asbestos-free Knorr 981 pads, squeal became common, and its amplitude and frequency increased considerably (Figure 2b) (3).

To correct the deteriorated squeal behavior, a series of on-car modifications were evaluated for an immediate solution (4). Laboratory investigations using a constant-speed dynamometer were also undertaken for long-term improvements (5,6). The on-car modifications included a variety of replacement pads and system modifications fitted to test trains run during nonrevenue hours. The on-car tests found one pad--the Abex 1389b--to be relatively squeal-free. This pad was selected as a suitable replacement pad with acceptable squeal behavior.

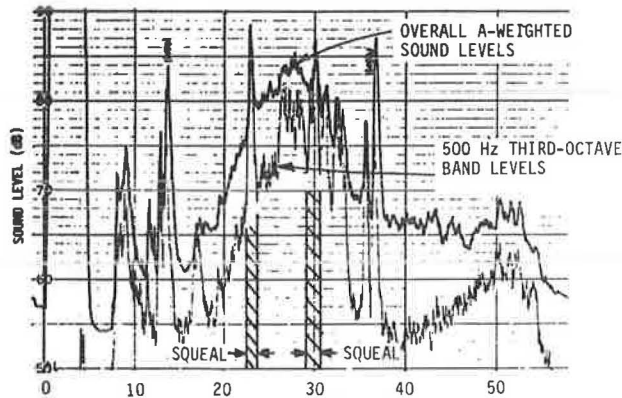
SQUEAL MECHANISM

The mechanism of brake squeal generation confounded investigators until two key observations were made (7):

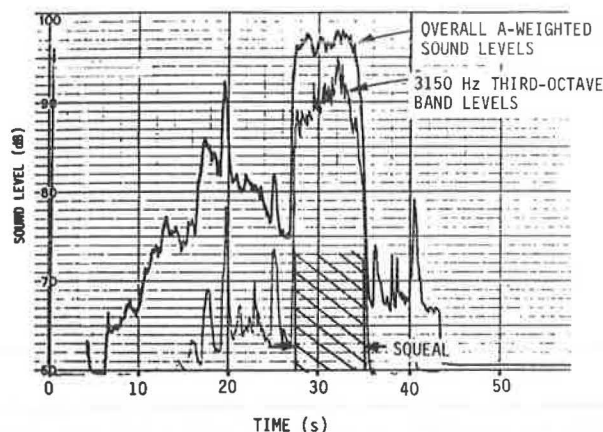
1. Squeal is a function of the direction of disc rotation (i.e., squeal might occur for only clockwise rotation and not for counterclockwise rotation), and

2. Deceleration measured during a squealing stop is somewhat higher than that measured for an essentially identical stop without squeal.

These observations suggested that squeal is related to an asymmetry of the contact area of the pad with the disc, such that the contact area is in a "sprag position" with respect to the backplate-piston contact point. This sprag configuration, or "digging in" of the pad to the disc, results in elastic deformation of the pad, which then reduces the binding forces and releases the pad to its original position from which the cycle can be repeated. This theory was tested by grinding a pad to an exaggerated asymmetry and varying the backplate-piston contact point. Squeal was observed consistent with the theory for the configuration shown in Figure 3 (7) for $\theta \approx \tan^{-1} \mu$, where μ is the pad friction coefficient. Further analysis indicated that squeal was possible for $0 < \theta < \tan^{-1} \mu$.



(a) Judiciary Square station, January 27, 1976



(b) McPherson Square station, February 20, 1981

FIGURE 2 Typical brake squeal time histories.

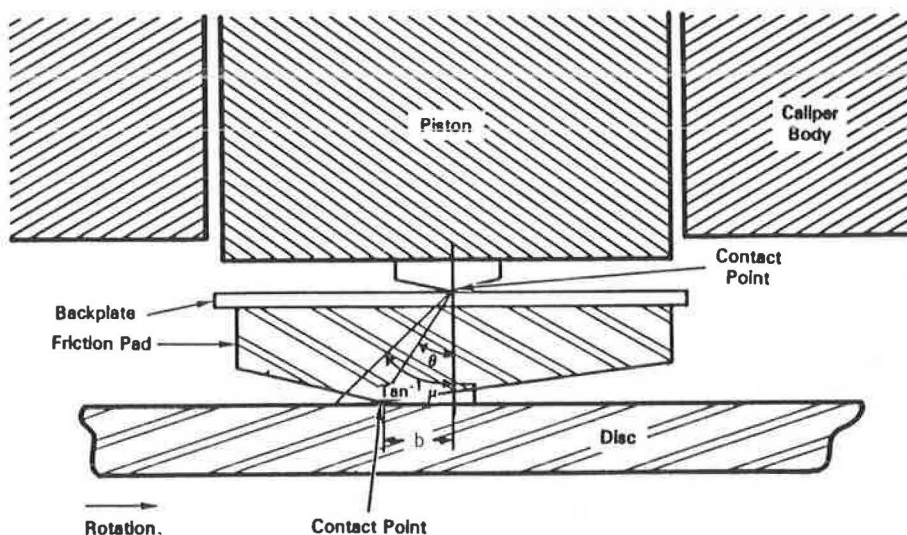


FIGURE 3 Disc, pad, and piston in squeal configuration (7).

Fundamental to the sprag-slip theory is the presence of the asymmetrical pad-disc contact area. The asymmetry is believed to arise from nonuniform pad wear, working of the backplate by the piston, or thermal distortion of the pad (7,8). A squeal-prone condition and slight backplate dishing have been observed after simply heating a pad to about 250°C and allowing it to cool. Thus heavy braking and subsequent cooling is likely to cause such distortions, as has been observed of squeal in in-service conditions. At low brake pressures the contact area is quite small due to the distortion; at high brake pressures the pad is flattened-out, thereby reducing the asymmetry. The result is less squeal at high brake pressures. The requirement that pad asymmetry exist probably accounts for the appearance of squeal in the Knorr 881 pad in the WMATA brake system only after a period of revenue service.

Investigators have noted that the frictional force on the face of the pad is resisted by a restraining force at the pad backplate resulting in a moment tending to rotate the leading edge of the pad toward the disc and causing more rapid wear at the leading edge (7). This moment also tends to shift the contact patch toward the leading edge--to a "spragging" position. This is shown in Figure 4. From translational equilibrium, all forces acting on the pad can be estimated in terms of the brake pressure force (N) and the friction coefficient. From rotational equilibrium, the offset (a) of the pad-disc effective contact point to the backplate-piston effective contact point must be $a = \mu t$, where t is the pad thickness. It is interesting to note that the maximum leading contact point offset (b) for squeal is equal to a. (Note that, even for the WMATA/Abex brake system, this offset is quite small. Specifically, for a new pad, $b \approx 0.25$ in. for a pad whose half-length is approximately 6 in.)

ANALYTICAL DESCRIPTION OF SQUEAL

The sprag-slip theory was supported and refined by a series of investigations (8-14). A mathematical description of a complex system such as a disc brake assembly requires a considerable number of simplifying assumptions. Expression of sprag-slip for a real (automotive) disc brake assembly, for example, consisted of a 6 degree of freedom (df) lumped-parameter model in which system damping was ignored (8). The interaction of the inner and outer pads was also ignored, such that the model was simplified to a single pad pressed against the disc. [Other work has demonstrated that the interaction of the pads does affect the parameter ranges that will result in squeal. However, the general trends indicated by the single-pad model are representative (14).] Thus this

model consists of three elements (the disc, pad, and caliper), with each possessing rotational and translational stiffness and mass. Element rotations are about an axis parallel to the disc radius and displacements are lateral (i.e., normal to the plane of the disc). Disc mass and stiffnesses are effective or equivalent values estimated for an equivalent beam from expected disc modal behavior during squeal.

When the equations of motion and boundary conditions are applied to the disc, pad, and caliper elements, a set of equations is obtained yielding solutions for the displacements of disc, pad, and caliper and the rotations of the disc and pad. These solutions have the form $y = Y e^{zt}$, where z can be imaginary; thus,

$$e^{zt} = e^{xt} e^{i\omega t} = e^{xt} [\cos(\omega t) + i \sin(\omega t)] \quad (1)$$

Therefore, the solutions are simple harmonic if $x = 0$, sinusoidal and damped if x is negative, and sinusoidal and diverging (i.e., unstable) if x is positive (15). Squeal is the self-excited oscillation that occurs when the brake system parameter values combine to yield an unstable solution to the displacement equations (i.e., positive x). In the literature the magnitude of positive x has been defined as the "squeal propensity" and $\omega/2$ has been called the "squeal frequency."

EFFECT OF BRAKE SYSTEM DESIGN ON SQUEAL

The fundamental squeal mechanism is understood. Simplified experimental and analytical models provide results that agree mutually and agree reasonably with specific real brake systems. However, behavior for one brake system may not be representative of that of another. Furthermore, the best current analytical model in the literature is still a considerable simplification of a complex system. Industry practice (both rail transit and automotive) for solving squeal problems remains basically trial-and-error modification of actual components. However, the analytical results are useful in guiding the types of modifications that may ultimately prove successful.

Brake Pad

Clearly, the brake pad plays a significant role in the squeal mechanism. When the original Abex 45109 pad was replaced by the Knorr 881 pad on the Metro-rail cars, squeal worsened considerably; when the Knorr 881 was replaced by the Abex 1389b, squeal was virtually eliminated (see Table 1). Interestingly, the presence of even one squeal-prone pad in a

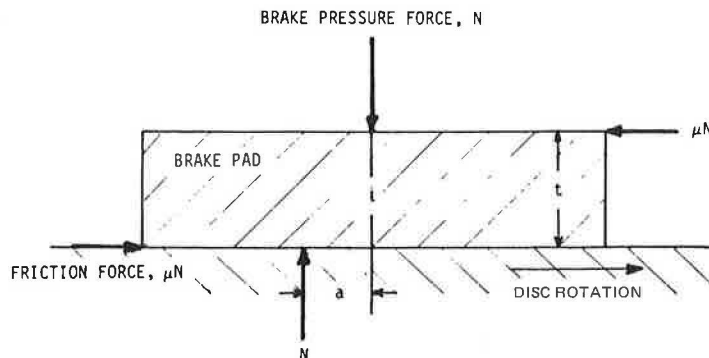


FIGURE 4 Forces acting on brake pad.

TABLE 1 Tests of WMATA On-Car Modifications

Pad	Disc	No. of Tests	L_{Amax}	Configuration
All	All	40	86	With various system modifications
Abex 45109	Abex	1	80	Original asbestos pads
Knorr 881	All	23	89	With various system modifications
Knorr 881-1	All	6	84	With various system modifications
Abex 1389b	All	7	77	With various system modifications
All	Knorr	10	88	With various system modifications
All	Abex	21	85	With various system modifications
NYAB	NYAB	1	79	Different brake assembly, including caliper
Knorr 881	All	7	92	With 0.01- to 0.10-in. rubber material behind backplate plus various other modifications
Knorr 881/881-1	All	5	89	With 0.125-in. steel plate inserted behind or welded to backplate plus various other modifications
Knorr 881	All	5	87	4-slot, 8-segment pads plus various other modifications
Knorr 881	All	4	90	1-slot, 2-segment pads plus various other modifications

Note: A test consisted of recordings of maximum slow-response A-weighted sound levels for at least six passbys of a two-car train fitted with a given brake system configuration. L_{Amax} is the average of the average maximum A-weighted sound levels for each test. Tests were performed at Union Station-Visitors Center Station, January 23 to April 7, 1981. Pads supplied by Knorr were manufactured by Jurid GmbH, Hamburg, West Germany.

caliper is sufficient to induce squeal (6,7). In tests on the same automotive disc brake assembly, four different friction materials tended to excite significantly different frequencies (16).

Increasing pad friction coefficient increases the range of pad contact point geometries ($0 < \theta < \tan^{-1} \mu$), which are squeal prone. Thus high-friction pad compositions tend to squeal more. Analytical results indicate that a minimum friction coefficient exists for which no squeal will be produced for any contact point geometry. In practice, for at least one actual system, this minimum friction coefficient was found to be 0.25 (9). When squeal is experienced, however, its sound level is independent of the friction coefficient (17).

Friction Material Stiffness

The 6 df model described in the previous section predicted squeal instability regions within fairly well-defined ranges of pad (Young's) modulus. However, the usefulness of pad modulus as a design parameter is limited by the pad modulus variability with temperature and pad distortion that causes the pad to become less stiff and more nonlinear (8).

In the WMATA laboratory tests, Battelle Columbus Laboratories measured the compressive static stiffnesses of Knorr 881 and Abex 1389b pads (5). The results are given in Table 2 (5) as a function of brake pressure. Note that in the load range representative of WMATA service, the quieter Abex pads are approximately twice as stiff at low braking effort (B1) and are approximately 20 percent stiffer at high braking effort (B5). The Abex 1389b pads have been characterized as "soft" (i.e., faster wearing) but less squeal prone. This behavior has

TABLE 2 Brake Pad Compressive Static Stiffness (5)

Braking Mode	Brake Press Range (psi)	Brake Force ^a (lb)	Stiffness (10^3 lb/in.)	
			Knorr 881	Abex 1389b
Snow	60-65	600	130	380
B1	110-130	1,200	180	340
B2	240-270	2,600	300	410
B3	290-310	3,000	320	420
B4	340-370	3,600	360	450
B5	427-473	4,500	420	490
Emergency	450-500	4,800	430	500

Note: The data are for static stiffness for increasing load.

^aTotal force approximated for brake pressure acting on two 2.5-in.-diameter pistons.

also been attributed to some automobile brake systems. However, neither squeal propensity nor service life has been found to be simply related to pad hardness.

Most disc brake pads are manufactured with at least one slot or "rain groove" (usually radial with respect to the disc). Somewhere in disc brake lore originated the nostrum that additional slots would quiet squealing systems, although no documented evidence of this has been found by the author. WMATA attempted this approach on the Knorr 881 pad by cutting an additional slot to form eight segments. This modification had no significant effect on average maximum squeal levels (see Table 1). The Office of Research and Experiments (ORE) of the European International Union of Railways (UIC) also tried this approach on a European-style (UIC-type) scissors-action caliper disc brake assembly and found the resultant squeal was prolonged and more objectionable (17). Battelle tried a further variation on this theme by cutting several radial slots through a Knorr 881 pad, including the backplate. The result of this modification was to reduce the number of squeal frequencies observed at high brake pressure, but it increased the number of squeal frequencies at lower brake pressure (5). Battelle also tried to remove friction material from one end of a brake pad to induce asymmetry and alter pad response (6). This modification did not alter squeal characteristics for either direction of disc rotation.

A simple geometric model of sprag indicates that prerequisite to squeal is a pad-disc contact offset (b) with $0 < b < (t \tan^{-1} \mu)$. The width ($t \tan^{-1} \mu$) was shown previously for the WMATA/Abex assembly to be relatively narrow compared with the circumferential length of the pad. Conceivably, removing the center portion of the friction material ($\pm t \tan^{-1} \mu$ about the center of the pad) could force the contact point geometry beyond the squeal range. This was apparently tried with an automotive brake assembly for which the pad center was milled out to within 0.75 in. of the pad ends. The result was an alteration of the observed frequencies, but apparently squeal was not eliminated (16).

Holographic interferometry experiments to determine component vibration behavior of an automotive disc brake assembly showed high vibration levels at the brake pad leading edge (18). This behavior is reasonably explained by the sprag-slip mechanism. These experimenters attempted to make the pad stiffer by testing the same pad type with and without a single central rain groove. Squeal frequency peaks for the ungrooved pad were reduced at least 15 dB. WMATA tested versions of the Knorr 881 with a

single slot instead of the standard three slots, with no benefit (see Table 1). Apparently no tests were made of a Knorr 881 with no slots, however.

Backplate Stiffness

The laser holography tests previously cited also showed high levels of pad backplate vibration. These results included "x" and "+" modal patterns exhibited on a square backplate with a centrally located pressure point. Results for an elongated pad (more similar to the WMATA pad geometry) gave a roughly radial nodal line somewhat comparable to the result obtained by Battelle for the Knorr 881 pad (6). The vigorous vibration of the backplate would appear to suggest that some modification might alter the system characteristics sufficiently to reduce squeal. Two approaches have been tried: stiffening bars and plates, and damping treatments.

The use of backplate inserts has been employed by the automotive industry, reportedly with some success. WMATA has tried a variety of backplate-stiffener modifications with a 0.125-in. steel plate (including some with a silicone rubber-fiberglass fabric bonded to the plate and some with a Teflon-type coating). These experiments showed no benefit (Table 1). Battelle also tried this approach with a 0.375 x 1.0 x 12-in. bar with similar lack of success (5). Reducing backplate stiffness by the previously mentioned slotted backplate was also ineffective. Insertion of thin elastomeric sheets behind the backplate also produced no benefit (Table 1).

Damping

In the Battelle compressive static stiffness measurements, both pads exhibited considerable hysteresis in compression with the "quiet" Abex pad exhibiting significantly greater hysteresis (consequently greater internal damping) than the "noisy" Knorr pad--an intuitively reasonable result (5). However, in dynamic tests on the two pads using an impedance hammer to explore the transverse bending behavior, the Knorr pad exhibited about 30 percent greater damping than the Abex pad. (Specifically, the results were Knorr 881, mean of 4.6 percent critical damping versus Abex 1389b, mean of 3.4 percent critical damping.) Similarly, in tests using a steady-state shaker excitation of suspended pads to explore the behavior of the friction material in a plane parallel to the disc and backplate, the Knorr pad exhibited about 90 percent greater damping than the Abex pad. (Specifically, the results were Knorr 881, mean of 2.5 percent critical damping versus Abex 1389b, mean of 1.3 percent critical damping.)

ORE performed pad damping experiments on an UIC-type brake assembly. In tests with an approximately 0.125-in. rubber coating to either the brake pad or the brake pad holder, no benefit was produced. In a test with about a 0.25-in.-thick "epoxy resin coating...on both the bearing surface of the pad and on the dove-tail seat...[such that] there was no longer any metallic connection between brake pad and brake pad holder," squeal was eliminated and sound level was reduced by 31 dB(A) (17). This treatment was not, however, considered suitable for operational use in its tested form. (Also, the treatment probably not only increased system damping but also significantly altered system stiffnesses.) Unfortunately, no damping capacity data were reported for the standard and modified assemblies.

Battelle tested a constrained-layer damping treatment on the Knorr pad backplate consisting of a

0.05-in. damping layer with a 0.25-in. steel constraining plate (6). This modification resulted in a 4 dB(A) reduction in squeal sound levels, but the pad had "squeal characteristics similar to those of the same pads before modification." This lack of success may be explained by the relatively limited increase (approximately 50 percent) in damping in the modified pad. (Damping measured by Battelle indicated that the standard pad had a mean of 4.9 percent critical damping, whereas the modified pad had a mean of 7.5 percent critical damping.)

Disc

The WMATA on-car tests showed no significant difference in maximum squeal levels between interchangeable discs provided by different manufacturers (Table 1). In tests using a simplified laboratory test rig with an 8-in.-diameter and approximately 0.1-in.-thick solid disc, a squeal frequency was observed "occurring near to the anti-resonance of the free disc between the (3,0) and (4,0) modes..." with the disc in a (3,0) mode when squealing (11). [Disc mode shape (D,C) corresponds to D nodal diameters and C nodal circles.]

Using a slightly different test rig, a (2,0) modal shape was observed for the squealing disc; and, with a significantly thicker disc, a (1,0) mode was observed with the nodal diameter line perpendicular to the radial line containing the contact point (13). Using holographic interferometry techniques on a small automotive disc brake assembly in squeal, six nodal radii were observed, with the 6th antinode "wholly suppressed by the brake pad" for an apparent (3,0) disc mode shape (18). Similarly, apparent (4,0) and (5,0) mode shapes were also observed. Battelle used a noncontacting displacement pick-up to probe a squealing Abex disc (6). Their findings implied a pattern similar to those obtained by the holographic work, with at least seven nodal radii indicated. Speculating the presence of an additional unobserved nodal radius just after the pad trailing edge and suppression of the 8th antinode by the pad suggests the disc is responding in a (4,0) mode.

Stiffness

A number of efforts have been made to "detune" the rotor to eliminate squeal. ORE tried two approaches (17): The removal of some of the cooling ribs of a rail transit brake disc to obtain an irregular rib distribution in 90-degree sectors gave no significant improvement. Machining one of the two disc friction surfaces (apparently to the wear limit) also produced no improvement. In an experiment similar to ORE but with cooling fin randomization over a full 360 degrees, Battelle found squeal frequency peaks were less intense but more numerous comparing modified and unmodified Abex rotors (5).

In the simplified laboratory test rig using 0.4-in.-diameter steel pins in place of brake pads, the effect of disc stiffness was explored by varying the radius of the contact point on the disc (13,14). Assuming disc stiffness

$$k_d \propto h^3/r^4 \quad (2)$$

where h is the disc thickness and r is the contact point radius, squeal instability regions were clearly defined as a function of disc stiffness, contact angle, and beam stiffness. (Beam stiffness was the experimental analog to pad and caliper stiffness.) However, as previously mentioned, a thicker disc squealed in a different mode, appar-

ently due to stiffness and mass effects, so that a simple thickness-cubed relationship is not valid. Apparently squeal cannot be eliminated in real systems by simple disc stiffness changes, although it is important in its interaction with caliper stiffness, as discussed in the following section.

A practical approach taken by the automotive industry has been to stiffen the rotor to increase the frequency of the disc modes out of the range of human hearing. However, the viability of this approach with the much more massive transit car discs is questionable.

Damping

An approach that has been explored by the automotive industry and is now in production for a number of automobiles is the use of high-damping discs. Gray iron is a generic cast iron commonly used in brake discs (including the Abex rotor). The internal damping capacity of gray irons has been found to be a function of its chemical composition--specifically, the equivalent iron carbon content. A number of batches of brake discs were cast and fitted to automobiles to be evaluated for squeal propensity; in addition, samples from these batches were tested for their damping capacity (19). The relationship of damping capacity (given in average percent critical damping for disc resonances greater than 2,000 Hz) with iron carbon equivalency (%CE) obtained from those tests is

$$\%C/C_0 = 0.302(\%CE) - 1.164 \quad (3)$$

with correlation coefficient $r = 0.83$ [from Miller (19)].

From the automobile tests in representative service, this study found that "about 0.2% critical damping was required to suppress squeal to a commercially acceptable level under the test conditions" and "essentially squeal-free brakes were obtained with 0.3% critically damped brake discs" (19). These conclusions are valid because the vehicles and brake pads ($\mu = 0.35$) were of the same type. However, the required numeric values of damping capacity are not universally applicable. For example, 0.2 percent critical damping may be only marginally acceptable for a different brake assembly or pad composition.

A disadvantage of high-damping gray irons is their inferior strength compared with other gray irons; thus, their use may necessitate rotor redesign, thereby reducing their suitability for retrofits. However, higher disc damping may alternatively be accomplished by mechanical damping devices.

Battelle measured the damping capacity of an Abex rotor (dynamometer-mounted without caliper and pads) by using a shaker to provide a white-noise excitation (5). The mean damping capacity over four measurement locations was 1.4 percent critical damping. Battelle also measured the damping capacity of the Abex rotor by using an impedance hammer (6). The mean damping capacity measured was 0.14 percent critical damping. (The difference in the two damping capacity results for the Abex rotor is unexplained; both the shaker and hammer methods are expected to agree more closely for the nominally identical installations.)

Battelle attempted to determine the effect of rotor damping capacity by filling the interior cooling passages of an Abex rotor with lead shot (5). Using the shaker and broadband excitation, the mean damping capacity over the four measurement locations was 6.4 percent critical damping--about 5 times greater damping than the standard rotor. (The in-

creased rotor mass was not reported.) When the shot-filled rotor was tested, squeal was experienced with fewer but more intense peak frequencies.

When an automotive disc with "four radial slots cut from the rim to the hub" was operated in a laboratory test, squeal was reported to be eliminated (16). Details of the modification were not provided, although it was not considered suitable for production. The mechanism of this modification apparently was increased damping because the un-slotted rotor had a bell-like ring when struck with a hammer, whereas the slotted rotor gave a very dead sound. Unfortunately, no other damping information was provided.

Caliper

In the laser holography experiments of various small automotive caliper configurations, the caliper structures were seen to participate in vigorous vibration. ORE measured lateral vibration on the brake pad holder on a UIC-type assembly and found high vibration levels. In on-train measurements of WMATA cars, a prominent caliper vibration frequency peak was observed that compared reasonably with a prominent airborne noise peak for the Abex brake assembly (20).

Mass and Stiffness

The 6 df model of the automotive disc brake assembly indicated that the squeal instability region is sensitive to both caliper mass and caliper stiffness (8). This model predicted three distinct narrow ranges of caliper mass where squeal instability is expected, with one range of significantly greater propensity [Figure 5a (8)]. With respect to caliper stiffness, the model predicted the system would tend to be stable at low stiffness and unstable with high squeal propensity at high stiffness, as shown in Figure 5b. Other experience both supports and contradicts these findings. Caliper mass modification has been effective in eliminating squeal in a squeal-prone brake assembly; at least one automobile is currently in production with additional caliper mass for this purpose. On the other hand, the same manufacturer has found that a stiffer caliper is less squeal prone. Apparently, the effect of stiffness changes is system specific.

This caliper stiffness experience correlates with findings obtained by using the simplified laboratory test rig (12-14). In these experiments beam stiffness (the experimental caliper and pad stiffness analog) interacted with disc stiffness in the definition of squeal instability regions for a given contact point geometry. For a given relatively narrow range of disc stiffness, the squeal instability was virtually independent of beam stiffness; further, for a given relatively narrow range of beam stiffness, the squeal instability was virtually independent of disc stiffness. This finding is shown in Figure 6 (12). (Note that the figure shows the pin-disc system's theoretical unstable regions for $\theta = 3$ degrees, $\mu = 0.4$.)

Damping

The presence of high vibration levels on the caliper structure suggests that the attachment of damping devices could dissipate significant squeal energy and potentially reduce or eliminate squeal propensity. Surprisingly, relatively little attention has been devoted to this approach. The ORE damped

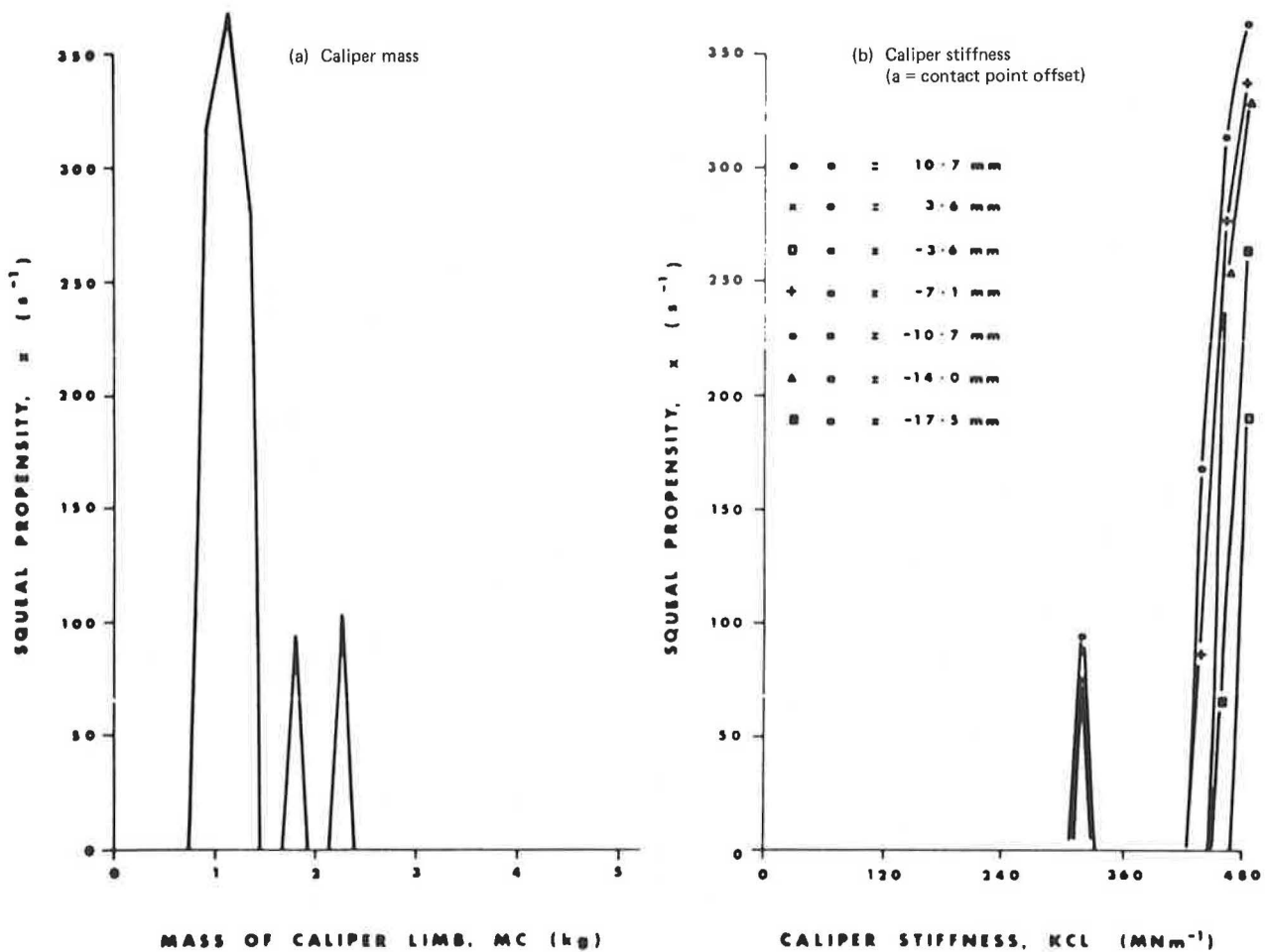


FIGURE 5 Effect of caliper parameters (8).

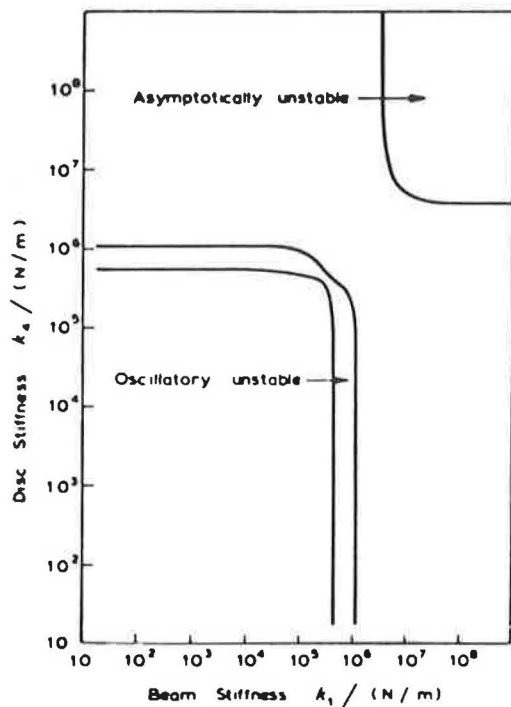


FIGURE 6 Effect of disc versus caliper stiffness (12).

pad holder, described previously, was effective. One of the experiments performed in conjunction with the laser holography studies included the application of adhesive damping pads to the caliper surface (18). This treatment was apparently effective in attenuating caliper vibration, although squeal was still experienced with that assembly.

CONCLUSIONS

Experience has shown that some brake systems are prone to squeal while others are not (e.g., WMATA versus BART). Further, even for squeal-prone systems, the response of the system to modification is system specific (i.e., modifications that are successful for one system have been unsuccessful for others). With these uncertainties in mind, some generalizations can be made.

1. Increasing backplate, disc, or caliper damping sufficiently is likely to reduce squeal propensity.
2. Increasing or decreasing disc stiffness, caliper mass, or caliper stiffness may move the brake system response out of the squeal instability region.
3. If a low friction coefficient pad ($\mu < 0.25$) can provide acceptable braking performance, it is a means to eliminate squeal.
4. Eliminating pad grooves may reduce squeal propensity.

ACKNOWLEDGMENTS

The author would like to acknowledge the following individuals for the information and insight they provided and not otherwise referenced: R. Scarbrough and V. Michalski, WMATA; G. Sastry, DeLeuw, Cather & Company; T. Flaim and R. Hickling, General Motors Corporation; and H. Burt, Knorr Brake Corporation. This work was sponsored in part by the Transportation Systems Center, U.S. Department of Transportation; R. Hinckley was the program director.

REFERENCES

1. L.A. Ronk and M.A. Staiano; ORI, Inc. Evaluation of Squeal Noise from the WMATA Transit Car Disc Brake System. Report UMTA-MA-06-0099-81-4. Transportation Systems Center, U.S. Department of Transportation, Cambridge, Mass., March 1981.
2. G.P. Wilson; Wilson, Ihrig, and Associates. Metrorail Operational Sound Level Measurements: Subway Station Sound Levels. Washington Metropolitan Area Transit Authority, Washington, D.C., Nov. 1979.
3. J.F. Waters. Metrorail Disc Brake Squeal Public Noise Exposure--Early 1981. Tech. Report 81-01. Waters Science Associates, Inc., Rockville, Md., March 1981.
4. G.N. Sastry and E.C. Green, Jr. A Quick Fix for Washington Metro Brake Squeal. *In* Transportation Research Record 896, TRB, National Research Council, Washington, D.C., 1982, pp. 71-74.
5. C.W. Rodman; Battelle Columbus Laboratories. Investigation of Noise Generated by Brakes of WMATA Rail Transit Vehicles. Transportation Systems Center, U.S. Department of Transportation, Cambridge, Mass., Sept. 15, 1981.
6. C.W. Rodman and M.W. Kurre; Battelle Columbus Laboratories. Phase II--Investigation of Noise Generated by Brakes of WMATA Rail Transit Vehicles. Transportation Systems Center, U.S. Department of Transportation, Cambridge, Mass., Sept. 15, 1982.
7. R.T. Spurr. Brake Squeal. *In* Vibration and Noise in Motor Vehicles, Proc., Institution of Mechanical Engineers, London, 1971, pp. 13-16.
8. N. Millner. An Analysis of Disc Brake Squeal. SAE Paper 780332. Presented at SAE Congress and Exposition, Detroit, Feb. 27-March 3, 1978.
9. S.W.E. Earles and G.B. Soar. Squeal Noise in Disc Brakes. *In* Vibration and Noise in Motor Vehicles, Proc., Institution of Mechanical Engineers, London, 1971, pp. 61-69.
10. M.R. North. A Mechanism of Disc Brake Squeal. Presented at 14th FISITA Meeting, June 1971.
11. S.W.E. Earles and G.B. Soars. A Vibrational Analysis of Pin-Disc System with Particular Reference to Squeal Noise in Disc Brakes. Presented at Stress Analysis Group Annual Conference, Institute of Physics, London, 1974.
12. S.W.E. Earles and C.K. Lee. Instabilities Arising from the Friction Interaction of a Pin-Disc System Resulting in Noise Generation. Trans. of ASME, Journal of Engineering for Industry, Vol. 98, Series B, No. 1, 1976, pp. 81-86.
13. S.W.E. Earles. A Mechanism of Disc-Brake Squeal. SAE Paper 770181. Presented at International Automobile Engineers Congress and Exposition, Detroit, Feb. 28-March 4, 1977.
14. S.W.E. Earles and M.N.M. Badi. On the Interaction of a Two-Pin-Disc System with Reference to the Generation of Disc-Brake Squeal. SAE Paper 780331. Presented at SAE Congress and Exposition, Detroit, Feb. 27-March 3, 1978.
15. R.H. Scanlan and R. Rosenbaum. Introduction to the Study of Aircraft Vibration and Flutter. Macmillan, New York, 1951.
16. J.H. Tarter. Disc Brake Squeal. SAE Paper 830530. Presented at SAE Congress and Exposition, Detroit, Feb. 28-March 4, 1983.
17. Tests to Reduce the Noise During Braking and Running Round a Sharp Curve: Results of Tests and Conclusions. Report C 137/RP 7. Office for Research and Experiments, International Union of Railways, Paris, Oct. 1977.
18. A. Filske, G. Hoppe, and H. Matthai. Oscillations in Squealing Disk Brakes--Analysis of Vibration Modes by Holographic Interferometry. SAE Paper 780333. Presented at SAE Congress and Exposition, Detroit, Feb. 27-March 3, 1978.
19. E.J. Miller. Damping Capacity of Pearlitic Gray Iron and Its Influence on Disc Brake Squeal Suppression. SAE Paper 690221. Presented at SAE Congress and Exposition, Detroit, 1969.
20. J.S. Rao; Stress Technology, Inc. Brake Assembly Problem Study. Washington Metropolitan Area Transit Authority, Washington, D.C., July 17, 1981.

Publication of this paper sponsored by Committee on Transportation-Related Noise and Vibration.

Research on a Device for Reducing Noise

KAZUYOSHI IIDA, YOSHIKAZU KONDOH, and YASUHIRO OKADO

ABSTRACT

The purpose of this research study is to describe a new device for reducing noise based on the principles of sound refraction and interference, which can effectively reduce noise from highway and railroad traffic. This device has a back sound barrier panel that effectively reduces sound when the system is used on an existing sound barrier. In a test at the proving ground of the Bridgestone Corporation, the device with a back barrier of glass fiber reduced the noise emanating from an 11-ton truck by 5 to 6 dB(A).

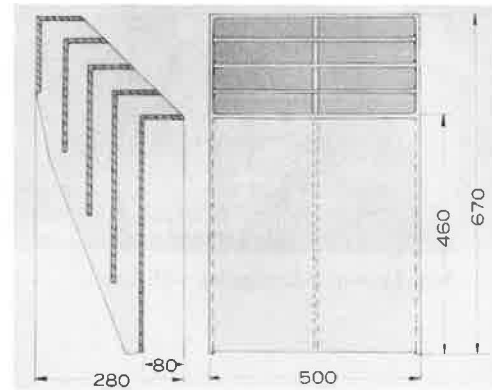


FIGURE 1 Construction of device.

PRINCIPLE AND EFFECT

This study is concerned with a new type of device for reducing noise based on the principles of sound refraction and interference. The device can effectively reduce the effect of noise emanating from highway and railroad traffic.

In order to reduce noise, it has been common practice to provide a noise barrier between the sound source and the receiver for the purpose of intercepting the propagation of the sound wave that causes the noise or to construct a barrier to completely surround and shield the noise source. However, the former is limited in its effectiveness to insulate the sound, whereas the latter requires additional devices for heat dissipation or ventilation, and hence becomes complex in construction, thereby making it difficult to install and make effective.

To overcome such disadvantages, attempts have been made to construct a high wall along a railroad or a highway. Such a high wall, however, obscures sunlight from nearby houses and blocks the passenger's field of vision; therefore, the wall has its own disadvantages.

Based on a consideration of these points, this study is concerned with the development of a device for reducing noise using the principles of sound refraction and interference.

DEVICE

The interference principle of the sound-reduction device is shown in Figure 1. On the right-hand side of the figure is the front elevation view from the sound source. The sound enters along the upper edge. The left-hand side shows a cross-sectional view of the device; shown are the hollow rectangular chambers located at right angles to each other, which are progressively longer from top to bottom.

The sound emanating from the source passes through the chambers and is refracted. It lags in phase compared with the sound passing over the top of the device. The device interferes with the two sounds, thus providing a region where the sound is reduced.

The underlying principle for this patented device is described by referring to Figures 2-5. The photographs show the sound distribution produced both in the absence and in the presence of the sound-reduction device. These photographs have been taken by using a special photographic method.

Analysis of Sound Pressure

In Figures 2 and 3 the brighter area represents the area where the sound pressure is higher (i.e., louder).

Figure 2 shows the distribution of a 1/3 octave band noise that has a center frequency of 2,000 Hz. The noise is emitted from noise a source (1) in the absence of the patented sound-reduction device.

Figure 3 shows the distribution of a 1/3 octave band noise that has a center frequency of 2,000 Hz. The noise is emitted from noise a source (1) and is refracted by the device (2). Area A represents sound that has been emitted from the source (1) that has passed over the top of the device (2). Area B represents sound that has passed and is delayed in phase

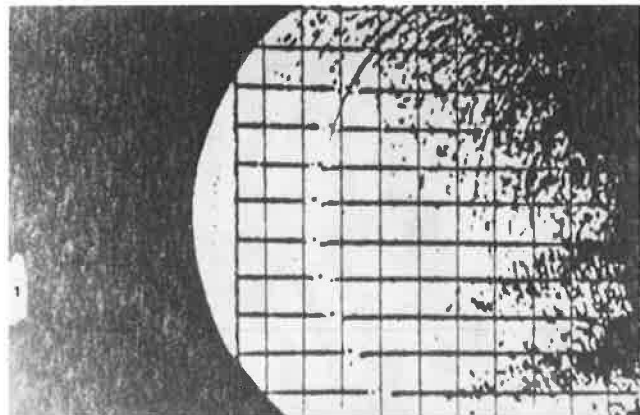


FIGURE 2 Sound pressure distribution without device.

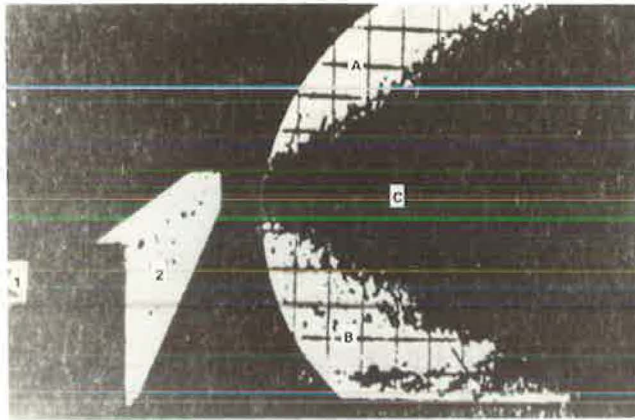


FIGURE 3 Sound pressure distribution with device.

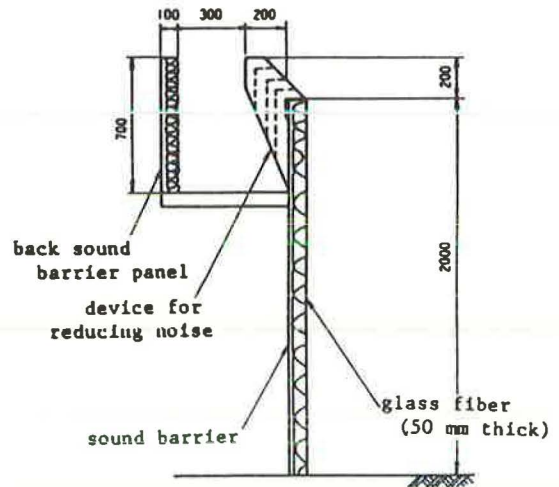


FIGURE 6 Cross section of sound-reduction system.

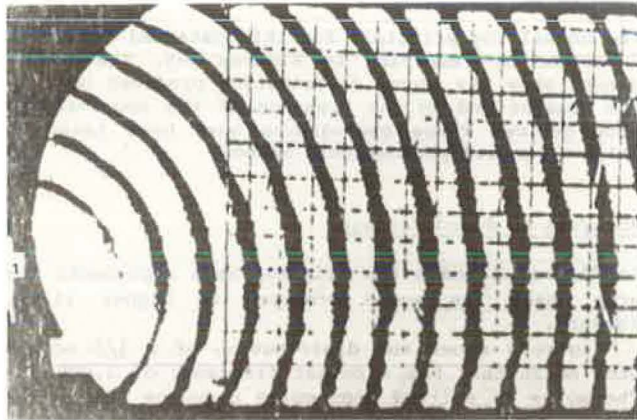


FIGURE 4 Sound wave without device.

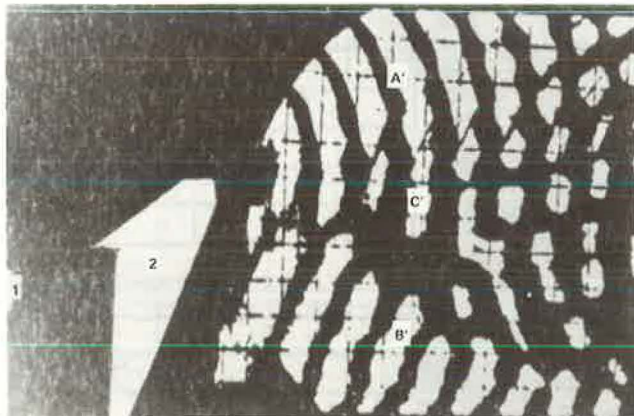


FIGURE 5 Sound wave with device.

as it passes through the chambers. Figure 3 shows that the device produces a low sound pressure area C between the two high sound pressure areas (A and B).

Analysis of Sound Wave Density

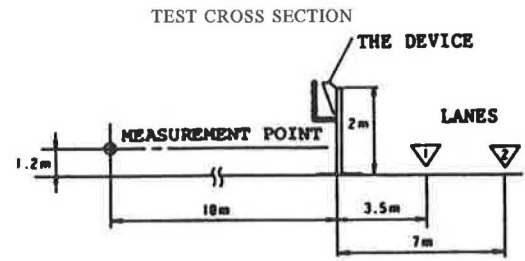
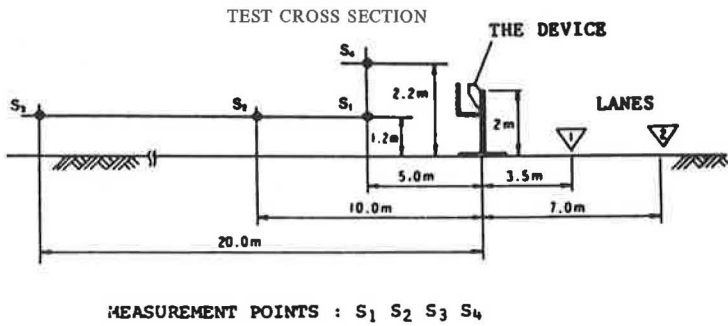
In Figures 4 and 5 the brighter areas represent sound waves of higher density.

Figure 4 shows the sound wave of a pure tone, which has a frequency of 2,000 Hz. The noise is emitted from the noise source (1) in the absence of the device. [The sound waves spread like ripples (concentric rings) in a pond after a stone has been thrown.]

Figure 5 shows the sound wave of a pure tone, which has a frequency of 2,000 Hz. The noise is emitted from the noise source (1) in the presence of the device (2). Figure 4 shows the pure tone emitted from the noise source (1) and propagated in a spherical wave without phase lag. The presence of the device in Figure 5, however, causes a sound wave B', which passes through the chambers and is propagated in a plane wave, to refract in a downward direction; this sound wave is delayed in phase compared with sound A', which has passed over the top of the device and is propagated in a spherical wave. As a result, the sound wave in region C' (located between sound A' and B') becomes a nonuniform wave, as shown in Figure 5. The nonuniform sound wave in region C' represents a destructive interference phenomenon. This phenomenon is produced between the direct sound wave A' passing over the top of the device and diffracted into the sound shadow behind the device, and the sound wave B' passing through the chambers of the device and refracted and delayed in phase. As a result the sound reduced in region C' is produced, as shown in Figure 5. The volume of the sound reduced in region C' due to the interference between sound B' and sound A' is determined by the size of the device, the difference in length between the chambers of the device, and the position of the noise source.

FIELD TESTS

Tests of this device were carried out at the Bridge-



MEASUREMENT POINTS : S₁ S₂ S₃ S₄

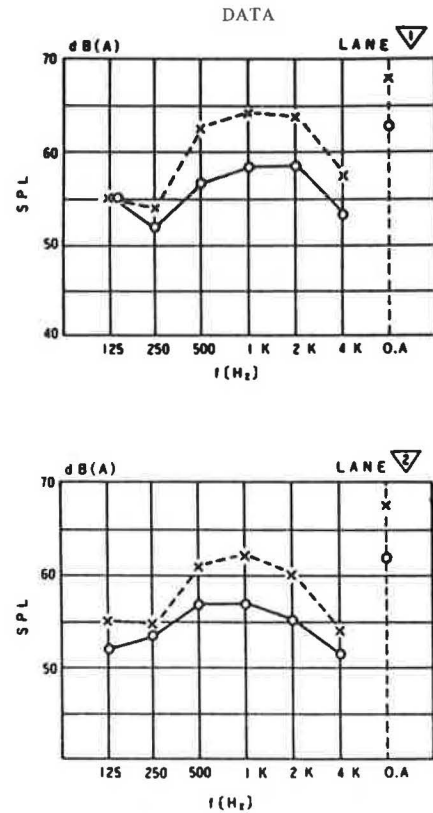
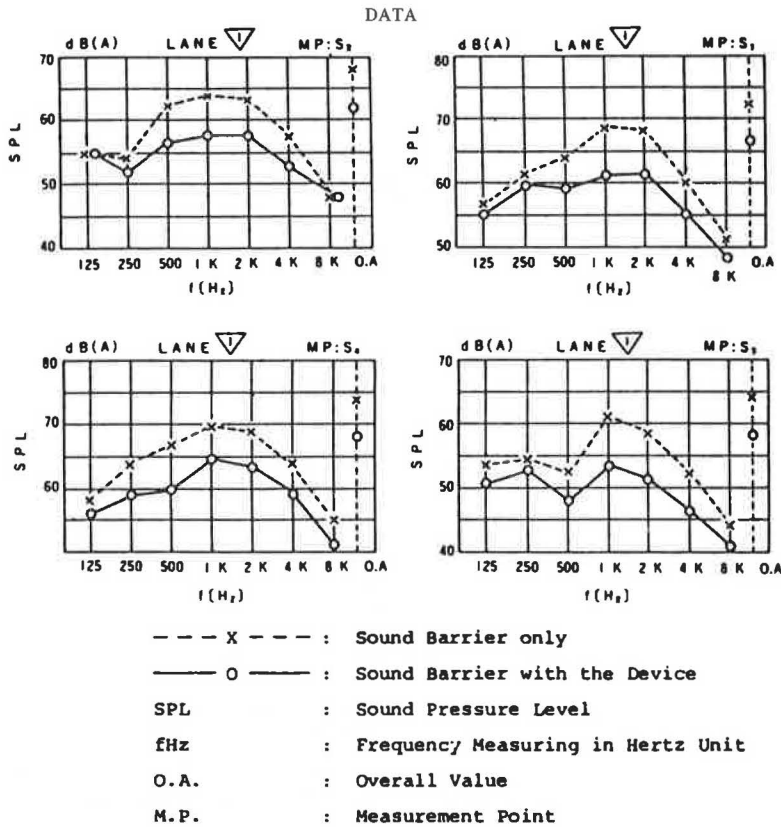


FIGURE 7 Data on frequency analysis at different measurement points.

FIGURE 8 Data of frequency analysis for different lanes.

stone Corporation proving ground on February 2, 1982. The tests were conducted under the following conditions:

1. Sound barrier--2.0 m high, coated with 50-mm-thick glass fiber on the front face for the purpose of sound absorption (Figure 6),
2. Test car--11-ton truck (Mitsubishi Fuso),
3. Speed--100 km/h (63 mph), and
4. Distance between the device and the noise source--3.5 and 7 m (11.5 and 23 ft).

The results of the test indicated that

1. The noise of the truck was reduced 5 to 6 dB(A) when the device was applied;
2. A similar degree of sound reduction was recorded at measurement points S₁ to S₄ in the range of 500 Hz to 4 kHz, as shown in Figure 7; and
3. A similar effect was recorded when the truck ran along a different lane, as shown in Figure 8; thus the device functioned efficiently, even if the noise source was distant. (The test setup is shown in Figure 9.)



FIGURE 9 Test setup.

CONCLUSIONS

Considerable reduction of sound can be expected when this device is used on existing sound barriers, without a big modification of the barriers. If new sound barriers are constructed, then the use of this device can contribute to the economical design of the sound barrier system by lowering the height and reducing the weight of the installation. This de-

vice, when combined with the back sound barrier panel that intercepts the refracted propagated noise, can effectively reduce the noise from sources such as railroads or highways.

Publication of this paper sponsored by Committee on Transportation-Related Noise and Vibration.

Review of Federal Noise Emission Standards for Interstate Rail Carriers

ERIC STUSNICK

ABSTRACT

The federal noise emission standards for interstate rail carriers, the most recent portion of which took effect on January 15, 1984, are reviewed. Some potential problems in carrying out various elements of these standards are described, and possible solutions to these problems are discussed.

The Noise Control Act of 1972 identified noise as a growing danger and declared that the policy of the United States was "to promote an environment for all Americans free from noise that jeopardizes their health and welfare." Included in the Act was the authorization to establish federal noise emission standards for products distributed in commerce, and the mandate for the U.S. Environmental Protection Agency (EPA) to coordinate federal activities in noise control. Section 17 of the Act specifically required EPA to promulgate standards and the U.S. Department of Transportation (DOT) to promulgate compliance regulations setting limits on "noise emission resulting from operation of the equipment and facilities of surface carriers engaged in interstate commerce by railroad." It further required that such regulations include noise emission standards that "reflect the degree of noise reduction achievable through the application of the best available technology, taking into account the cost of compliance."

In accordance with Section 17 of the Act, EPA issued final railroad noise emission standards on December 31, 1975. These standards applied to all railroad cars and all locomotives, except steam locomotives. On August 23, 1977, FRA published Railroad Noise Emission Compliance Regulations setting forth procedures for enforcing the EPA standards.

In June 1977 the Association of American Railroads (AAR), along with several railroad companies,

challenged the EPA regulation in the U.S. Court of Appeals on the basis that it did not include standards for all railroad equipment and facilities as required by the Noise Control Act. The concern of the railroad industry was that, lacking federal preemption of all railroad noise source regulations, there could develop a great variety of differing and inconsistent standards in every jurisdiction along the railroad's routes. In addition, local communities would not necessarily be bound by the protective, requirement in the Noise Control Act for use of the "best available technology, taking into account the cost of compliance."

The judgment of the court was in favor of the railroad industry. As a result EPA published proposed noise regulations for additional railroad equipment and facilities in April 1979. These proposed regulations would have established federal standards for overall railroad facility and equipment noise, as well as specific standards for retarders, refrigerator cars, and car-coupling operations.

After an extended public comment period, EPA published final rules on January 4, 1980, establishing standards for noise from four specific sources, namely, switcher locomotives, retarders, car couplings, and locomotive load cell test stands. These new standards took effect on January 15, 1984.

Although at the time of preparation of this paper DOT had not yet promulgated compliance regulations for these new standards, draft regulations were in the process of being prepared.

LOCOMOTIVE STANDARDS

The data in Table 1 summarize the standards for noise emission from all locomotives, except steam locomotives, operated or controlled by railroads within the continental United States.

The original standards, issued in 1975, differentiated among three different operating conditions:

1. Stationary at idle throttle setting,

TABLE 1 Locomotive Noise Emission Standards

Operating Condition	Noise Metric	Meter Response	Meas't Location	Locomotive Type	
				Non-Switchers Built On or Before 31 Dec 79	All Switchers; Non-Switchers Built After 31 Dec 79
Stationary, Idle	L _{max}	Slow	100 Feet	73 dB(A)	70 dB(A)
Stationary, Non-Idle	L _{max}	Slow	100 Feet	93 dB(A)	87 dB(A)
Moving	L _{max}	Fast	100 Feet	96 dB(A)	90 dB(A)

* Switchers are in compliance if L₉₀(Fast) ≤ 65 dB(A) on receiving property. L₉₀ measurement must be validated by showing that L₁₀(Fast) - L₉₉(Fast) ≤ 4 dB(A).

- 2. Stationary at a throttle setting other than idle, and
- 3. Moving at any throttle setting.

The standards also differentiated between two classes of locomotive:

- 1. Those built on or before December 31, 1979, and
- 2. Those built after December 31, 1979.

The standards for locomotives built after December 31, 1979, were from 3 to 6 dB lower than those for the older locomotives, depending on the mode of operation. All standards specified the maximum A-weighted sound level that could occur at a distance of 100 ft from the source. Instrumentation, test site clearance, weather condition, and background noise criteria for these measurements were also defined in the standards.

The new addition to these standards, which took effect on January 15, requires that all switcher locomotives meet the lower, more stringent standards, regardless of their year of manufacture. Switcher locomotives are those locomotive models that are designated as a switcher by the builder or reported to the Interstate Commerce Commission (ICC) as a switcher by the operating or owning railroad. Appendix A of Subpart A of the standard lists those locomotive models that are considered to be switchers.

In addition to extending the more stringent 100-ft sound levels to switcher locomotives of all manufacture dates, the new standard introduces the con-

cept of a "trigger" level. Recognizing that noise from switcher locomotives operating in a railroad yard is a community problem only if the sound level at the boundary of the yard is excessive, these standards deem all switcher locomotives in a yard to be in compliance if the L₉₀ sound level on neighboring receiving property due to stationary switcher locomotives does not exceed 65 dB(A) when measured for a period of at least 15 min. If this 65-dB(A) trigger level is exceeded on any receiving property, then 100-ft maximum sound level measurements must be made to determine the compliance of locomotives within the yard.

To ensure that any L₉₀ measurement on receiving property is restricted to essentially steady-state noise sources (presumably stationary switcher locomotives in the yard), the new standard defines a validation procedure for the L₉₀ measurement, which requires that the difference between L₁₀ and L₉₉ be 4 dB or less. Meeting this requirement indicates that the sound being measured changes only slightly with time and thus emanates from steady-state sources.

RAIL CAR STANDARDS

The pre-1980 noise emission standards on rail cars have not been changed by the promulgation of the new standards. As noted by the data in Table 2, these standards differentiate between two operating conditions:

- 1. Speeds less than or equal to 45 mph, and
- 2. Speeds exceeding 45 mph.

TABLE 2 Noise Emission Standards for Railroad Equipment Other than Locomotives

Noise Source	Operating Condition	Noise Metric	Meter Response	Meas't Location	Standard dB(A)	
Railroad Cars	Speed ≤ 45 mph	L _{max}	Fast	100 Feet	88	
	Speed > 45 mph	L _{max}	Fast	100 Feet	93	
Active Retarders	Any	L _{adj.ave. max.}	Fast	Rec.Prop.	83	
Car-Coupling	Any	L _{adj.ave. max.}	Fast	Rec.Prop.	92	
Locomotive Load Cell Test Stands	Any	L ₉₀ *	Fast	Rec.Prop.	65	
	or	(a) Primary Standard	L _{max}	Slow	100 Feet	78
		(b) If (a) Is Not Feasible	L ₉₀ *	Fast	Rec.Prop. >400 Feet	65

* L₉₀ measurement must be validated by showing that L₁₀(Fast) - L₉₉(Fast) ≤ 4 dB(A)

The standards specify the maximum fast-response A-weighted sound level that can occur 100 ft from the centerline of the track as the rail car passes by. Instrumentation, track construction and curvature, test site clearance, weather condition, and background noise criteria for these measurements are also defined in the standard.

RETARDER AND CAR-COUPLING STANDARDS

Standards on two new railroad noise sources--active retarders and rail car couplings--went into effect on January 15. The data in Table 2 indicate that the metric used to measure sound from these two intermittent sources is the adjusted average sound level measured on neighboring receiving property. The adjusted average sound level is the energy-average of the maximum fast-response A-weighted sound levels measured for a sequence of events (either retarder sounds or car-coupling impacts, but not both), adjusted by a factor that takes into account the rate at which these events occur. At a rate of one event per minute, the adjustment factor is zero; at a rate of two events per minute, 3 dB is added to the computed energy-average level; at a rate of four events per minute, 6 dB is added; and so on. At a rate of one event every 2 min, 3 dB is subtracted from the calculated energy-average level; at a rate of one event every 4 min, 6 dB is subtracted; and so on.

In measuring the sequence of retarder or car-coupling sound levels, at least 30 consecutive events must be included and the measurement period must be at least 60 min and not more than 240 min. An event is defined as the occurrence of a sound in which the maximum fast-response A-weighted sound level during the occurrence exceeds the level immediately before the occurrence by at least 10 dB. Instrumentation, test site clearance, and weather condition criteria for the measurements are defined in the standard. Correction factors for the use of type 2 sound level measurement instrumentation are also specified.

LOCOMOTIVE LOAD CELL TEST STAND STANDARDS

Also taking effect on January 15 were standards on the noise emissions from locomotive load cell test stands. These test stands are large, fixed banks of resistors (usually fan cooled) that are connected to the electric generator of a stationary diesel-electric locomotive to provide an electrical load for testing the operation of the diesel engine and the electrical system.

Typically, these tests involve operating the locomotive for several minutes at each of a series of throttle settings. The noise emissions during such tests originate from locomotives under test, the test stand cooling fans, and possibly the resistor bank. Maximum noise levels usually occur when the locomotive is operating at the maximum throttle setting.

The data in Table 2 indicate that the standard defines the maximum slow-response A-weighted sound level as measured at 100 ft from the geometric center of the locomotive being load tested. As in the case of the new switcher locomotive standard, an L_{90} trigger level, as measured on neighboring receiver property, is defined. If this level is not exceeded, all locomotive load cell test stands in the railroad facility are deemed to be in compliance with the standard. This L_{90} measurement must be validated by showing that L_{99} minus L_{10} does not exceed 4 dB.

Instrumentation, test site clearance, and weather condition criteria are also defined in the standard. Because the test site clearance requirements are not often satisfied around existing load cell test stands, the standard defines an alternate measurement in terms of the maximum L_{90} sound level on receiving property at least 400 ft away from the test stand. This alternate standard may only be applied when the clearance requirements for the 100-ft measurement cannot be met.

POTENTIAL PROBLEMS

Several problems may potentially exist in carrying out some of the measurements required by the new standard. For example, it is required that the measurement of the L_{90} trigger level associated with the switcher locomotive standards and the locomotive load cell test stand standards be validated by demonstrating that L_{99} minus L_{10} does not exceed 4 dB. The purpose of this requirement is to ensure that the noise at the receiving property measurement site primarily consists of nearly steady-state railroad noise, presumably from nearby stationary locomotives or load cell testing. The data on which these statistical sound levels are based must be measured over a period of at least 15 min or, if manual sampling techniques are being used, until 100 measurements at intervals of 10 sec are made.

If the measured value of L_{90} so obtained is not validated (i.e., if $L_{99} - L_{10} > 4$ dB), then the standard states that "measurements may be taken over a longer period to attempt to improve the certainty of the measurement and to validate L_{90} ." No guidance is provided as to when to terminate attempts to validate the L_{90} measurement. Because many railroad yards are located in or near large cities with heavy automobile, truck, and aircraft traffic nearby, it may often be the case that the measured noise field is not nearly steady-state and validation of L_{90} is impossible.

The intent, of course, is to eliminate sites in such heavily trafficked areas from this part of the standard, because the switcher locomotives and load cell test stands are probably not major sources of environmental noise. Without guidance, however, the potential exists for many hours of wasted effort as inexperienced personnel attempt to validate the measurement.

A second problem may occur in the case in which the L_{90} measurement is validated. In such a case, to determine the applicability of the standard the observer is required to determine "the principal direction of nearly steady-state sound at the measurement location...by listening to the sound and localizing its apparent source(s)." In the envisioned situation in which nearby stationary locomotives or load test stands or both are the only major noise sources, there should be no real problem in identifying the source.

In the more common case, however, in which road vehicle and aircraft passbys contribute to the measurement, it is impossible even for the experienced professional to determine the major contributor(s) to L_{90} without a detailed study of a strip chart of the continuous sound level on which has been annotated the identification of the principal noise source at each instant of time. No existing automatic equipment can determine the contribution to the L_{90} measurement of only the railroad noise.

Thus, without some detailed guidelines in this area, the potential exists for gross errors in the identification of the major source of receiving property noise. A need exists for better procedures to identify major contributors to statistical sound

level measurements where there are several noise sources present.

A third potential problem relates to the way in which the trigger level portion of the regulation may be applied to switcher locomotives. The standard states that all switcher locomotives that operate in a particular railroad facility are deemed to be in compliance with this standard if the L_{90} trigger level on nearby receiving property does not exceed 65 dB. If this trigger level is exceeded, then presumably an inspector may require a 100-ft sound level measurement for each switcher locomotive in the railroad yard.

It is not too difficult to envision a situation in which one or more locomotives that meet the 100-ft sound level standard (70 dB at idle throttle setting) cause the trigger level of 65 dB to be exceeded because they are normally parked close to the receiving property measurement site. The obvious solution to any community noise problem caused by these locomotives is to move them further from the edge of the railroad yard, even though they meet the 100-ft standard. Yet the standard can be interpreted to require that all other switcher locomotives in the yard be tested at 100 ft and any exceeding the specified maximum be modified, even though those locomotives are not contributing to the trigger level at the receiving property measurement site.

Clearly, some discretionary judgment should be allowed both enforcement officials and railroad

personnel in solving a noise problem such as this. A solution that reduces the L_{90} at the receiving property below the trigger level should be acceptable, even if it does not involve making 100-ft measurements of all other switcher locomotives in the yard.

CONCLUSIONS

Because elements of the new railroad noise emission regulations attempt to cover many complex situations, they can be implemented in a manner that is counterproductive to cost-efficient noise control. Proper training of both enforcement and railroad personnel will be required, along with the use of reasonable judgment on the part of these persons, in order that the intents of the noise act be carried out in an effective manner.

ACKNOWLEDGMENT

The preparation of this paper was supported by the Association of American Railroads.

Publication of this paper sponsored by Committee on Transportation-Related Noise and Vibration.

Use of Microcomputers in Highway Noise Data Acquisition and Analysis

PHILIP J. GREALY, SIMON SLUTSKY, and WILLIAM R. McSHANE

ABSTRACT

A microcomputer-based noise data acquisition and analysis system has been designed that expands the capabilities currently available for monitoring highway traffic noise. The system was designed for research activities investigating the effects of pavement and tire design on highway noise levels, and it incorporates the state of the art in microcomputer interfacing equipment design. The system is designed to allow the high-speed collection and analysis of both A-weighted and 1/3 octave noise data for multiple microphone configurations. The components of the system are described, and a discussion of the hardware and software development, as well as the specific application the system is used for, is included. It is suggested that there are other applications that the system could be easily adapted to, and some insight into the effect that continued ad-

vancements in microelectronics may have on such a system is provided.

Conventional methods of acquiring highway noise data have made use of systems consisting of a series of microphones, sound level meters, and tape recorders. Collected data are then generally brought back to the laboratory for playback and analysis [see Figure 1 (1)]. This analysis is usually accomplished by using various types of filter systems coupled together with a computer. Although this method provides the necessary capabilities to carry out a detailed analysis of data, it requires large capital outlays for equipment and tends to be a time-consuming, labor-intensive, and thus costly activity.

With the advancements in the field of microelectronics in the past 5 to 10 years, the prospects of more compact and even portable equipment have been greatly improved. The evolution of the computer from vacuum tubes to transistors to integrated circuits

HIGHWAY NOISE RECORDING SYSTEM

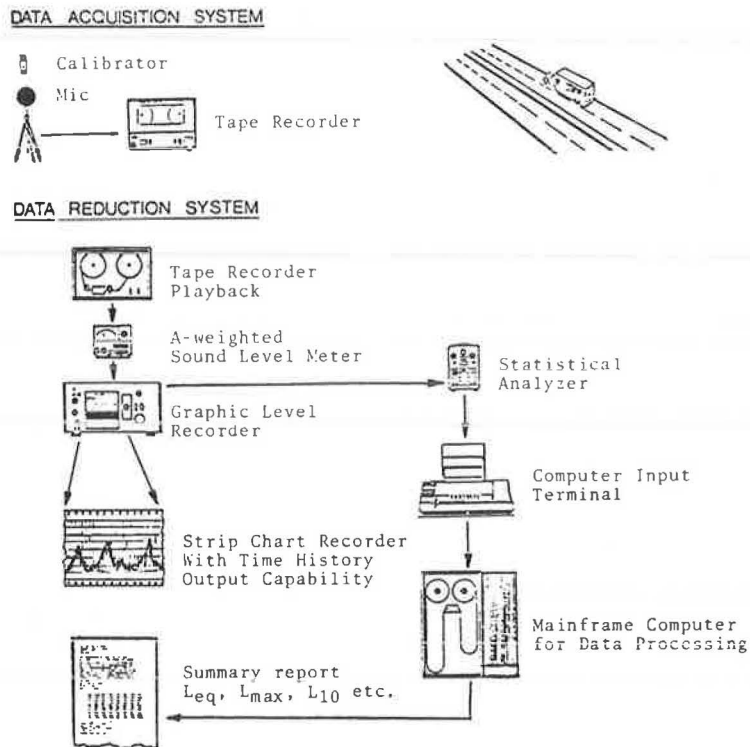


FIGURE 1 Typical highway noise data acquisition system (1).

has created new possibilities in the instrumentation and data acquisition fields. The availability of microcomputers with 16K, 64K, and now as much as 256K of random access memory (RAM) has made it possible to modify the method in which noise data are collected and analyzed.

In the following sections the details of a microcomputer-based noise data acquisition system, which was designed to incorporate some of these technological advancements, are discussed.

DATA ACQUISITION REQUIREMENTS OF CURRENT RESEARCH ACTIVITY

The Transportation Training and Research Center of the Polytechnic Institute of New York (PINY) was awarded a contract by FHWA to develop and demonstrate a tire-pavement noise assessment procedure. From recently completed research (2), it has been found that at highway speeds, tire noise is a predominant source of highway noise; thus the type of pavement selected can make a significant difference [3 to 8 dB(A)] in the resulting highway noise level. In some areas such a reduction may in fact negate the need to construct extensive and expensive barriers. By providing the states with a means of assessing these differences in highway noise impacts due to variations in pavement designs, the pavement design engineer will have the ability to recommend the use of a "quieter" pavement in noise-sensitive areas.

As part of the demonstration program, it was necessary to develop, implement, and recommend a field measurement program that the states could exercise easily in collecting their own data. Although there are several other activities associated with the overall study, the data in this paper deal

primarily with the approach taken to meet the data-collection needs.

In the initial development phases of this field measurement procedure, it was determined that to develop a procedure that could be used both easily and cost effectively by the states, efforts should be directed toward establishing an on-board data-collection method. Thereby, data collected could be incorporated into other agency inventory activities such as collection of pavement condition data, skid resistance measurements, and photologging--all necessary inputs to an effective pavement management system.

To justify the use of such a method, it was deemed necessary to conduct simultaneous measurements of both on-board and wayside microphones at various test sites, and from these measurements develop correlations between a vehicle-mounted on-board microphone and a microphone located at the roadside at the standard reference distance of 50 ft (see Figure 2).

Consequently, the investigators examined the possibility of designing a system capable of high-speed data acquisition from a multimicrophone configuration, with the ability of providing the following information for a test vehicle as it passes through a typical measurement trap:

1. A-weighted and 1/3 octave time history of the on-board microphone,
2. A-weighted and 1/3 octave time history of the microphone located 50 ft from the test vehicle, and
3. Position sensing and speed tracking of the vehicle.

To obtain this information at sufficient sampling rates (i.e., 1,000 samples per second), it was found both useful and necessary to have a data-collection

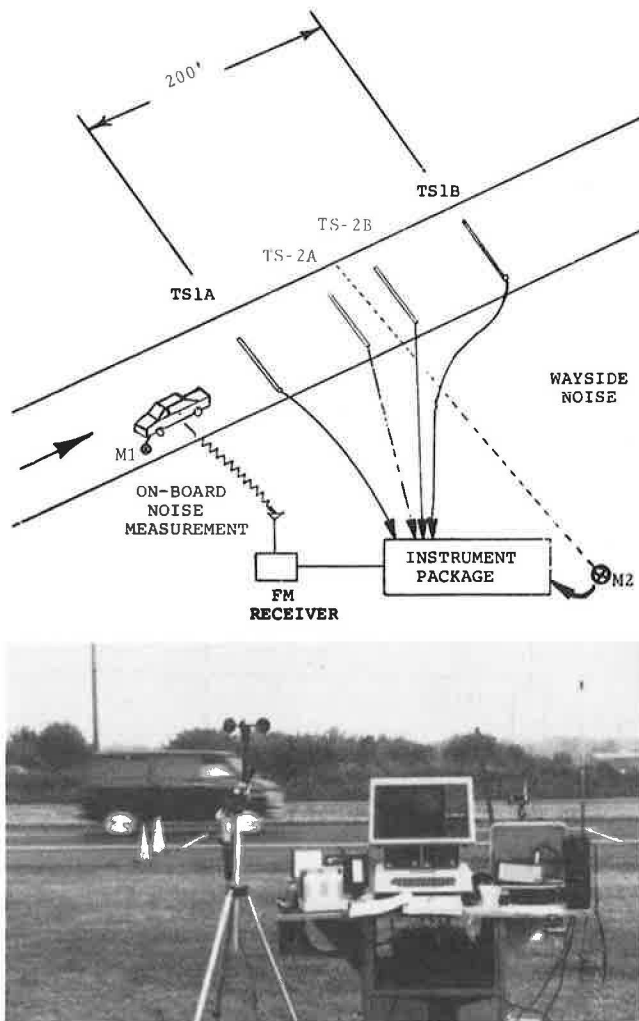


FIGURE 2 Equipment configuration used for passby on-board and wayside noise measurements.

system structured around a microcomputer. With this in mind, several possible equipment configurations were investigated. Due partially to the availability of certain in-house equipment, the conceptualization of the new system began with an APPLE II+ microcomputer and an IVIE Electronics IE-30A (3) real-time spectrum analyzer as the main components.

At the time the design of the system began, the APPLE II+ was found to be one of the most convenient microcomputers on the market, with a fairly broad base of hardware and software peripherals readily available. Two such peripherals that became integral parts of the system were a real-time clock and a 16-channel analog-to-digital (A/D) interface card.

Beyond component acquisition, the more complex problem of accessing and processing the various output signals of the different microphones and spectrum analyzers needed to be addressed. The most difficult of these tasks was the sampling of the 1/3 octave outputs of the IVIE IE-30A. To accomplish this, a combination of software and hardware development was necessary. The details of the hardware design specifications and software documentation are described elsewhere (4,5), but the general principles applied are described herein.

INTERFACING EQUIPMENT DESIGN

The IVIE/APPLE noise monitoring interfacing hardware

consists of signal-conditioning units that can be classified into several groups. The first of these units, which is used with the various sound level meters and individual microphones systems, has the function of converting the wide-band, low-voltage audio signal from these systems into a slowly varying direct current (dc) voltage of between -5 to +5 V, which in turn can be input directly to the A/D interface card located inside the APPLE. The hardware for this purpose includes a voltage amplifier and an alternating current (ac) to RMS converter with a logarithmic output channel. This system provides a dynamic range of 50 dB, which can be adjusted to fit incremental ranges of acoustic levels from 50 to 140 dB for the individual microphones.

The second series of signal conditioners is designed specifically for the IVIE IE-30A's and is somewhat more complex. In general, however, they serve to sequentially sample both the 1/3 octave and A-weighted outputs from the IVIE and adjust them to fit into the appropriate voltage range for the A/D board of the APPLE. The output from the IVIE signal conditioner consists of a reference pulse followed by 29, 1/3 octave band samples that correspond to frequencies from 25 Hz to 16 kHz. The dynamic range of the third octave output from the system is 40 dB, whereas the A-weighted sound pressure level (SPL) has a dynamic range of 50 dB(A). This range is variable from 30 to 140 dB(A), depending on the reference setting of the IVIE.

CURRENT PINY WAYSIDE DATA ACQUISITION SYSTEM

Figure 2 shows the typical equipment configuration used by the research team. In general, the setup involves the placement of microphones on board the vehicle and at the roadside at 50 ft from the centerline of the vehicle's travel path. The instrumentation system referred to in this figure is shown in more detail in Figure 3, which is a block diagram of the equipment configuration. The individual components of this system are described in the following paragraphs.

As discussed previously, the heart of this system is an APPLE II+ microcomputer (64K RAM), which is used to monitor, store, and analyze several different channels of noise and speed data. The peripherals used in conjunction with the APPLE are

1. Four 5.25-in. disk drives,
2. One 16-channel A/D interface card,
3. One real-time clock interface card, and
4. One 12-in. monitor.

Note that the system can operate with a minimum of two disk drives; however, the use of the two additional drives allows the collected data to be sorted by vehicle type. Thus drive 1 is reserved to run the data-collection program while drives 2, 3, and 4 are used to store data collected for the vehicle categories of automobile, van, and truck, respectively. This in turn enables successive sampling of the various types of test vehicles without removing or changing storage disks.

In addition to these peripherals, there are several microphones and other components that complete the system:

1. One Bruel & Kjaer 2203 sound level meter;
2. Two IVIE-30A spectrum analyzers;
3. Four temporary roadway electronic sensing devices (tapeswitches);
4. A portable 800-w Honda gasoline-powered ac/dc electric generator;
5. Three short-range wireless FM transmitters;

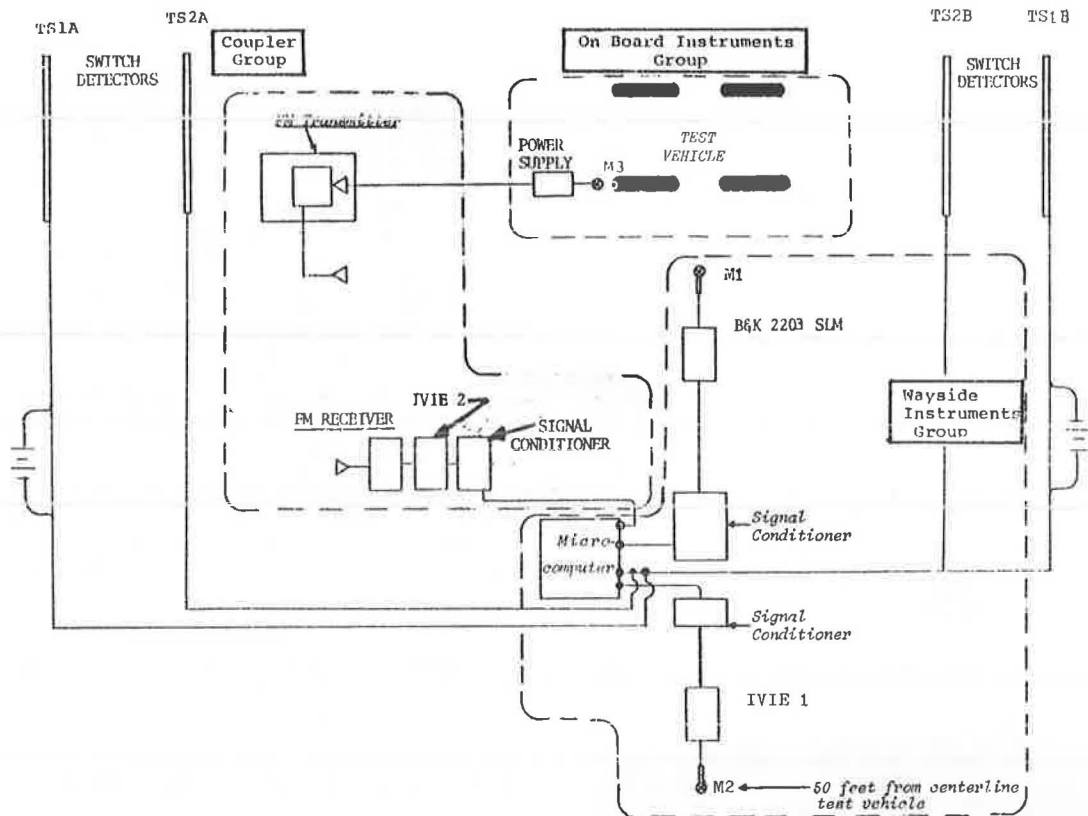


FIGURE 3 Block diagram of passby data acquisition instrumentation.

6. One FM receiver with a crystal matched to the transmitter;
7. Three test vehicles, including a passenger car, a van, and a truck; and
8. Three vehicle-mounted microphone systems (GenRad 0.5-in. condenser microphone with P-42 pre-amplifier and an 18-V power supply).

Of these components, those of particular interest are the FM telemetering system and the portable generator. The latter is noted because of its excellent power output, low exhaust noise levels, and compactness--factors that are essential for the types of measurements involved.

The telemetry system is also an essential component of the measurement system. The telemetering equipment consists of three short-range wireless FM transmitters coupled with a matched crystal FM receiver. The transmitters are mounted on each of the three test vehicles and are used to transmit the noise signals sensed directly behind the tire as a vehicle passes through the measurement trap.

The transmitted signal is picked up by the FM receiver located at the wayside. The output from the receiver is then transferred to the IVIE spectrum analyzer. The use of the system enables the on-board and wayside measurements to be recorded sequentially by the computer located at the roadside. There are, however, certain limiting factors associated with its use.

The first factor is the limited transmission range of approximately 150 ft. This limitation is partly overcome by placing the receiver at the midpoint of the measurement trap, thus expanding the effective trap distance to as much as 300 ft, which is adequate for these measurements.

The sound problem is the limited dynamic range of the telemetering system, which is on the order of 30

to 35 dB. The effect of this limited dynamic range is mitigated by the nature of the on-board signal, which experiences only minor fluctuations in levels over the entire measurement trap. Still, because the range of noise levels for the three vehicle types exhibits a greater variation, care must be taken in adjusting these levels to obtain a maximum useful dynamic range for the system.

In order to combine and coordinate the equipment into an interactive system capable of processing and storing the various events occurring during a vehicle passby through the measurement trap, an extensive software package was designed. The individual components of this package are discussed in the next section.

DATA ACQUISITION SOFTWARE

The data acquisition software consists of three main routines, including (a) test inventory data, (b) data collection and memory storage, and (c) disk data storage. The first routine, which is written in APPLESOFT BASIC, serves the purpose of inputting inventory information to be stored with the data collected for each run. This includes general information such as the vehicle, tire, and pavement types being tested, as well as the date, time, and meteorological information.

The second routine is actually the key part of the package and is written in APPLE-6502 assembly language. This routine serves the purpose of reading the starting and ending time of each run and storing the individual data samples in the memory of the microcomputer. After the data collection is completed, the program returns to a BASIC routine, which saves the data to disk for future analysis. The data are stored in the format shown in Figure 4.

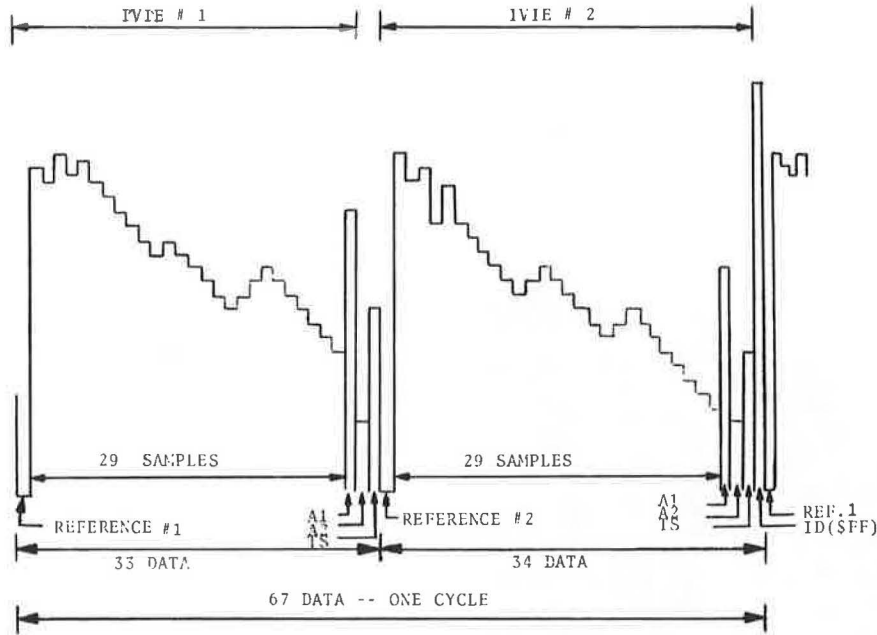


FIGURE 4 Data storage format.

The tapeswitch (TS-1A) referred to previously in Figure 2 serves to automatically trigger the assembly language software used to collect the data from the various instruments. Tapeswitches TS-2A and TS-2B isolate a smaller trap in the region where the peak is expected to occur. The last tapeswitch (TS-1B) terminates the acquisition of samples from the various microphones and enables the data to be written to disk.

As shown in Figure 4, a complete cycle consists of 67 pieces of data. The cycle begins with a reference signal from IVIE no. 1 followed by 29, 1/3 octave band samples that correspond to frequencies from 25 Hz to 16 kHz. This is followed by an A-weighted signal from the wayside nearfield microphone and an A-weighted signal from IVIE no. 1. An indication of the tapeswitch status follows, with the remainder of the cycle consisting of a repeat of identical information for the second IVIE. The last data value in the cycle is an identification signal that marks the end of the cycle. As many as 100 cycles can be collected and stored in memory during a typical run.

The sampling rate of the measurement system is limited by the processing rate of the IVIE IE-30A. It takes approximately 11.5 milliseconds to sample the 1/3 octave spectrum and A-weighted outputs from a single IVIE. However, when acquiring data from two IVIEs, as in the case here, the time to read the data from both can range from 23 to 34 milliseconds. This is due mainly to the internal clocks of the IVIEs, which may or may not be fully synchronized with one another. Nonetheless, for a typical trap distance of 200 ft, the number of cycles collected during a single 55 mph passby run is on the order of 75 cycles. With a cycle consisting of 67 data points, this corresponds to a total of 5,025 pieces of data for a single run.

ON-BOARD DATA ACQUISITION SYSTEM

The data-collection system previously described is for a combination of on-board and wayside noise measurements. Variations of this system exist for separate collection of either on-board or wayside

measurements. For wayside-only measurements, the change requires no more than elimination of the transmitted on-board signal from the process. The on-board process is less trivial; it is described in detail in the following paragraphs.

Initially, the on-board measurement procedure consisted of a microphone mounted behind the tire, as shown in Figure 5. To reduce the effect of wind noise around the microphone, a specially designed windscreen was developed. Based on prior work conducted by Rosenheck and Hofmann (6), the use of a tear-drop-shaped windscreen was investigated. Be-

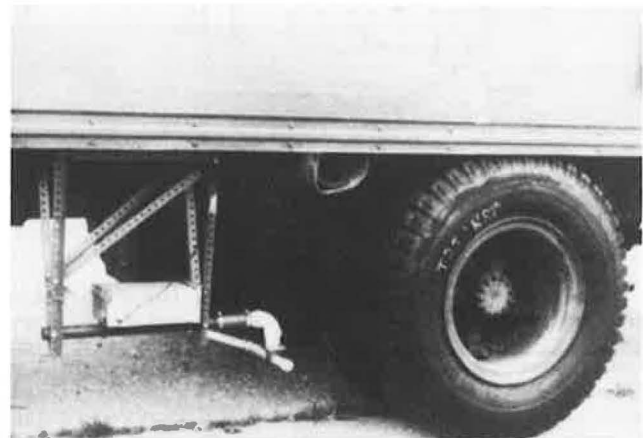
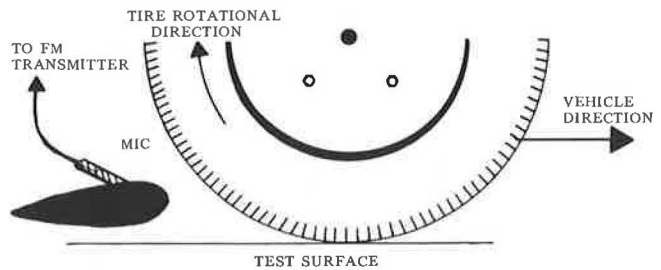


FIGURE 5 Typical mounting of on-board microphone system.

cause this type of windscreen is not commercially available, it was necessary to construct one in-house. Figure 6 shows one of these windscreens mounted directly behind a test tire. Based on the results of a simulated wind tunnel test, it was found that the use of this windscreen enabled consideration of measurements with frequencies as low as 200 Hz, which otherwise would have been submerged by the wind noise.

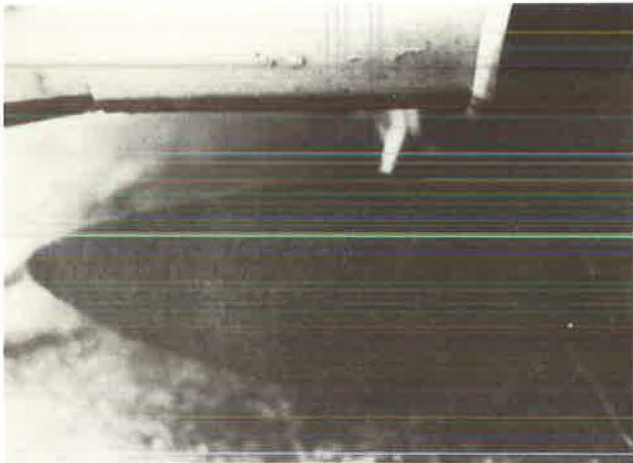


FIGURE 6 Windscreen used with on-board microphone.

Care was also taken in mounting the microphone on the vehicles to minimize vibrational effects. A rigid mounting system that consisted of polyvinylchloride (PVC) piping was used. In addition to providing support for the microphone and preamplifier, the piping was lined with foam rubber and the microphone cable was run through it for added protection.

The remainder of the on-board system consists of the IVIE/APPLE interface system previously described coupled with a speed pick-up device that constantly inventories the vehicle speed during measurements (see Figure 7). Figure 8 shows the typical on-board instrumentation setup in the test van.

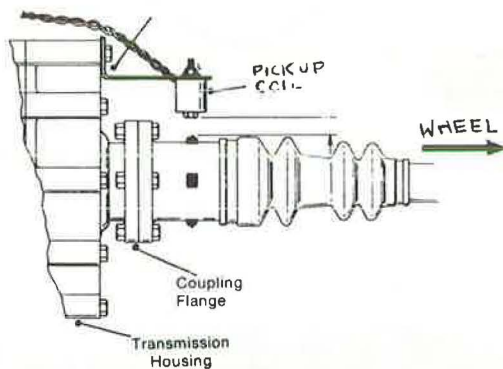


FIGURE 7 Placement of speed-sensing device.

After gaining some experience with the telemetering of noise signals with the FM transmission system, it became apparent that the possibility of testing two vehicles simultaneously was feasible. In this configuration, one test vehicle is equipped with (a) a microcomputer system, (b) two IVIEs, (c) a speed pick-up unit, and (d) two FM receivers with different crystals. The data from this first vehicle

are fed directly through the IVIE and into the microcomputer system. The data from the second vehicle are transmitted to the first vehicle by the transmitters. One channel transmits the noise data and the other transmits the speed data for the second vehicle. When these data are received by the receivers in vehicle one, the speed data are input directly to the microcomputer, and the noise data are processed through the second IVIE and then stored in the microcomputer.

DESCRIPTION OF DATA ANALYSIS SOFTWARE SYSTEM

The data analysis software consists of various programs that serve such functions as recalling the raw data from disk, performing various statistical computations, and printing paper copies of these results. The details of each of these are described in the following paragraphs.

The Recall/Data program simply recalls the raw data from disk according to the format in which it was initially stored. The data are read back into memory where it can be used in any of a series of computations.

The Data/Analysis program is used in computing L_{eq} (L-equivalent), L_{max} , and average on-board and wayside levels for each frequency; it is also used in the preparation of time histories for the various microphones. This program has several variations, depending on whether the data are for wayside and on-board measurements or simply for on-board measurements. There are also several printing options available for printing hard-paper copies of these results. Figure 9 is a typical output of the available data. The printed record data include such items as the identification number, date, test conditions, and data sampling rate. The data outputs include a time history of the various microphones and an indication of L_{max} and L_{eq} . The last portion of this printout is a summary of the maximum and average levels by 1/3 octave for each microphone.

To summarize and compare the results of several individual runs for the same site and vehicle and tire combination, there is also an Analysis/Summary program that takes the results of these runs and computes the mean levels and variances for all runs. These results can then be used in further statistical analyses and presentation of results.



FIGURE 8 On-board instrumentation system.

SUMMARY OF DATA COLLECTION				1/3 OCT READINGS FOR TRAP1													
FILE ID	DATE	VEHICLE TYPE	TIRE TYPE	PAVEMENT TYPE	NO OF CYCLES	SAMPLE RATE	MIC#2	TRAP1	TRAP	FREQ	WAYSIDE READINGS			DNBD RDS	TRANSFER FUNCTIONS		
											MAX	IAVG	EL50	AVG	TF(MAX)	TF(IAVG)	TF(EL50)
01-2	8583	CAR	T7C		74	29.78 CYCLES/SEC				25.0 HZ	66	67.6	66.5				
										31.5 HZ	65.2	67.2	66.3				
										40.0 HZ	63	65.4	64.7				
										50.0 HZ	62.5	63.4	62.6				
										65.0 HZ	59.9	61.5	60.2				
										80.0 HZ	59.1	60.4	59.3				
										100 HZ	59.4	59.8	58.8				
										125 HZ	55.5	54.1	53.6				
										160 HZ	54.5	54.3	53.6				
										200 HZ	60.1	58.8	58.3	83.5	-23.4	-24.7	-25.2
										250 HZ	60.1	58.4	58.1	81	-20.9	-22.6	-22.9
										315 HZ	59.9	56.6	56.6	82.1	-22.2	-25.5	-25.5
										400 HZ	60.8	56.9	56.9	84.6	-23.8	-27.7	-27.7
										500 HZ	59.4	56.8	56.5	83.3	-23.9	-26.5	-26.8
										630 HZ	61.8	59.5	59.5	83.4	-21.6	-23.9	-23.9
										800 HZ	66.9	63.2	63.3	88.1	-21.2	-24.9	-24.8
										1 K	67.9	63.3	63.3	90.3	-22.4	-27	-27
										1.25 K	61.3	60.7	60.2	91.2	-29.9	-30.5	-31
										1.6 K	60.1	59.6	58.9	87.5	-27.4	-27.9	-28.6
										2 K	58.4	57.5	56.9	85.2	-26.8	-27.7	-28.3
										2.5 K	57.2	56.4	55.9	82.9	-25.7	-26.5	-27
										3.15 K	54.5	53.3	52.8	76.7	-22.2	-23.4	-23.9
										4 K	52.3	51.2	50.8	73.8	-21.5	-22.6	-23
										5 K	50.6	49.1	48.8	70.5	-19.9	-21.4	-21.7
										6.3 K	48.6	47.6	47.2	49.3	-1.700	-1.7	-2.09
										8 K	45.7	44.8	44.4	61.8	-16.1	-17	-17.4
										A-W	72.4	69.7	69.6	97.6	-25.2	-27.9	-28

FIGURE 9 Sample printout of data analysis results.

AUTOMATION CONCEPTS

Although the use of the microcomputer eliminated the stage of playing back a recorded tape, it is still a somewhat time-consuming process to complete a detailed analysis of the raw data. To overcome the loss of time and personnel necessary for running the analysis, a procedure to automate this stage was developed. Considering that it can take up to 25 min on the microcomputer to analyze a typical run, and that a total of 35 runs are taken for each vehicle at each site, it was necessary to structure a program that would allow multiple runs to be analyzed without operator interaction; that is, to successively read and analyze the individual files and then save the results on disk. This was accomplished through software, with the resulting data processing time reduced by between 30 and 50 percent.

This automated method of reading successive files also proved to be useful when printing paper copies of the results. The operator only has to load a disk into the microcomputer, answer a few questions, and then return later with all files printed automatically.

CONCLUSIONS

By taking advantage of the recent technological advancements in microelectronics, a more cost-effective

highway noise data acquisition system has been designed, tested, and implemented. With such a system the amount of useful data that can be feasibly collected and analyzed by highway engineers is greatly expanded.

Although the system described herein was designed specifically for the acquisition of highway noise data, it has the potential of being used for other applications. Some of these other uses could include noise-monitoring systems for airports, subway systems, and industrial applications, where the concern for noise levels is a sensitive issue.

In summary, the present system is limited by the amount of available storage and the number of channels of data that can be handled because it was designed around an 8-bit, 64K (RAM) microcomputer. However, since the time it was initially designed, other 16-bit microcomputers with 256K (RAM) or greater and additional A/D channels have become commercially available. By configuring the present system around one of these more advanced microcomputers, the capabilities will be greatly increased.

ACKNOWLEDGMENTS

The research reported on herein is being conducted under an FHWA contract, "Tire-Pavement Noise Assessment Procedure." Fred Romano is the FHWA technical monitor. The authors wish to acknowledge the inputs

of many others associated with the design and implementation of the research reported on here. Special thanks are expressed to Loyal Chow, Patrick Hanley, James Goon, and Conrad Moses for their contributions to the design of the hardware and software systems presented here. Appreciation is also extended to Michael Leonard, Nassy Srour, and Horace Patterson for their assistance in the data-collection efforts.

REFERENCES

1. Guide on Evaluation and Attenuation of Traffic Noise. AASHTO, Washington, D.C., 1974.
2. J.C. Walker and R.D. Oakes. The Reduction of Tyre-Road Interaction Noise. Dunlop Corp., England, 1981.
3. IVIE IE-30A Audio Analysis System Owner's Manual. IVIE Electronics, Salt Lake City, Utah, March 1978.
4. L. Chow and P. Grealy. IVIE/APPLE Interfacing System. Polytechnic Institute of New York, Brooklyn, Sept. 1982.
5. P. Hanley and P. Grealy. Tire-Noise Data Processing Software--User's Manual. Polytechnic Institute of New York, Brooklyn, July 1983.
6. A.S. Rosenheck and R.F. Hofmann. Measurement of Automobile Tire Noise in a Moving Vehicle and Comparison with Drum Measurements. Proc., International Tire Noise Conference, Stockholm, Sweden, 1979.

This paper was produced as part of a program of research sponsored by FHWA, U.S. Department of Transportation. The results and views expressed are the product of this research and statements expressed in this paper are those of the authors and do not necessarily reflect those of the FHWA.

Publication of this paper sponsored by Committee on Instrumentation Principles and Applications.